Time is of the essence - investigating kinetic interactions between drug, endogenous neuropeptides and receptor

Nederpelt, I.

Time is of the essence

Investigating kinetic interactions between drug, endogenous neuropeptides and receptor

Cover design: Rochelle Vergroesen & Indira Nederpelt

Cover art: Rochelle Vergroesen

Thesis lay-out: Indira Nederpelt

Printing: GVO drukkers & vormgevers B.V., Ede

ISBN: 978-94-6332-161-7

Time is of the essence

Investigating kinetic interactions between drug, endogenous neuropeptides and receptor

Proefschrift

Ter verkrijging van de graad van Doctor aan de Universiteit Leiden,

op gezag van Rector Magnificus Prof. Dr. C.J.J.M. Stolker,

volgens besluit van het College voor Promoties te verdedigen op donderdag 6 April 2017

klokke 16:15 uur

Door

Indira Nederpelt

Geboren te Rotterdam, Nederland

In 1988

Promotor: Prof. Dr. A.P. IJzerman

Co-promotor: Dr. L.H. Heitman

Promotie commissie:

Prof. Dr. H. Irth (chair)

Prof. Dr. J.A. Bouwstra (secretary)

Dr. E.C. de Lange (assistant professor of pharmacology at the LACDR, Leiden University)

Prof. Dr. G. Vauquelin (professor of molecular pharmacology at the Vrije Universiteit Brussel)

Prof. Dr. R.A. Adan (professor of molecular pharmacology at the Utrecht Medical Centre)

The research described in this thesis was performed at the department of Medicinal Chemistry of the Leiden Academic Centre for Drug Research (LACDR), Leiden University (Leiden, The Netherlands). The research was financially supported by EU/EFPIA Innovative Medicines Initiative Joint Undertaking, K4DD grant n° 115366.

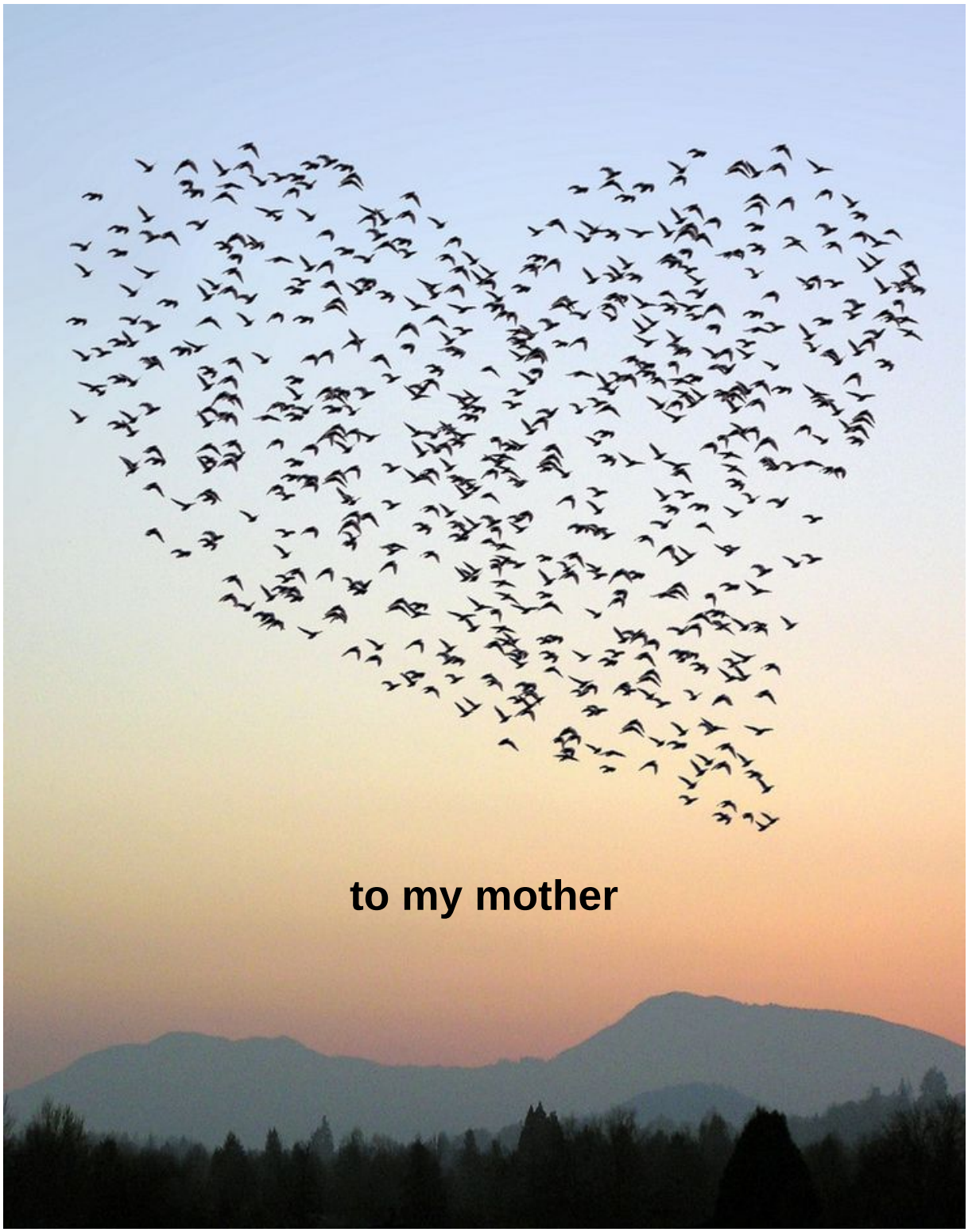
to my mother

Index

Chapter 1

General introduction

The search for effective drugs treating diseases has been an age-old quest. While drug design and development have witnessed major progress over the last decades, one of the main challenges still resides in the lack of efficacy. Consequently, traditional lead selection procedures like Lipinski's rule of five and affinity-based selection need to be reconsidered. Over the past 10-years, binding kinetics, i.e. the association and dissociation rate of a drug to and from its target, have been proposed as better predictive parameters in assessing the potential of novel drugs [1-6]. Although the importance of binding kinetics is increasingly recognized, there is still a need for robust assays suitable to study association and dissociation rates of potential drug candidates. Additionally, many successful drugs achieve their effect by competing with endogenous ligands for the same binding site. Therefore, understanding the pharmacological and physiological behavior, such as binding kinetics, of endogenous ligands in the human body is crucial. This is of particular importance for endogenous ligands since they are often released temporally at locally high concentrations. Finally, to bridge the gap between *in vitro* and *in vivo* studies, functional assays that can reliably translate binding kinetics to *in vitro* functional effects are crucial.

To illustrate the importance and relevance of the research performed in this thesis, this chapter provides a general introduction. Firstly, the superfamily of G protein-coupled receptors (GPCRs) will be introduced, followed by an introduction of the sub-family of neuropeptide receptors which are predominantly GPCRs. Consequently, the background of two well-known neuropeptide receptors, namely the gonadotropin-releasing hormone (GnRH) receptor and neurokinin 1 (NK1) receptor, will be outlined as the experimental chapters of this thesis are centered around these receptors. Furthermore, the concept of binding kinetics will be defined, including the challenges of measuring these kinetic binding parameters. Lastly, the aim and outline of this thesis will be explained.

G protein-coupled receptors

The GPCR family is one of the largest and most diverse receptor families and nearly 800 genes encoding GPCRs have to date been identified [7]. GPCRs are composed of seven transmembrane helices with extracellular and intracellular loops and an extracellular (N-terminal) and intracellular (C-terminal) tail. GPCRs are coupled to intracellular G proteins and can be activated by a wide range of ligands, such as peptides, neurotransmitters, hormones, growth factors, odorant molecules and even photons [8] (Figure 1). GPCR activation results in a conformational change of the receptor, causing GDP to be exchanged for GTP. Consequently, this leads to dissociation of the Gαβγ-heterotrimer into the βγ-dimer and the α-subunit. The four main Gα-subunits are; $G\alpha_i$, $G\alpha_s$, $G\alpha_q$ and $G\alpha_{12/13}$. The activation and inhibition of diverse G protein-dependent pathways makes GPCRs essential in cell

signaling [9]. Targeting the GPCR super-family has led to approximately 30% of the marketed drugs and to date GPCRs are vital targets in drug research due to their role in (patho-) physiology throughout the body [10].

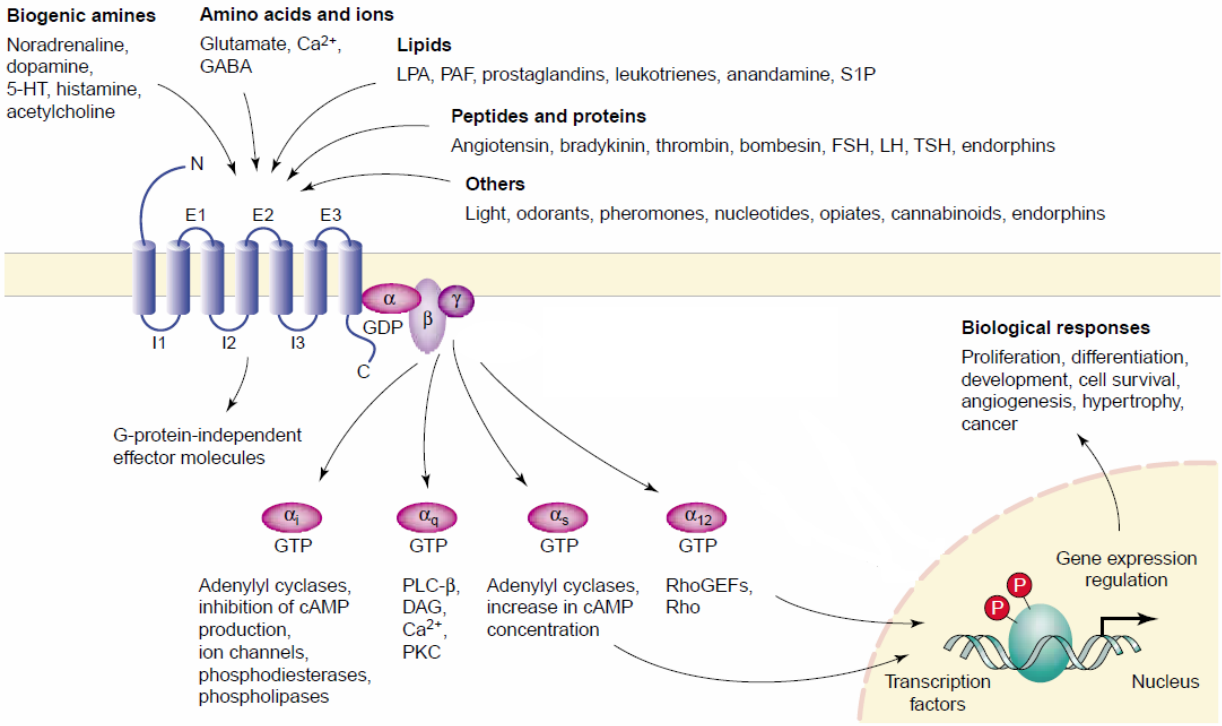

Figure 1: Schematic overview of ligands binding to G protein-coupled receptors and their four main signaling pathways. A wide range of ligands can bind and activate GPCRs through G protein-dependent (i.e. $G\alpha_s$, $G\alpha_q$, $G\alpha_i$ and $G\alpha_{12}$ proteins) and G protein-independent (e.g. β-arrestin) pathways. These signaling pathways can regulate pivotal cellular functions such as proliferation [8].

Neuropeptide receptors

Neuropeptides are (poly)peptides and can be short as kisspeptin-10 (e.g. 3 amino acids) or as long as neurexophilin-1 (e.g. 250 amino acids). Neuropeptides mediate neuronal communication by binding to neuropeptide receptors expressed on either neuronal substrates such as glial cells or on non-neuronal target cells [11]. The neuropeptide receptor family consists of over 44 receptor families which are predominantly GPCRs. Neuropeptide receptors and their endogenous ligands are involved in numerous behavioral and physiological functions such as blood pressure, body temperature, feeding behavior, pain regulation, reproduction, learning, memory and sleep [12]. Consequently, neuropeptide transmission is an attractive focal area for drug design in numerous therapeutic areas, such as inflammatory conditions, epilepsy and psychiatric diseases [13-15].

GnRH receptor

One of the most well-known neuropeptide receptors is the gonadotropin-releasing hormone (GnRH) receptor. This receptor binds endogenous GnRH and upon activation stimulates the production of follicle stimulating hormone (FSH) and luteinizing hormone (LH). The GnRH receptor belongs to the superfamily of GPCRs and is (predominantly) coupled to $G\alpha_{q/11}$ proteins This receptor is involved in maintaining hormone levels in both males and females which makes it an attractive drug target in the treatment of hormone-dependent diseases such as fertility disorders, precocious puberty, and cancers of the endometrium, ovary, prostate and mammary [16, 17]. Sustained receptor exposure to GnRH or GnRH analogs leads to desensitization of GnRH receptor-mediated gonadotropin secretion. This desensitization or blockade of the GnRH receptor is called chemical castration and underlies the therapeutic use of GnRH analogs. The first GnRH analog to reach the market was nafarelin acetate in 1998 and soon after many more GnRH analogs were FDA approved, such as leuprolide acetate, goserelin acetate, degarelix and triptorelin [18-20]. To date, many peptide GnRH receptor agonists and antagonists are on the market to treat hormone-dependent disorders [17, 21-24] and available patient information suggest that the pharmacokinetic and pharmacodynamic profiles are very comparable. Accordingly, insights into the *in vitro* binding parameters, such as drug-target binding kinetics, could improve the understanding of the mechanism of action of these well-known drugs.

NK1 receptor

Another well-known neuropeptide receptor is the neurokinin 1 (NK1) receptor or tachykinin 1 receptor. This receptor belongs to the tachykinin receptor family that consists of NK1, NK2 and NK3 receptors. The NK1 receptor belongs to class A GPCRs and is functionally coupled to $G\alpha_{q/11}$ proteins and $G\alpha_{s}$ proteins. Multiple endogenous tachykinins bind to the NK1 receptor, including Substance P (SP), neurokinin A (NKA) and neurokinin B (NKB). Each tachykinin has a specific rank order to activate tachykinin receptors with regard to potency and affinity, namely SP > NKA > NKB for the NK1 receptor, NKA > NKB > SP for the NK2 receptor and NKB > NKA > SP for the NK3 receptor. The NK1 receptor plays an imperative role in the brain with respect to the regulation of affective behavior and emesis, as well as nociception in the spinal cord [25].

Presently, only two drugs are on the market targeting the NK1 receptor for the treatment of chemotherapy-induced nausea and vomiting (CINV). Aprepitant, a high affinity, selective NK1 receptor antagonist was FDA approved in 2003 [26]. This small molecule

antagonist was the first NK1 antagonists to reach the market as previous clinical trials were predominantly aimed towards clinical pain states [27]. Interestingly, a distinguishing feature of aprepitant is its so-called PK/PD discrepancy *in vivo*, i.e. aprepitant levels in the brain were below the limit of quantification while a strong inhibitory effect was still present, which researchers attest to its slow receptor dissociation rate [28]. In 2014, a combination drug of a NK1 small molecule antagonist (netupitant) and a 5-HT_3 antagonist, was approved for the treatment of CINV [29]. *In vitro* studies demonstrated that netupitant was wash-out resistant for up to 5 hours and the action of netupitant was therefore deemed insurmountable [30]. These two drug examples allude to the importance of being aware of and consequently optimizing kinetic binding parameters.

Binding kinetics, a retrospective analysis

Traditional drug discovery programs are predominantly focused on equilibrium-based parameters such as K_i and IC_{50} values. However, candidate drugs with high affinity and potency often fail in clinical trials due to target toxicity and/or lack of *in vivo* efficacy [31, 32]. Therefore, other, more predictive parameters than affinity and potency values are warranted. Binding kinetics are a collective term for the association (k_{on}) and dissociation (k_{off}) rate constant of a drug to and from its target. Additionally, the so-called drug-target residence time is reflective of the life-time of the drug-target complex and is defined as the reciprocal of k_{off} [3]. Over the past 10 years binding kinetics are increasingly acknowledged to be vital for the mechanism of action of a potential drug [33]. Moreover, many blockbuster drugs have been retrospectively been examined for their binding kinetics and were found to have distinct kinetic profiles [34]. For example, quetiapine, a dopamine D_2 receptor antagonist approved for the treatment of schizophrenia and bipolar disorder, has significantly less adverse effects and on-target toxicity in comparison to other dopamine D_2 receptor antagonists due to its fast dissociation rate [35]. However, more often slow dissociation rates are favorable. Tiotropium, a muscarinic M_3 receptor antagonist, is a well-known long-acting muscarinic antagonist. Since the muscarinic M_3 receptor is mainly targeted to treat chronic diseases, a long duration of action is desirable to achieve prolonged efficacy and thus improve patient compliance [36]. Another advantage, aside from the long duration of action of tiotropium, is that it has kinetic selectivity (i.e. faster dissociation rates from other muscarinic receptor subtypes) over other muscarinic receptors thereby minimizing off-target toxicity [37]. Finally, negative allosteric CCR5 modulator maraviroc, was the first drug targeting CCR5 to get FDA approval and proved to be highly efficacious in inhibiting HIV cell infection[38]. Watson and colleagues reported very slow dissociation rates for this compound and the reversal of antagonism rate was found to be longer than 136 hours at room temperature [39]. All these case studies

demonstrate the importance of binding kinetics in achieving high *in vivo* efficacy and/or minimizing (target) toxicity.

Challenges of incorporating binding kinetics in the drug discovery paradigm

While the previous examples greatly emphasize the impact of binding kinetics, kinetic binding parameters are often only taken into account in retrospect, if at all. Concerns are regularly expressed about suitable high-throughput assays to study binding kinetics in a time-efficient manner, such that they might be introduced in an earlier stage of the drug discovery process.

Labeled binding assays

The most recognized assays to study binding kinetics are radioligand binding experiments, where the ligand of interest is radiolabeled and association and dissociation experiments are performed to directly measure k_{on} and k_{off} values. However, since radiolabeling every potential drug candidate is very costly and time consuming, novel protocols and techniques have been proposed over the past years [34, 40].

In 1984, Motulsky and Mahan introduced a pharmacological approach in which the binding kinetics of unlabeled ligands can be quantitatively measured by only using one labeled tracer[41]. This so-called competition association method has to date been used to determine the binding kinetics of numerous potential drug candidates [42-44]. Recently, a more medium-throughput dual-point competition association assay was developed [45]. This assay makes use of only two time points and the specific binding of the labeled tracer at these time points generates a qualitative measure of the dissociation kinetics of the (competitive) unlabeled ligand. This screening assay has already been successfully applied to multiple targets [46-48].

Considering the disadvantages of working with radioactivity, alternative labeling techniques have been explored. Schiele *et al* developed a universal homogeneous kinetic probe competition assay (kPCA) that allowed accurate and cost-effective measurements of binding kinetics in a high-throughput format [49]. They compared binding kinetics of three target groups (GPCRs, protein-protein interactions and enzymes) measured with radioligand binding studies, kPCA and surface plasmon resonance (SPR) spectroscopy. Results were highly correlated and the authors proposed that the time-resolved fluorescence energy transfer (TR-FRET) method used for kPCA combines the time resolution of SPR and related biosensors while maintaining the versatility of radioligand binding studies. Notably, one of the

disadvantages of kPCA is the need for not only a fluorescently labeled tracer but also an engineered fluorescently labeled receptor.

Label-free binding assays

Alternative methods to measure binding kinetics are label-free techniques such as SPR and surface acoustic wave (SAW) biosensors [50, 51]. These assays enable real-time quantitative measurements of association and dissociation rates of unlabeled ligands targeting membrane proteins. Advantages of both assays are the capability of using relatively small quantities of materials in addition to the high time resolution [52-54]. The need for having an immobilized receptor protein represents a serious disadvantage when studying GPCR binding as these proteins rapidly disintegrate when taken out of their natural environment.

More recently, a label-free mass spectrometry (MS) ligand binding assay was developed for the adenosine A_1 and A_{2A} receptors [55]. The authors were able to perform saturation, association, dissociation and displacement studies without an internal standard making it a true label-free assay suitable to study binding kinetics. Results from the MS experiments were highly correlated to radioligand binding studies. An inconvenience of this assay is the need for an elaborate sample quantification procedure that needs technical expertise.

Functional assays

Another method to qualitatively study binding kinetics of agonists and antagonists is by measuring their functional effects.

To examine the binding kinetics of agonists, a functional wash out can be conducted. Cells are pre-incubated with the agonist of interest to allow the binding of agonist to the receptor. Consequently, cells are washed and the effects of agonist binding can be measured. In theory, agonists with fast dissociation kinetics should be readily washed out while slowly dissociating agonists should still be bound to the receptor thereby maintaining most of the functional effect [56].

The binding kinetics of antagonists can be measured by examining their functional insurmountability. For these experiments cells are pre-incubated with a competitive antagonist prior to addition of an (endogenous) agonist. The maximal response of the agonist with and without antagonist pre-incubation can then be compared. If the maximal response of the agonist is significantly decreased upon antagonist pre-incubation, the antagonist is deemed insurmountable which is often correlated to its slow dissociation rate [57, 58]. A

drawback of functional assays predicting binding kinetics is that these only provide an indication for the dissociation rate of a ligand while the association rate might also be of importance.

Objectives and outline of this thesis

Objective

The objective of this thesis was to provide kinetic binding parameters of well-known neuropeptides and competitive drugs targeting the GnRH receptor and NK1 receptor to advance the understanding of these ligand-receptor interactions. Additionally, we aimed to design, validate and compare various kinetic assays to supply a more diverse toolbox suitable for studying binding kinetics. The kinetic assays that were used and discussed in this thesis are radioligand binding, TR-FRET, label-free xCELLigence and real-time cAMP assays (Figure 2). Lastly, correlations between binding kinetics and functional effects *in vitro* were explored. A schematic overview of the contents of this thesis is presented in Figure 3.

Outline

In **Chapter 2** the kinetic profile of neuropeptide – receptor interactions is reviewed to provide a clear overview of the importance of binding kinetics and other kinetic interactions. This chapter also includes the potential of neuropeptide receptors in drug discovery. Furthermore the relevance of not only characterizing the drug candidate but also the endogenous ligand and target, with particular focus on their kinetic aspects, is explained.

The binding kinetics of well-known GnRH receptor agonists are analyzed in **Chapter 3**. For this purpose two kinetic binding assays were designed, validated and compared (Figure 2A and 2B).

Endogenous GnRH and a slowly dissociating analog (buserelin) were further studied in **Chapter 4**. The receptor activation profiles induced by both agonists were examined with a label-free impedance-based assay measuring changes in cell morphology (Figure 2C). This assay allowed for real-time measurements of cellular effects. A wash-out assay was also designed to examine the long-lasting effects of both agonists.

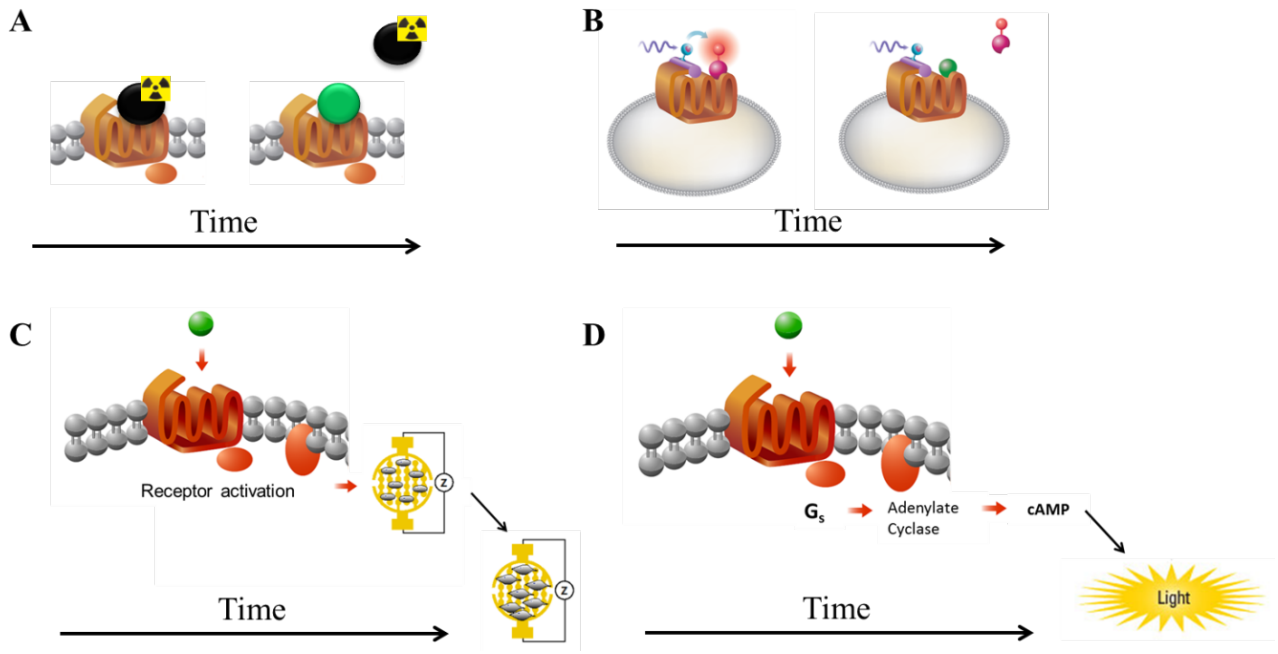

Figure 2: Schematic depiction of the kinetic binding assays (A and B) and kinetic functional assays (C and D) used in this thesis. (A) Radioligand binding assay. Assay requirements are cell membrane preparations and high affinity radiolabeled tracer. Over time the unlabeled ligand of interest will displace the radiolabeled tracer and from this the k_{on}, k_{off} and residence time (RT) values of the unlabeled ligand can be calculated. (B) TR-FRET™ assay. Assay requirements are whole cells with a SNAP-tagged receptor and a high affinity fluorescent tracer. When the fluorescent tracer and tagged receptor are in close proximity a FRET signal can be detected, over time the unlabeled ligand of interest will displace the fluorescent tracer and from this the k_{on}, k_{off} and RT values of the unlabeled ligand can be calculated. (C) Real-time functional label-free xCELLigence assay. Assay requirements are whole cells, no tracer or labeling necessary. Receptor activation can be followed over time by monitoring the cell morphology through impedance. (D) Real-time functional GloSensor™ cAMP assay. Assay requirements are whole cells transfected with GloSensor plasmid, this cAMP-biosensor undergoes a conformational change upon cAMP binding, followed by the turnover of Luciferin resulting in an increase in luminescence. cAMP production can be followed over time by monitoring luminescence.

In **Chapter 5** the binding kinetics of well-known endogenous tachykinins targeting the NK1 receptor are examined using radioligand binding studies (Figure 2A). Moreover, functional parameters such as potency and maximal response values were determined in label-free impedance-based experiments (Figure 2C).

In **Chapter 6** the relationship between *in vitro* drug-target binding kinetics and cellular responses is investigated to improve the understanding of drug efficacy *in vivo*. The functional effects of slowly (aprepitant) and fastly (DFA) dissociating NK1 receptor antagonists were examined in the presence of endogenous agonists SP or NKA. Two different kinetic functional assays were compared, namely a real-time morphology-based assay and a real-time cAMP assay (Figure 2C and 2D). Moreover, we examined the onset of receptor activation, providing a novel method to examine binding kinetics in a functional assay.

Chapter 7 provides an overall conclusion of the novel findings presented in this thesis and new perspectives and opportunities for the research toward GPCRs, including neuropeptide receptors, and kinetic interactions are discussed. Hopefully this thesis will inspire researchers in academia and industry to implement kinetic binding studies to their research programs.

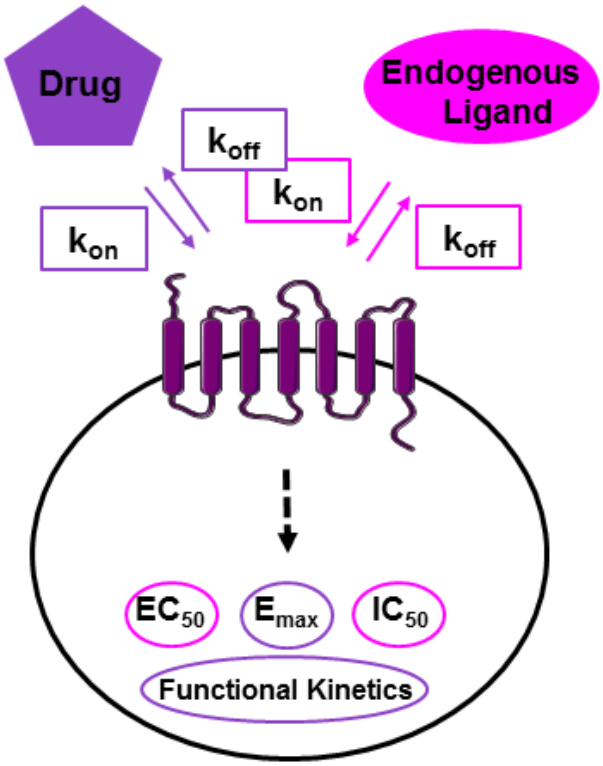

Figure 3: Schematic overview of the contents of this thesis. The main focus of this thesis is on the binding kinetics (k_{on}, k_{off} and RT) of endogenous ligands and competitive drugs targeting the GnRH receptor or the NK1 receptor. Furthermore, the translation of these varying binding kinetics to *in vitro* functional effects, such as E_{max}, are explored.

References

1. Zhang, R. and F. Monsma, *The importance of drug-target residence time.* Current opinion in drug discovery & development, 2009. **12**(4): p. 488-96.
2. Dahl, G. and T. Akerud, *Pharmacokinetics and the drug-target residence time concept.* Drug Discov Today, 2013. **18**(15-16): p. 697-707.
3. Copeland, R.A., D.L. Pompliano, and T.D. Meek, *Drug-target residence time and its implications for lead optimization.* Nature reviews. Drug discovery, 2006. **5**(9): p. 730-9.
4. Vauquelin, G. and I. Van Liefde, *Slow antagonist dissociation and long-lasting in vivo receptor protection.* Trends in pharmacological sciences, 2006. **27**(7): p. 356-9.
5. Tummino, P.J. and R.A. Copeland, *Residence time of receptor-ligand complexes and its effect on biological function.* Biochemistry, 2008. **47**(20): p. 5481-92.
6. Swinney, D.C., et al., *The Role of Binding Kinetics in GPCR Drug Discovery.* Curr Top Med Chem, 2015. **15**(24): p. 2504-22.
7. Bjarnadottir, T.K., et al., *Comprehensive repertoire and phylogenetic analysis of the G protein-coupled receptors in human and mouse.* Genomics, 2006. **88**(3): p. 263-73.
8. Marinissen, M.J. and J.S. Gutkind, *G-protein-coupled receptors and signaling networks: emerging paradigms.* Trends Pharmacol Sci, 2001. **22**(7): p. 368-76.
9. Fredriksson, R., et al., *The G-protein-coupled receptors in the human genome form five main families. Phylogenetic analysis, paralogon groups, and fingerprints.* Mol Pharmacol, 2003. **63**(6): p. 1256-72.
10. Jacoby, E., et al., *The 7 TM G-protein-coupled receptor target family.* ChemMedChem, 2006. **1**(8): p. 761-82.
11. Wang, Y., et al., *NeuroPep: a comprehensive resource of neuropeptides.* Database (Oxford), 2015. **2015**: p. bav038.
12. Hoyer, D. and T. Bartfai, *Neuropeptides and neuropeptide receptors: drug targets, and peptide and non-peptide ligands: a tribute to Prof. Dieter Seebach.* Chem Biodivers, 2012. **9**(11): p. 2367-87.
13. Griebel, G. and F. Holsboer, *Neuropeptide receptor ligands as drugs for psychiatric diseases: the end of the beginning?* Nat Rev Drug Discov, 2012. **11**(6): p. 462-78.
14. Pinter, E., et al., *Neuropeptide receptors as potential drug targets in the treatment of inflammatory conditions.* Br J Clin Pharmacol, 2014. **77**(1): p. 5-20.
15. Clynen, E., et al., *Neuropeptides as targets for the development of anticonvulsant drugs.* Mol Neurobiol, 2014. **50**(2): p. 626-46.
16. McArdle, C.A., *Gonadotropin-releasing hormone receptor signaling: biased and unbiased.* Mini Rev Med Chem, 2012. **12**(9): p. 841-850.
17. Labrie, F., *GnRH agonists and the rapidly increasing use of combined androgen blockade in prostate cancer.* Endocrine-related cancer, 2014: p. 301-317.
18. Garner, C., *Uses of GnRH agonists.* J Obstet Gynecol Neonatal Nurs, 1994. **23**(7): p. 563-70.
19. Al-Inany, H.G., et al., *Gonadotrophin-releasing hormone antagonists for assisted reproductive technology.* Cochrane Database Syst Rev, 2016. **4**: p. CD001750.

20. Rosario, D.J., et al., *The role of gonadotrophin-releasing hormone antagonists in the treatment of patients with advanced hormone-dependent prostate cancer in the UK.* World J Urol, 2016.
21. Prapas, Y., et al., *GnRH antagonist versus long GnRH agonist protocol in poor IVF responders: a randomized clinical trial.* Eur J Obstet Gynecol Reprod Biol, 2012: p. 43-46.
22. Maggi, R., et al., *GnRH and GnRH receptors in the pathophysiology of the human female reproductive system.* Hum Reprod Update, 2015.
23. Lewis, K.A., et al., *A single histrelin implant is effective for 2 years for treatment of central precocious puberty.* The Journal of pediatrics, 2013. **163**(4): p. 1214-6.
24. Leone Roberti Maggiore, U., et al., *Triptorelin for the treatment of endometriosis.* Expert Opin Pharmacother, 2014. **15**(8): p. 1153-79.
25. Garcia-Recio, S. and P. Gascon, *Biological and Pharmacological Aspects of the NK1-Receptor.* Biomed Res Int, 2015. **2015**: p. 495704.
26. Wang, S.Y., et al., *Aprepitant in the prevention of vomiting induced by moderately and highly emetogenic chemotherapy.* Asian Pac J Cancer Prev, 2014. **15**(23): p. 10045-51.
27. Hill, R., *NK1 (substance P) receptor antagonists--why are they not analgesic in humans?* Trends Pharmacol Sci, 2000. **21**(7): p. 244-6.
28. Lindstrom, E., et al., *Neurokinin 1 receptor antagonists: Correlation between in vitro receptor interaction and in vivo efficacy.* Journal of Pharmacology and Experimental Therapeutics, 2007. **322**(3): p. 1286-1293.
29. Navari, R.M., *Profile of netupitant/palonosetron (NEPA) fixed dose combination and its potential in the treatment of chemotherapy-induced nausea and vomiting (CINV).* Drug Des Devel Ther, 2015. **9**: p. 155-61.
30. Rizzi, A., et al., *In vitro and in vivo pharmacological characterization of the novel NK(1) receptor selective antagonist Netupitant.* Peptides, 2012. **37**(1): p. 86-97.
31. Arrowsmith, J., *Trial watch: phase III and submission failures: 2007-2010.* Nat Rev Drug Discov, 2011. **10**(2): p. 87.
32. Arrowsmith, J., *Trial watch: Phase II failures: 2008-2010.* Nat Rev Drug Discov, 2011. **10**(5): p. 328-9.
33. Copeland, R.A., *The drug-target residence time model: a 10-year retrospective.* Nat Rev Drug Discov, 2015.
34. Guo, D., et al., *Drug-target residence time-a case for G protein-coupled receptors.* Medicinal research reviews, 2014. **34**(4): p. 856-92.
35. Carboni, L., et al., *Slow dissociation of partial agonists from the D-2 receptor is linked to reduced prolactin release.* International Journal of Neuropsychopharmacology, 2012. **15**(5): p. 645-656.
36. Tashkin, D.P., *Is a long-acting inhaled bronchodilator the first agent to use in stable chronic obstructive pulmonary disease?* Current opinion in pulmonary medicine, 2005. **11**(2): p. 121-8.
37. Disse, B., et al., *Ba 679 BR, a novel long-acting anticholinergic bronchodilator.* Life Sci, 1993. **52**(5-6): p. 537-44.

38. Woollard, S.M. and G.D. Kanmogne, *Maraviroc: a review of its use in HIV infection and beyond.* Drug Des Devel Ther, 2015. **9**: p. 5447-68.
39. Watson, C., et al., *The CCR5 receptor-based mechanism of action of 873140, a potent allosteric noncompetitive HIV entry inhibitor.* Molecular pharmacology, 2005. **67**(4): p. 1268-82.
40. de Witte, W.E., et al., *Mechanistic models enable the rational use of in vitro drug-target binding kinetics for better drug effects in patients.* Expert Opin Drug Discov, 2016. **11**(1): p. 45-63.
41. Motulsky, H.J. and L.C. Mahan, *The kinetics of competitive radioligand binding predicted by the law of mass action.* Molecular pharmacology, 1984. **25**(1): p. 1-9.
42. Sykes, D.A., M.R. Dowling, and S.J. Charlton, *Exploring the mechanism of agonist efficacy: a relationship between efficacy and agonist dissociation rate at the muscarinic M3 receptor.* Molecular pharmacology, 2009. **76**(3): p. 543-51.
43. Slack, R.J., et al., *Pharmacological characterization of GSK1004723, a novel, long-acting antagonist at histamine H(1) and H(3) receptors.* British journal of pharmacology, 2011. **164**(6): p. 1627-41.
44. McNeely, P.M., et al., *A2AR Binding Kinetics in the Ligand Depletion Regime.* J Biomol Screen, 2016.
45. Guo, D., et al., *Dual-Point Competition Association Assay: A Fast and High-Throughput Kinetic Screening Method for Assessing Ligand-Receptor Binding Kinetics.* J Biomol Screen, 2012.
46. van Veldhoven, J.P., et al., *Affinity and kinetics study of anthranilic acids as HCA2 receptor agonists.* Bioorg Med Chem, 2015. **23**(14): p. 4013-25.
47. Louvel, J., et al., *Structure-kinetics relationships of Capadenoson derivatives as adenosine A1 receptor agonists.* Eur J Med Chem, 2015. **101**: p. 681-91.
48. Pompeu, T.E., et al., *Partial agonism and fast dissociation of LASSBio-579 at dopamine D2 receptor.* Prog Neuropsychopharmacol Biol Psychiatry, 2015. **62**: p. 1-6.
49. Schiele, F., P. Ayaz, and A. Fernandez-Montalvan, *A universal homogeneous assay for high-throughput determination of binding kinetics.* Anal Biochem, 2015. **468**: p. 42-9.
50. Patching, S.G., *Surface plasmon resonance spectroscopy for characterisation of membrane protein-ligand interactions and its potential for drug discovery.* Biochimica et biophysica acta, 2014. **1838**(1 Pt A): p. 43-55.
51. Gronewold, T.M., *Surface acoustic wave sensors in the bioanalytical field: recent trends and challenges.* Analytica chimica acta, 2007. **603**(2): p. 119-28.
52. Rich, R.L. and D.G. Myszka, *Higher-throughput, label-free, real-time molecular interaction analysis.* Analytical biochemistry, 2007. **361**(1): p. 1-6.
53. Gronewold, T.M., et al., *Kinetic binding analysis of aptamers targeting HIV-1 proteins by a combination of a microbalance array and mass spectrometry (MAMS).* Journal of proteome research, 2009. **8**(7): p. 3568-77.

54. Segala, E., et al., *Biosensor-based affinities and binding kinetics of small molecule antagonists to the adenosine A(2A) receptor reconstituted in HDL like particles.* FEBS Lett, 2015. **589**(13): p. 1399-405.
55. Massink, A., et al., *Mass spectrometry-based ligand binding assays on adenosine A1 and A2A receptors.* Purinergic Signal, 2015. **11**(4): p. 581-94.
56. Casarosa, P., et al., *Functional and biochemical rationales for the 24-hour-long duration of action of olodaterol.* The Journal of pharmacology and experimental therapeutics, 2011. **337**(3): p. 600-9.
57. Vauquelin, G., et al., *Insurmountable AT(1) receptor antagonism: the need for different antagonist binding states of the receptor.* Trends in pharmacological sciences, 2001. **22**(7): p. 343-4.
58. Kenakin, T., S. Jenkinson, and C. Watson, *Determining the potency and molecular mechanism of action of insurmountable antagonists.* The Journal of pharmacology and experimental therapeutics, 2006. **319**(2): p. 710-23.

Chapter 2

Kinetic profile of neuropeptide – receptor interactions

Indira Nederpelt

Julia Bunnik

Adriaan P. IJzerman

Laura H. Heitman

Adapted from *Trends in Neurosciences* **2016** *39 (12): 830–839*

Abstract

Currently, drug discovery focusses only on quantifying pharmacological parameters, sometimes including binding kinetics, of drug candidates. For a complete understanding of a drug's desired binding kinetics, the kinetics of both the target and its endogenous ligands should be considered. This is because the release and binding kinetics of endogenous ligands in addition to receptor internalization rates are significant contributors to drug-target interactions.

Here, we discuss the kinetic profile of three neuropeptides and their receptors; gonadotropin-releasing hormone receptor (GnRHR), neuropeptide Y receptors, and corticotropin-releasing factor receptor 1 (CRF_1R). These three examples provide new insights into the importance of kinetic profiles which could improve the understanding of desired drug-target binding kinetics and advance drug discovery for various neurological and psychiatric illnesses.

Background of neuropeptides in drug discovery

Over the past 40 years, many neuropeptides have been identified in the central nervous system (CNS) and the peripheral nervous system (PNS). Neuropeptides are 3-100 amino acid long polypeptides and are synthesized by neurons. Neuropeptides act on either neural substrates, such as neurons and glial cells or on non-neuronal target cells [1]; they mediate neuronal communication by acting on neuropeptide receptors. Neuropeptide receptors include over 44 receptor families, of which most are G protein-coupled receptors (GPCRs). Neuropeptides and their cognate receptors are involved in many physiological and behavioral functions, such as pain regulation, blood pressure, body temperature, feeding behavior, reproduction, sleep, and learning and memory [2]. Therefore, neuropeptide transmission is an attractive area for drug discovery in several therapeutic areas, including inflammatory conditions [3], epilepsy [4] and psychiatric diseases [5]. Release of endogenous neuropeptides is often pulsatile or in bursts in response to stress, resulting in instant high local concentrations which adds complexity to the development of drugs targeting neuropeptide receptors [6].

Optimized ligand-receptor binding kinetics is an emerging concept in drug discovery research

Many drug candidates have failed in clinical trials, over 50% due to a reported lack of efficacy [7]. Several studies suggest that binding kinetics, particularly the lifetime of the ligand-receptor binary complex, may be more relevant for *in vivo* drug efficacy than their typical equilibrium parameters obtained *in vitro,* such as target affinity (K_i) and potency (IC_{50}) [8-10]. This lifetime can be expressed as the drug-target residence time (RT) and is reflected by the dissociation rate constant (k_{off}) of the ligand or drug. The k_{off} value can simply be converted to RT, which is equal to the reciprocal of k_{off} ($RT = 1/k_{off}$).

Currently, several successfully marketed drugs in the GPCR field have been proven in retrospect to have long RT [11]. These drugs illustrate the benefits of optimized binding kinetics in drug discovery represented by lower dosages, increased efficacy and/or safety. For example, the NK1 receptor antagonist aprepitant has superior *in vivo* efficacy in comparison to other NK1 receptor antagonists due to its slow receptor dissociation [11]. As another example, patients with asthma or chronic obstructive pulmonary disease (COPD) can benefit from the slowly dissociating β_2-adrenoreceptor agonist olodaterol [12]. The bronchodilating effects of this drug last up to 24 h. which allows for once-daily administration. However, it is important to note that slow dissociation rates are not always desired. Long RT can also lead to adverse effects and thereby decrease drug safety in the patient [10]. An example of a successful drug with a short residence time is quetiapine, a dopamine D_2

receptor antagonist approved for the treatment of schizophrenia and bipolar disorder. This antipsychotic drug was shown to have fewer (on-target) side effects than other dopamine D_2 receptor antagonists on the market [13]. Altogether, incorporating optimized binding kinetics prospectively could improve the success rate in drug discovery and development and thus of drugs entering the market.

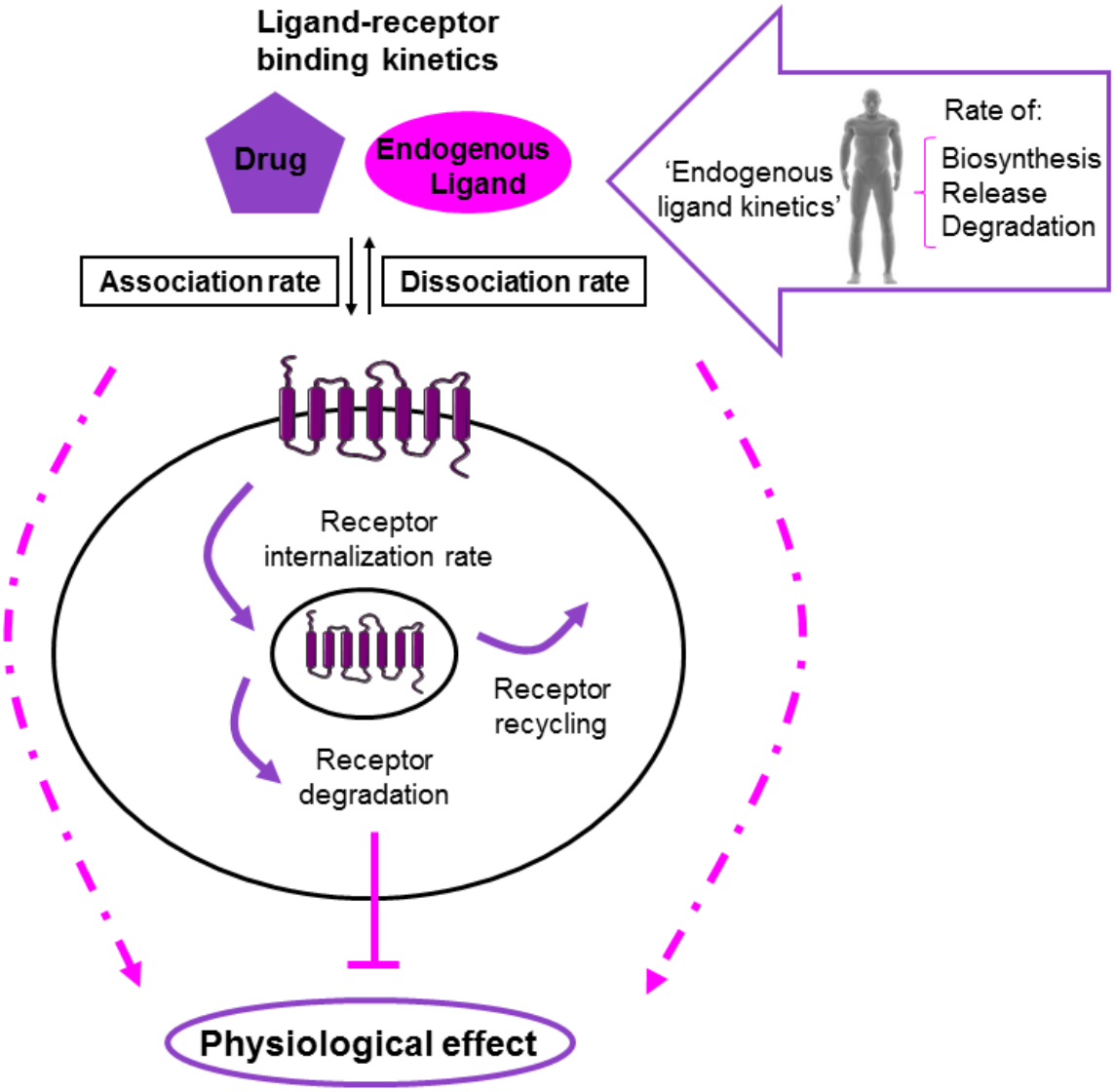

Figure 1. Schematic representation of the structure of this review. Drugs are often competing with endogenous ligands but the kinetic profile of the target receptor and its endogenous ligand(s) are often overlooked. In this review the endogenous ligand release kinetics, endogenous ligand binding kinetics and receptor fate (e.g., internalization kinetics and degradation pathways), i.e. kinetic profiles, of three exemplary and diverse neuropeptide receptor classes and their endogenous ligands will be discussed.

The kinetic profile of a target receptor and its endogenous ligand

The majority of successful drugs achieve their effect by competing with endogenous ligands for the same binding site. Therefore, understanding the pharmacological and physiological behavior of endogenous ligands in the human body is crucial. In contrast to the *in vitro* test tube situation, the human body is an open system. Consequently, the concentration of endogenous ligand, drug and target receptor change over time as these molecules enter and leave the system [10, 14]. Moreover, in order to comprehend desired drug-target kinetics, awareness of the kinetic profile of the target receptor and its endogenous ligand(s) is essential. Firstly, it is imperative to consider the time scale and rate of endogenous ligand release as this can result in temporarily high local concentrations. Secondly, knowledge of the rates of association to and dissociation from the receptor not only of the drug candidate but also of the endogenous ligand should be considered as these parameters can be a limitation to the availability of the unoccupied receptor. Finally, to get a better understanding of the *in vivo* effects of a drug candidate, insight into the rate at which receptors desensitize or internalize under normal and pathophysiological conditions is necessary [15]. Agonist responses are usually regulated by receptor desensitization and internalization and this can limit the effect and duration of receptor signaling [16]. Moreover, receptor complexation with receptor activity-modifying proteins (RAMPs) [17], as well as receptor ubiquitination and other degradation steps are of influence on receptor half-life [18] and although literature on this topic is sparse more knowledge could aid drug discovery [19]. Accordingly, the impact of a long RT drug may be diminished when receptors are rapidly degraded or recycled [15, 20]. Attempts to simultaneously address these aspects in mathematical models that allow such an in vitro/in vivo translation are encouraging. These models can be of great value to analyze experimental data and simulate various cases of drug treatment in a comprehensive and integrative fashion [21].

In brief, to improve drug discovery more insight towards the kinetic characteristics of both drug and the endogenous ligand and its target, i.e. the full kinetic profile, is crucial (Figure 1). We propose a new perspective to drug discovery, where increased attention is paid to 1) release frequency of endogenous ligands (Box 1, Box 2 and Figure 2), 2) binding kinetics of endogenous ligands, and 3) internalization and degradation rates of target receptors. To demonstrate the diversity in kinetic profiles of neuropeptide receptors, we provide a synthesis of the kinetic profiles of three exemplary and diverse neuropeptide receptors and their endogenous ligands, i.e. gonadotropin-releasing hormone receptor (GnRHR), neuropeptide Y receptors, and corticotropin-releasing factor receptor 1 (CRF_1R) (Figure 1).

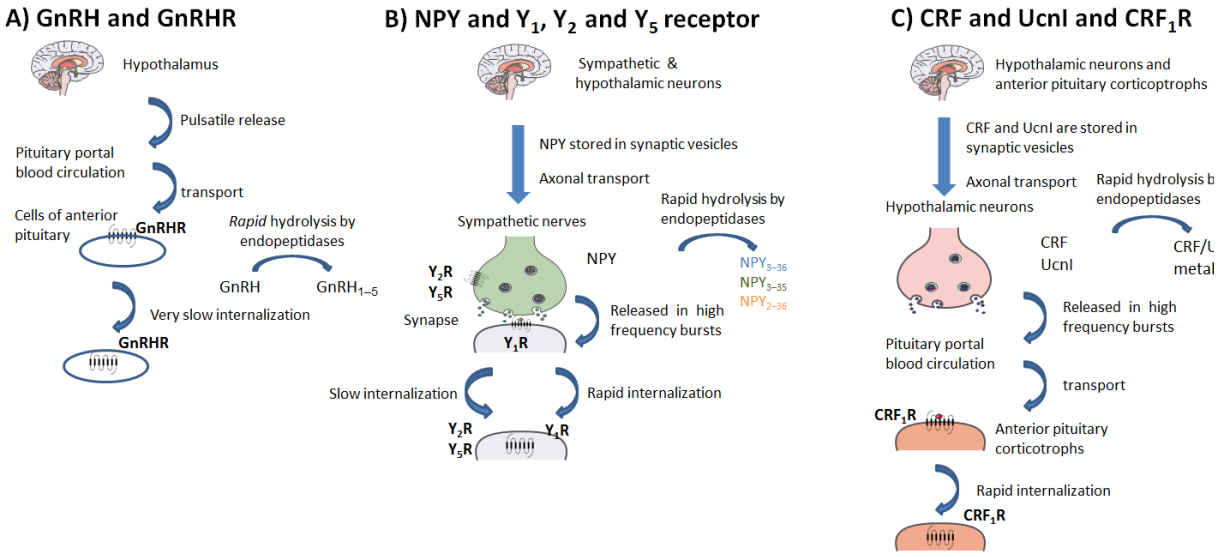

Figure 2. Schematic representation of biosynthesis, release and degradation kinetics ('endogenous ligand kinetics') of endogenous neuropeptides GnRH (A), NPY (B) and CRF (C) in the human body at physiological conditions. This cartoon describes the location of synthesis of the neuropeptide, followed by release, transport, and binding at its cognate receptor. Finally, the endogenous neuropeptide is degraded by endopeptidases. Sources of medical illustrations: Somersault1824 Library of Science & Medical Illustrations [22] and Servier medical art. [23].

Kinetic profile of neuropeptide receptors and their endogenous ligands

GnRH and the GnRHR

Gonadotropin-releasing hormone (GnRH) is a neuropeptide that mediates the central control of the reproductive system and is released by the hypothalamus. GnRH activates GnRH receptors (GnRHRs) in the anterior pituitary and subsequently stimulates secretion of follicle-stimulating hormone (FSH) and luteinizing hormone (LH). GnRH is released in high and low frequency pulses dependent on gender and reproductive cycles (Box 1 and Figure 2) [24], and plasma concentrations range from 0.1-2.0 pg/ml (i.e. 84.5 nM – 1.7 µM) [25]. GnRHR belongs to the class A rhodopsin-like family of GPCRs and GnRHR is predominantly coupled to $G\alpha_{q/11}$ proteins. A unique feature of the GnRHR is that it, unlike all other GPCRs, lacks an intracellular C-terminal tail [26]. GnRHR is successfully targeted to treat hormone-dependent diseases such as prostate cancer [27] with either antagonists or agonists that act as functional antagonist.

In 1979 a study demonstrated that radiolabeled GnRH (i.e., ^{125}I-GnRH) associated rapidly to ovine anterior pituitary homogenates with a k_{on} value of 0.78 nM^{-1} min^{-1}.

Dissociation of the agonist was extremely rapid, with a k_{off} value of 0.18 min^{-1}, translating into a RT of 5.6 min which was calculated from the initial slope of the dissociation curve [28].

More recently [29], two novel competition association assays were developed that allowed for the first time the determination of kinetic receptor binding characteristics of a series of peptide agonists for the human GnRH receptor, including its endogenous ligand GnRH. Firstly, a novel radioligand binding competition association assay was developed in

Box 1: Biosynthesis, release and degradation of endogenous neuropeptides

Neuropeptides are generally synthesized from larger precursors in the neuronal cell body upon stress stimuli [6]. The precursors are stored in vesicles, where they are degraded by convertases into active peptides. Neuropeptides are transported to the release sites at neurons and released by exocytosis, where they bind their cognate receptor [30]. The kinetics of neuropeptide synthesis, release and degradation is presented in Figure 2.

Gonadotropin-releasing hormone

- GnRH is synthesized in the hypothalamus from a precursor polypeptide by enzymatic processing [31-33].
- GnRH is released in pulses from the hypothalamus. GnRH secretion is regulated both by the feedback actions of gonadal steroids and neural input from higher cognitive and sensory centers [33]. The pattern of pulsatile GnRH secretion ranges from minutes to hours and varies between sexes, during reproductive life and during the menstrual cycle in females [24] and ranges in frequency between 30 min and 3-4 hours [34].
- GnRH is rapidly hydrolyzed (half-life 2-4 min) into GnRH 1-5 by thimet oligopeptidase (EC 3.4.24.15) both in the hypothalamus and the anterior pituitary [35-37].

Neuropeptide Y

- NPY is synthesized in the hypothalamus and in the peripheral nervous system by sympathetic neurons [38]
- NPY is released in high frequency bursts (every 5 min) from sympathetic nerve terminals, upon stress stimuli or pathological conditions [39, 40].
- NPY is rapidly hydrolysed (half-life approximately 12 min) by peptidases, including dipeptidyl peptidase IV (EC 3.4.14.5)) and aminopeptidase P (EC 3.4.11.9) [41, 42].

Corticotropin-releasing factor and Urocortin I

- CRF and UcnI are synthesized and released by the paraventricular nucleus of the hypothalamus [43].
- The axons of hypothalamic neurons release CRF and UcnI (approximately every 5 min) into the hypophyseal portal blood in reaction to stress [6].
- CRF and UcnI are rapidly hydrolyzed (half-life 12-73 min) by endothelin-converting enzyme 1 (ECE1, EC 3.4.24.71) in the brain [44, 45].

which GnRH had k_{on}, k_{off} and RT values of 0.06 ± 0.01 nM^{-1} min^{-1}, 0.2 ± 0.02 min^{-1}, and 6.3 ± 0.6 min at room temperature, respectively (Table 1).

Secondly, a homogenous time-resolved fluorescence (TR-FRET) Tag-lite™ method was developed as an alternative assay for the same purpose. These TR-FRET experiments provided similar k_{on}, k_{off} and RT values for GnRH of 0.02 ± 0.01 $nM^{-1}min^{-1}$, 0.44 ± 0.3 min^{-1}, and 2.3 ± 1.6 min at room temperature, respectively [29] (Table 1).

Table 1. Qualitative overview of the kinetic profile, i.e. the release kinetics of the endogenous ligand(s), binding kinetics and receptor internalization rates, of the GnRH receptor, NPY receptors and CRF1 receptor (see also Box 1).

Neuropeptide system			Fast*	Medium*	Slow*
GnRH	Release kinetics**	GnRH	**X**		**X**
	Binding kinetics	GnRH-GnRHR	**X**		
	Internalization kinetics	GnRHR			**X**
NPY	Release kinetics***	NPY	**X**		
	Binding kinetics	NPY-Y_1R	**k_{on}**	**k_{off}**	
		NPY-Y_2R	**k_{on}**		**k_{off}**
		NPY-Y_5R	**k_{on}**	**k_{off}**	
	Internalization kinetics	Y_1R	**X**		
		Y_2R			**X**
		Y_5R			**X**
CRF	Release kinetics***	CRF	**X**		
		UCNI	**X**		**X**
	Binding kinetics	CRF-CRF_1R	**k_{on}**		**k_{off}**
		UCNI-CRF_1R		**X**	
	Internalization kinetics	CRF_1R	**males**		**females**

* Fast, medium and slow kinetics are an arbitrary categorization in proportion to the target system, exact rates can be found in the corresponding paragraph.

** GnRH release is pulsatile ranging from minutes to hours and depends on gender, age and menstrual cycle, see also Box 1.

*** NPY, CRF and UCNI are released in high frequency bursts in response to stress or pathological conditions, see also Box 1.

The lack of an intracellular C-terminal tail on the GnRH receptor results in the absence of rapid arrestin-mediated desensitization and in very slow internalization rates [26, 46]. Madziva *et al.* showed less than 50% internalization after 60 min stimulation with a GnRH analogue [47]. Additionally, Pawson *et al.* showed that mammalian GnRHRs (human

and rat) undergo slow, constitutive (i.e. agonist-independent) internalization [46]. The importance of a C-terminal tail for receptor internalization was shown by two studies; firstly, the catfish GnRH receptor that does possess an intracellular C-terminal tail displayed rapid desensitization and internalization. It was shown that approximately 50% of the catfish GnRH receptors were internalized after 15 min stimulation with chicken II GnRH (endocytosis rate constant = 0.099 min^{-1}) [48]. Secondly, addition of a functional intracellular C-terminal tail of the thyrotropin-releasing hormone receptor (TRHR) to the rat GnRHR produced rapid desensitization and increased receptor internalization rates [48].

In brief, drugs targeting the GnRHR are competing with fast association and dissociation kinetics of endogenous GnRH that is released in pulses ranging from minutes to hours reaching plasma concentrations up to 1.7 µM. In particular, high frequency GnRH bursts should be considered when designing drugs competing with GnRH. In addition, the GnRHR internalizes slowly and is thus not a limiting factor for drugs to be effective. We hypothesize that (functional) antagonists targeting the GnRH receptor should have a long residence time to overcome the high frequency pulses and fast association kinetics of the endogenous ligand. This is particularly beneficial when chronic treatment is desired, e.g. for treatment of prostate cancer or endometriosis.

Box 2: Alternative mechanisms involved in regulating ligand concentrations

Neuropeptides are generally degraded by peptidases, and reuptake systems or binding proteins are often not involved in regulating free ligand concentrations. However, a few exceptions have been reported where alternative mechanisms are proposed to regulate high neuropeptide concentrations.

For instance, a binding protein has been discovered, called the CRF binding protein (CRF-BP), that binds CRF, Ucn1 and their associated peptides with high affinity [49]. This protein is broadly distributed throughout the brain and its predominant role is to bind and clear CRF from the blood. CRF-BP is also expressed in the liver and placenta where it is believed to modulate CRF levels and protect the body from increased plasma CRF levels, particularly during late stages of pregnancy [50].

Another exception is reported for cholecystokinin octapeptide (CCK8). The degradation of CCK8 by peptidases is much slower in comparison to other neuropeptides and therefore an alternative control mechanism was hypothesized. A highly selective uptake mechanism was reported that together with peptidases enables termination of CCK8 activity [51].

Taken together, ligand-binding proteins and reuptake systems, although rare, can play a role in regulating free neuropeptide concentrations and should therefore be considered regarding endogenous neuropeptide concentrations.

Neuropeptide Y and Neuropeptide Y receptors

Neuropeptide Y (NPY) is a 36 amino acid neuropeptide hormone that acts as a neurotransmitter in the central nervous system (CNS). NPY is the principal endogenous agonist at neuropeptide Y type 1 (Y_1), type 2 (Y_2) and type 5 (Y_5) receptors. NPY is released in high frequency bursts upon stress stimuli (Box 1 and Figure 2) [39] and plasma concentrations are reported to be around 10 µM [52]. NPY receptors belong to class A GPCRs and are coupled to G_i or G_o proteins [53]. NPY receptors and their endogenous ligands are involved in the control of appetite, inhibition of anxiety in the CNS, presynaptic inhibition of neurotransmitter release in the CNS and periphery, the modulation of circadian rhythm and pain transmission [54]. NPY receptors are mainly targeted to treat stress-related disorders but also in pain treatment, cancer and epilepsy [2].

The kinetic binding profile of endogenous neuropeptide Y ligands to human Y_1, Y_2, and mouse Y_5 receptors was extensively studied by Dautzenberg *et al.* At 22°C, ^{125}I-NPY displays rapid association to hY_1, hY_2 and mY_5 receptors (Table 1). Dissociation of ^{125}I-NPY from the mY_5 receptor and hY_1 receptor provided residence times between 50 and 80 min. In contrast, minimal dissociation (approximately 20%) of ^{125}I-NPY from both recombinant and endogenous Y_2 receptor was observed after 24 h incubation. These findings indicate a pseudo-irreversible binding mode of NPY to the hY_2 receptor [55], which adds complexity to drug development targeting the hY_2 receptor.

Receptor internalization rates, as well as subsequent degradation or resensitization differ substantially between the different NPY receptor subtypes. Upon human NPY exposure, the Y_1 receptor is rapidly internalized via clathrin-dependent endocytosis [56-58]. In addition, resensitization studies demonstrated that the Y_1 receptor is rapidly recycled back to the cell membrane [56, 58, 59]. In contrast, Y_2 receptors neither internalize nor desensitize [56], or only to a small extent with extremely slow internalization rates after prolonged agonist exposure [57, 60]. Internalization of Y_5 receptors has not been extensively studied yet. However, it was reported that this receptor internalizes to a much slower extent than Y_1 [60-62].

In conclusion, target kinetics for the NPY receptor subtypes vary greatly and NPY is released in high frequency bursts upon stress stimuli with plasma concentrations around 10 µM. Rapid association and dissociation kinetics as well as internalization rates were observed for the NPY-hY_1 receptor complex. In contrast, while the binding kinetics of NPY to the hY_2 receptor are similar to the hY1 receptor, internalization of hY2 is extremely slow. hY5 internalization has also been reported to be slow, with fast association and slow dissociation rates of NPY. Therefore, we postulate that drugs with fast binding kinetics are desirable when targeting the hY_1 receptor, while fast association and slow dissociation kinetics are beneficial for hY_2 and hY_5 receptors. Slowly dissociating agonists are particularly interesting

for cancer treatment as they might accelerate receptor internalization [63] while a slowly dissociating antagonist could be beneficial for the treatment of obesity [64].

CRF, UcnI and the CRF_1R

Corticotropin releasing factor (CRF) and urocortin 1 (UcnI) are hormones that are the primary CNS neuromodulators of the hypothalamic-pituitary-adrenal axis. CRF and UcnI regulate adrenocorticotropic hormone (ACTH) secretion by the pituitary and are critical neurotransmitters in the neuroendocrine and behavioral response to stress [67]. CRF and UcnI are released in high frequency bursts in response to stress (Box 1 and Figure 2) [6]. UcnI is mainly expressed in cell bodies of the Edinger Westphal nucleus in the brain while CRF is more widely expressed in the CNS [68]. Plasma concentrations of UcnI are reported to reach up to 5 µM, while maximal CRF concentrations are much lower (around 2 pM). During stress and/or pathological conditions levels of both endogenous ligands increase, which is most noticeable for CRF of which levels can go up to 0.5 mM [69-71]. CRF and UcnI exert their effect by activation of two CRF receptor subtypes, CRF_1 and CRF_2 receptors. These receptors both belong to the secretin-like class B subfamily of GPCRs and are primarily coupled to G_s proteins. Several studies have indicated the involvement of the CRF system in human stress disorders, such as anxiety, depression and addiction [72].

Box 3: Examples of drugs targeting neuropeptide GPCRs with optimized binding kinetics.

As this was all studied in retrospect, these examples demonstrate the need for a better understanding of the kinetic profile of the target receptor and its endogenous ligands, in addition to the drug candidate.

Candesartan is a marketed angiotensin II subtype-1 (AT_1) receptor antagonists for the treatment of hypertension. It has a residence time of 173 min (37°C) [11].

Aprepitant and **netupitant** are marketed NK_1R antagonists to treat chemotherapy-induced emesis. Aprepitant has a residence time of 154 min (22°C) [11] and netupitant has been reported as an insurmountable antagonist with antagonistic effects lasting over 5 hours [65].

Suvorexant is a dual orexin receptor antagonist to treat insomnia. It has a residence time of 83 min for the orexin type 2 (OX_2) receptor (room temperature) [66].

Buserelin is a GnRH peptide agonist used to treat hormone dependent diseases. It has a reported residence time of 111 min at 25 °C [29].

Ligand binding kinetics studies of CRF and UcnI to the CRF_1 receptor are limited (Table 1). In an early study De Souza *et al.*, studied the binding of ^{125}I-[Tyr^0] CRF (^{125}I-rCRF) to rat olfactory membranes at different temperatures [73]. This study demonstrated temperature-dependent ^{125}I-rCRF association to rat CRF_1 receptors with a k_{on} value of 0.52 nM^{-1} min^{-1} at 23°C. At this temperature, dissociation was reversible and monophasic, with a k_{off} value of 0.007 min^{-1} and

RT of 143 min while association and dissociation were more rapid at physiological temperature [73]. In contrast, [^{3}H]-UcnI association to the human CRF_1 receptor was slow and monophasic with a k_{on} value of 0.06 ± 0.024 nM^{-1} min^{-1} while dissociation was faster in comparison to CRF with a reported k_{off} value of 0.017 ± 0.007 min^{-1} and RT of 58 min at room temperature [74].

CRF_1 receptors undergo rapid desensitization and internalization during continuous exposure to CRF or UcnI [75]. Although UcnI- and CRF-induced CRF_1 receptor internalization occurred to a similar degree, the receptor was shown to recycle and resensitize more efficiently after CRF stimulation [44]. Moreover, there is evidence of sex differences in CRF_1 receptor signaling and trafficking [76]. In male rats, a swim stress paradigm promoted CRF_1 receptor β-arrestin2 association, and internalization in LC neurons. However, in female rats stress-induced CRF_1 receptor-β-arrestin 2 association remained low, and stress-induced CRF_1 receptor internalization was impaired [76]. Valentino *et al.* suggested that sex biases in both CRF_1 receptor coupling to G proteins, and CRF_1-β-arrestin 2 association makes females more sensitive to acute stress and less able to adapt to chronic stress [77].

To summarize, although ligand binding kinetics studies on the CRF_1 receptor are limited, it is likely that drugs targeting the CRF_1 receptor are competing with fast binding kinetics of CRF but slower binding kinetics of UcnI. Additionally, CRF_1 receptor desensitization and internalization is fast in males but slow in females. These gender-specific internalization kinetics should be taken into account in the design of novel agonistic drugs targeting the CRF_1 receptor when treating e.g. depression. Antagonists targeting the CRF1 receptor to treat e.g. addiction should have fast association and slow dissociation rates to overcome the slow dissociation kinetics of CRF and high plasma concentrations of both CRF and UCNI during stress. Considering that stress-related disorders often need chronic treatment, patients could benefit from slowly dissociating drugs.

Concluding remarks

Drug-target association and dissociation rates play an important role in achieving safe and efficacious drug action *in vivo*. For example, numerous drugs have been proven in retrospect to be highly efficacious due to their slow dissociation rates (Box 3). Currently, drug discovery efforts are moving towards incorporating optimized binding kinetics prospectively. As many successful drugs on the market achieve their effects by competing with endogenous ligands, a better understanding of the pharmacological and physiological behavior of endogenous ligands and their receptors in the human body is crucial. This is particularly important for neuropeptides, since their release is generally pulsatile or in bursts consequent to stress stimuli, ultimately resulting in instant high local concentrations.

Moreover, to understand desired binding kinetics for the target of interest, insights into receptor internalization kinetics are beneficial, as this arguably terminates a drug's effect.

In this review we have presented evidence of varying ligand binding kinetics for the endogenous ligands of three exemplary neuropeptide receptors. In addition to the observed variability in ligand binding kinetics across these three exemplars, receptor internalization kinetics were also largely different for all three discussed neuropeptide receptors. Thus, collectively, this small case overview demonstrates a broad array of kinetic profiles for neuropeptide receptors, i.e. endogenous ligand release rates, binding kinetics and receptor internalization rates. Presently, drug discovery focusses mainly on characterizing drug candidates only, while the kinetic profile of the target receptor and its endogenous ligand(s) are most often neglected. Therefore, we believe it is a great opportunity for future drug research to include the kinetic profile of the target receptor and its endogenous ligand(s) to the drug discovery paradigm. Knowledge of these complete kinetic profiles could improve our understanding of desired binding kinetics and in turn lead to less attrition in (pre-) clinical phases of drug development and to more efficacious drugs.

References

1. Wang, Y., et al., *NeuroPep: a comprehensive resource of neuropeptides.* Database (Oxford), 2015. **2015**: p. bav038.
2. Hoyer, D. and T. Bartfai, *Neuropeptides and neuropeptide receptors: drug targets, and peptide and non-peptide ligands: a tribute to Prof. Dieter Seebach.* Chem Biodivers, 2012. **9**(11): p. 2367-87.
3. Pinter, E., et al., *Neuropeptide receptors as potential drug targets in the treatment of inflammatory conditions.* Br J Clin Pharmacol, 2014. **77**(1): p. 5-20.
4. Clynen, E., et al., *Neuropeptides as targets for the development of anticonvulsant drugs.* Mol Neurobiol, 2014. **50**(2): p. 626-46.
5. Griebel, G. and F. Holsboer, *Neuropeptide receptor ligands as drugs for psychiatric diseases: the end of the beginning?* Nat Rev Drug Discov, 2012. **11**(6): p. 462-78.
6. Kormos, V. and B. Gaszner, *Role of neuropeptides in anxiety, stress, and depression: from animals to humans.* Neuropeptides, 2013. **47**(6): p. 401-19.
7. Arrowsmith, J. and P. Miller, *Trial watch: phase II and phase III attrition rates 2011-2012.* Nat Rev Drug Discov, 2013. **12**(8): p. 569.
8. Swinney, D.C., et al., *The Role of Binding Kinetics in GPCR Drug Discovery.* Curr Top Med Chem, 2015. **15**(24): p. 2504-22.
9. Dahl, G. and T. Akerud, *Pharmacokinetics and the drug-target residence time concept.* Drug Discov Today, 2013. **18**(15-16): p. 697-707.
10. Copeland, R.A., *The drug-target residence time model: a 10-year retrospective.* Nat Rev Drug Discov, 2016. **15**(2): p. 87-95.
11. Guo, D., et al., *Drug-Target Residence Time—A Case for G Protein-Coupled Receptors.* Medicinal Research Reviews, 2014. **34**(4): p. 856-892.
12. Cazzola, M., et al., *Assessing the clinical value of fast onset and sustained duration of action of long-acting bronchodilators for COPD.* Pulm Pharmacol Ther, 2015. **31**: p. 68-78.
13. Carboni, L., et al., *Slow dissociation of partial agonists from the D-2 receptor is linked to reduced prolactin release.* International Journal of Neuropsychopharmacology, 2012. **15**(5): p. 645-656.
14. Vauquelin, G., *Impact of target binding kinetics on in vivo drug efficacy: k , k and rebinding.* Br J Pharmacol, 2016.
15. Vauquelin, G. and I. Van Liefde, *Slow antagonist dissociation and long-lasting in vivo receptor protection.* Trends Pharmacol Sci, 2006. **27**(7): p. 356-9.
16. Hothersall, J.D., et al., *Can residence time offer a useful strategy to target agonist drugs for sustained GPCR responses?* Drug Discovery Today, 2015.
17. Hay, D.L. and A.A. Pioszak, *Receptor Activity-Modifying Proteins (RAMPs): New Insights and Roles.* Annu Rev Pharmacol Toxicol, 2016. **56**: p. 469-87.
18. Alonso, V. and P.A. Friedman, *Minireview: ubiquitination-regulated G protein-coupled receptor signaling and trafficking.* Mol Endocrinol, 2013. **27**(4): p. 558-72.

19. Guo, D., L.H. Heitman, and I.J. AP, *The Role of Target Binding Kinetics in Drug Discovery.* ChemMedChem, 2015. **10**(11): p. 1793-6.
20. Guo, D., L.H. Heitman, and I.J. AP, *Kinetic Aspects of the Interaction between Ligand and G Protein-Coupled Receptor: The Case of the Adenosine Receptors.* Chem Rev, 2016.
21. de Witte, W.E., et al., *Mechanistic models enable the rational use of in vitro drug-target binding kinetics for better drug effects in patients.* Expert Opin Drug Discov, 2016. **11**(1): p. 45-63.
22. Lahortiga, I. and L. Cox, *Library of Science and Medical Illustrations. Scientific illustration for the research scientist*. 2015: somersault18:24
23. *Servier medical art. Powerpoint image bank 2015*. Available from: http://www.servier.com/.
24. Maggi, R., et al., *GnRH and GnRH receptors in the pathophysiology of the human female reproductive system.* Hum Reprod Update, 2015.
25. Araki, S., et al., *Reevaluation of immunoreactive gonadotropin-releasing hormone (GnRH) levels in general circulation in women: changes in levels and episodic patterns before, during and after gonadotropin surges.* Endocrinol Jpn, 1986. **33**(4): p. 457-68.
26. Finch, A.R., et al., *Trafficking and signalling of gonadotrophin-releasing hormone receptors: an automated imaging approach.* Br J Pharmacol, 2010. **159**(4): p. 751-60.
27. Labrie, F., *GnRH agonists and the rapidly increasing use of combined androgen blockade in prostate cancer.* Endocrine-related cancer, 2014: p. 301-317.
28. Wagner, T.O., T.E. Adams, and T.M. Nett, *GNRH interaction with anterior pituitary. I. Determination of the affinity and number of receptors for GNRH in ovine anterior pituitary.* Biol Reprod, 1979. **20**(2): p. 140-9.
29. Nederpelt, I., et al., *Characterization of 12 GnRH peptide agonists - a kinetic perspective.* Br J Pharmacol, 2016. **173**(1): p. 128-41.
30. Bergquist, F. and M. Ludwig, *Neuropeptide release*, in *Intercellular Communication in the Nervous System*, R. Malenka, Editor. 2009, Academic Press.
31. Anthony, E.L., J.C. King, and E.G. Stopa, *Immunocytochemical localization of LHRH in the median eminence, infundibular stalk, and neurohypophysis. Evidence for multiple sites of releasing hormone secretion in humans and other mammals.* Cell Tissue Res, 1984. **236**(1): p. 5-14.
32. Stopa, E.G., et al., *Computer-assisted mapping of immunoreactive mammalian gonadotropin-releasing hormone in adult human basal forebrain and amygdala.* Endocrinology, 1991. **128**(6): p. 3199-207.
33. Arnold, A.P., et al., *Hormones, brain and behavior*. Vol. 5. 2002, San Diago, California, USA: Academic Press, Elsevier Science.
34. Marshall, J.C. and M.L. Griffin, *The role of changing pulse frequency in the regulation of ovulation.* Hum Reprod, 1993. **8 Suppl 2**: p. 57-61.

35. Herman, A., et al., *Gonadoliberin (GnRH) and its copper complex (Cu-GnRH) enzymatic degradation in hypothalamic and pituitary tissue in vitro.* J Physiol Pharmacol, 2012. **63**(1): p. 69-75.
36. Larco, D.O., et al., *The Novel Actions of the Metabolite GnRH-(1-5) are Mediated by a G Protein-Coupled Receptor.* Front Endocrinol (Lausanne), 2013. **4**: p. 83.
37. Kumar, P. and A. Sharma, *Gonadotropin-releasing hormone analogs: Understanding advantages and limitations.* J Hum Reprod Sci, 2014. **7**(3): p. 170-4.
38. Adrian, T.E., et al., *Neuropeptide Y distribution in human brain.* Nature, 1983. **306**(5943): p. 584-6.
39. Heilig, M., *The NPY system in stress, anxiety and depression.* Neuropeptides, 2004. **38**(4): p. 213-24.
40. Woller, M.J. and E. Terasawa, *Changes in pulsatile release of neuropeptide-Y and luteinizing hormone (LH)-releasing hormone during the progesterone-induced LH surge in rhesus monkeys.* Endocrinology, 1994. **135**(4): p. 1679-86.
41. Abid, K., et al., *Kinetic study of neuropeptide Y (NPY) proteolysis in blood and identification of NPY3-35: a new peptide generated by plasma kallikrein.* J Biol Chem, 2009. **284**(37): p. 24715-24.
42. Grouzmann, E., et al., *Disappearance rate of catecholamines, total metanephrines, and neuropeptide Y from the plasma of patients after resection of pheochromocytoma.* Clin Chem, 2001. **47**(6): p. 1075-82.
43. Swanson, L.W., et al., *Organization of ovine corticotropin-releasing factor immunoreactive cells and fibers in the rat brain: an immunohistochemical study.* Neuroendocrinology, 1983. **36**(3): p. 165-86.
44. Hasdemir, B., et al., *Endothelin-converting enzyme-1 actions determine differential trafficking and signaling of corticotropin-releasing factor receptor 1 at high agonist concentrations.* Mol Endocrinol, 2012. **26**(4): p. 681-95.
45. Schulte, H.M., et al., *Corticotropin-releasing factor: pharmacokinetics in man.* J Clin Endocrinol Metab, 1984. **58**(1): p. 192-6.
46. Pawson, A.J., et al., *Mammalian type I gonadotropin-releasing hormone receptors undergo slow, constitutive, agonist-independent internalization.* Endocrinology, 2008. **149**(3): p. 1415-22.
47. Madziva, M.T., et al., *The carboxy-terminal tail or the intracellular loop 3 is required for beta-arrestin-dependent internalization of a mammalian type II GnRH receptor.* Mol Cell Endocrinol, 2015. **411**: p. 187-97.
48. Heding, A., et al., *Gonadotropin-releasing hormone receptors with intracellular carboxyl-terminal tails undergo acute desensitization of total inositol phosphate production and exhibit accelerated internalization kinetics.* J Biol Chem, 1998. **273**(19): p. 11472-7.
49. Behan, D.P., E.A. Linton, and P.J. Lowry, *The Human-Plasma Crf-Binding Protein - Its Isolation Using Affinity-Chromatography.* Journal of Physiology-London, 1988. **399**: p. P90-P90.

50. Ardati, A., et al., *Pharmacological characterisation of the recombinant human CRF binding protein using a simple assay.* Journal of Neuroscience Methods, 1998. **80**(1): p. 99-105.
51. Migaud, M., B.P. Roques, and C. Durieux, *Evidence for a high-affinity uptake system for cholecystokinin octapeptide (CCK8) in rat cortical synaptosomes.* Eur J Neurosci, 1995. **7**(5): p. 1074-9.
52. Nam, S.Y., et al., *Cerebrospinal fluid and plasma concentrations of leptin, NPY, and alpha-MSH in obese women and their relationship to negative energy balance.* J Clin Endocrinol Metab, 2001. **86**(10): p. 4849-53.
53. Michel, M.C., et al., *XVI. International Union of Pharmacology recommendations for the nomenclature of neuropeptide Y, peptide YY, and pancreatic polypeptide receptors.* Pharmacol Rev, 1998. **50**(1): p. 143-50.
54. Babilon, S., K. Morl, and A.G. Beck-Sickinger, *Towards improved receptor targeting: anterograde transport, internalization and postendocytic trafficking of neuropeptide Y receptors.* Biol Chem, 2013. **394**(8): p. 921-36.
55. Dautzenberg, F.M. and S. Neysari, *Irreversible binding kinetics of neuropeptide Y ligands to Y2 but not to Y1 and Y5 receptors.* Pharmacology, 2005. **75**(1): p. 21-9.
56. Gicquiaux, H., et al., *Rapid internalization and recycling of the human neuropeptide Y Y(1) receptor.* J Biol Chem, 2002. **277**(8): p. 6645-55.
57. Ouedraogo, M., et al., *Distinct motifs of neuropeptide Y receptors differentially regulate trafficking and desensitization.* Traffic, 2008. **9**(3): p. 305-24.
58. Pheng, L.H., et al., *Agonist- and antagonist-induced sequestration/internalization of neuropeptide Y Y1 receptors in HEK293 cells.* Br J Pharmacol, 2003. **139**(4): p. 695-704.
59. Parker, S.L., et al., *Cloned neuropeptide Y (NPY) Y1 and pancreatic polypeptide Y4 receptors expressed in Chinese hamster ovary cells show considerable agonist-driven internalization, in contrast to the NPY Y2 receptor.* Eur J Biochem, 2001. **268**(4): p. 877-86.
60. Walther, C., K. Morl, and A.G. Beck-Sickinger, *Neuropeptide Y receptors: ligand binding and trafficking suggest novel approaches in drug development.* J Pept Sci, 2011. **17**(4): p. 233-46.
61. Bohme, I., et al., *Agonist induced receptor internalization of neuropeptide Y receptor subtypes depends on third intracellular loop and C-terminus.* Cell Signal, 2008. **20**(10): p. 1740-9.
62. Parker, S.L., et al., *Ligand internalization by cloned neuropeptide Y Y5 receptors excludes Y2 and Y4 receptor-selective peptides.* Eur J Pharmacol, 2003. **474**(1): p. 31-42.
63. Li, J., Y. Tian, and A. Wu, *Neuropeptide Y receptors: a promising target for cancer imaging and therapy.* Regen Biomater, 2015. **2**(3): p. 215-9.
64. Hallberg, M., *Neuropeptides: metabolism to bioactive fragments and the pharmacology of their receptors.* Med Res Rev, 2015. **35**(3): p. 464-519.
65. Rizzi, A., et al., *In vitro and in vivo pharmacological characterization of the novel NK(1) receptor selective antagonist Netupitant.* Peptides, 2012. **37**(1): p. 86-97.
66. Mould, R., et al., *Binding kinetics differentiates functional antagonism of orexin-2 receptor ligands.* Br J Pharmacol, 2014. **171**(2): p. 351-63.

67. Dautzenberg, F.M., et al., *Corticotropin-releasing factor receptors: CRF1 receptor.* IUPHAR/BPS Guide to PHARMACOLOGY, 2015.
68. Bale, T.L. and W.W. Vale, *CRF and CRF receptors: role in stress responsivity and other behaviors.* Annu Rev Pharmacol Toxicol, 2004. **44**: p. 525-57.
69. Florio, P., et al., *Plasma urocortin levels in the diagnosis of ovarian endometriosis.* Obstet Gynecol, 2007. **110**(3): p. 594-600.
70. Catalan, R., et al., *Plasma corticotropin-releasing factor in depressive disorders.* Biol Psychiatry, 1998. **44**(1): p. 15-20.
71. Goland, R.S., et al., *Plasma corticotropin-releasing factor concentrations in the baboon during pregnancy.* Endocrinology, 1992. **131**(4): p. 1782-6.
72. Bortolato, A., et al., *Structure of Class B GPCRs: new horizons for drug discovery.* Br J Pharmacol, 2014. **171**(13): p. 3132-45.
73. De Souza, E.B., *Corticotropin-releasing factor receptors in the rat central nervous system: characterization and regional distribution.* J Neurosci, 1987. **7**(1): p. 88-100.
74. Gottowik, J., et al., *Labelling of CRF1 and CRF2 receptors using the novel radioligand, [3H]-urocortin.* Neuropharmacology, 1997. **36**(10): p. 1439-46.
75. Dautzenberg, F.M. and R.L. Hauger, *The CRF peptide family and their receptors: yet more partners discovered.* Trends Pharmacol Sci, 2002. **23**(2): p. 71-7.
76. Bangasser, D.A., et al., *Sex differences in corticotropin-releasing factor receptor signaling and trafficking: potential role in female vulnerability to stress-related psychopathology.* Mol Psychiatry, 2010. **15**(9): p. 877, 896-904.
77. Valentino, R.J., E. Van Bockstaele, and D. Bangasser, *Sex-specific cell signaling: the corticotropin-releasing factor receptor model.* Trends Pharmacol Sci, 2013. **34**(8): p. 437-44.

Chapter 3

Characterization of 12 GnRH peptide agonists – a kinetic perspective

Indira Nederpelt

Victoria Schuldt

Felix Schiele

Katrin Nowak-Reppel

Amaury E. Fernández-Montalván

Adriaan P. IJzerman

Laura H. Heitman

Adapted from *British Journal of Pharmacology* **2016** *173 (1): 128-41*

Abstract

Drug-target residence time is an important, yet often overlooked, parameter in drug discovery. Multiple studies have proposed an increased residence time to be beneficial for improved drug efficacy and/or longer duration of action.

Currently there are many drugs on the market targeting the gonadotropin-releasing hormone (GnRH) receptor for the treatment of hormone-dependent diseases. Surprisingly, the kinetic receptor binding parameters of these analogues have not yet been reported. Therefore, this project focused on determining the receptor binding kinetics of twelve GnRH peptide agonists, including many marketed drugs.

We successfully developed and optimized a novel radioligand binding competition association assay for the human GnRH receptor with the use of a radiolabeled peptide agonist, ^{125}I-triptorelin. In addition to radioligand binding studies, a homogenous time-resolved fluorescence (TR-FRET) Tag-lite™ method was developed as an alternative assay for the same purpose. Both assays were applied to determine the kinetic receptor binding characteristics of twelve high affinity GnRH peptide agonists. Results obtained from both methods were highly correlated. Interestingly, the binding kinetics of the peptide agonists were more divergent than their affinities with residence times ranging from 5.6 min (goserelin) to 125 min (deslorelin).

Our research provides new insights by incorporating kinetic, next to equilibrium, binding parameters in current research and development that can potentially improve future drug discovery targeting the GnRH receptor.

Introduction

Drug target residence time is emerging as an important parameter in the drug discovery process. Multiple studies provide evidence that the binding kinetics of drug target interactions rather than the typical equilibrium binding parameters are important for *in vivo* efficacy [1-4]. Several marketed drugs in the field of G protein-coupled receptors (GPCRs) have *retrospectively* been shown to display slow receptor dissociation rates, or, in other words, long receptor residence times [5]. For instance, the histamine H_1 receptor antagonist desloratidine was found to have a long residence time, which could explain its high potency and 24 hours duration of action observed in clinical studies [6]. Another example is the insurmountable antagonist for the angiotensin II subtype-1 (AT_1) receptor, telmisartan. The authors deemed the insurmountability and therefore improved efficacy of telmisartan to be partly due to its very slow dissociation from AT_1 receptors [7].

The hypothalamic neuropeptide gonadotropin-releasing hormone (GnRH) is a central mediator of reproductive functions. This decapeptide binds to a class A GPCR, namely the GnRH receptor (GnRHR) located mainly on pituitary gonadotrophs. Along with the pituitary, GnRH receptors are expressed in reproductive tissues, both normal and malignant, such as those of the prostate and mammary gland [8-11]. Upon receptor activation, the gonadotropins luteinizing hormone (LH) and follicle stimulating hormone (FSH) are synthesized and secreted from gonadotrophic cells. LH and FSH consecutively induce follicle stimulation and ovulation in females and promote steroidogenesis in both males and females [12].

The pulsatile release of GnRH from the hypothalamus is essential for the maintenance of ovarian function. Sustained exposure of GnRHR to GnRH or GnRH analogues leads to activation, commonly named ''flare'', followed by desensitization of GnRHR-mediated gonadotropin secretion. Accordingly, blockade by antagonists or desensitization of GnRHR-mediated gonadotropin secretion both ultimately reduce circulating levels of gonadotropins and gonadal steroids [13, 14]. This so called chemical castration underlies the therapeutic use of GnRH analogues to treat sex hormone-dependent diseases [15-17].

Consequently, considerable efforts have been put towards the development of agonists and antagonists targeting the GnRH receptor [18-22]. Only a few studies have examined the receptor binding kinetics of GnRH ligands. A paper of Heise *et al.* [23] described a scintillation proximity assay to qualitatively distinguish between fast and slowly dissociating antagonists for the GnRH receptor. The authors demonstrated that slow dissociation rates were responsible for large discrepancies between a ligand's K_i value determined at 30 minutes versus 10 hours and they suggested using the K_i ratio as a

screening method to select slowly dissociating compounds. Two other studies focused on a quantitative determination of receptor binding kinetics of small molecule GnRH antagonists. Here, a direct correlation between the insurmountability and slow dissociation rates of these antagonists was shown [24, 25].

Currently multiple peptide GnRH analogues have been approved for the treatment of advanced prostatic cancer, endometriosis, *in vitro* fertilization and more [15-17, 26-29]. Remarkably, the receptor binding kinetics of peptide GnRH receptor ligands have never been reported. Therefore, we developed a novel radioligand binding competition association assay that allowed us to determine the kinetic binding parameters and focused on twelve GnRH peptide agonists, including many marketed drugs (Table 1). In addition, we compared these kinetic parameters with those from a newly developed homogenous time-resolved fluorescent (HTRF) assay. Both assays may improve future drug discovery targeting the GnRH receptor by incorporating kinetic receptor binding parameters into current research and development trajectories.

Material & methods

Reagents and peptides

Deslorelin and fertirelin (Table 1) were obtained from Genway Biotech Inc. (San Diego, CA, U.S.A.) and American Peptide Company (Sunnyvale, CA), respectively. All other peptide analogs (Table 1) and bovine serum albumin (BSA) were purchased from Sigma-Aldrich Chemie B.V. (Zwijndrecht, The Netherlands). BCA (bicinchoninic acid) protein assay reagent was obtained from Pierce Chemical Company (Rockford, IL, U.S.A.). ^{125}I-triptorelin (specific activity 2200 Ci/mmol) was purchased from PerkinElmer (Groningen, The Netherlands). Chinese Hamster Ovary cells stably expressing the human gonadotropin-releasing hormone receptor (from now on CHOhGnRH cells) were kindly provided by MSD (Oss, The Netherlands). Tag-lite™ HEK293 cells containing a stably overexpressed human GnRH receptor labeled with Tb (from now on Tag-lite™ GnRH cells) were obtained as frozen stocks from Cisbio (Codolet, France). A buserelin-derived tracer, labeled at the ^{6th} position with a red emitting fluorophore and Tag-lite™-buffer (TLB) were also purchased from Cisbio (Codolet, France). All other chemicals and cell culture materials were obtained from standard commercial sources. The molecular target nomenclature (GnRHR) conforms to 'The Concise Guide to PHARMACOLOGY 2013/14: G Protein-Coupled Receptors' [30].

Cell Culture

For radioligand binding assays, CHOhGnRH cells were grown in Ham's F12/DMEM (1:1) medium supplemented with 10% normal bovine serum, 2 mM glutamine, penicillin (100 IU/mL), streptomycin (100 µg mL^{-1}) and G418 (200 µg mL^{-1}) at 37 °C in 5% CO_2.

For TR-FRET experiments, 1 ml (7 *10^6 cells ml^{-1}) of Tag-lite™ GnRH cells were thawed, washed with 15 ml ice-cold TLB, resuspended in 5 ml TLB and immediately used.

Membrane Preparation

CHOhGnRH cells were scraped from the plates in 5 mL PBS, collected and centrifuged at 700 *g* (3000 rpm) for 5 min. Derived pellets were pooled and resuspended in 50 mM Tris HCl buffer pH 7.4 at 25 °C supplemented with 2 mM $MgCl_2$, and subsequently homogenized with an UltraThurrax (Heidolph Instruments, Germany). The cytosolic fraction and membranes were separated by centrifugation at 100 000 *g* (31 000 rpm) in an Optima LE-80K ultracentrifuge (Beckman Coulter, Fullterton, CA, U.S.A.) for 20 min. at 4 °C. The pellet was resuspended and centrifugation was repeated. The obtained pellet was resuspended, membranes were aliquoted and stored at -80 °C. Membrane protein concentrations were determined using the BCA method with BSA as a standard [31].

Table 1: Amino acid sequences of the twelve examined GnRH peptide agonists. The differences between the peptides are expressed in bold.

	1	2	3	4	5	6	7	8	9	10
GnRH	pGlu*	His	Trp	Ser	Tyr	**Gly**	Leu	Arg	Pro	**Gly-NH_2**
Triptorelin	pGlu*	His	Trp	Ser	Tyr	**D-Trp**	Leu	Arg	Pro	**Gly-NH_2**
[D-Ala^6]-GnRH	pGlu*	His	Trp	Ser	Tyr	**D-Ala**	Leu	Arg	Pro	**Gly-NH_2**
[D-Lys^6]-GnRH	pGlu*	His	Trp	Ser	Tyr	**D-Lys**	Leu	Arg	Pro	**Gly-NH_2**
Fertirelin	pGlu*	His	Trp	Ser	Tyr	**Gly**	Leu	Arg	Pro	**NHEt***
Alarelin	pGlu*	His	Trp	Ser	Tyr	**D-Ala**	Leu	Arg	Pro	**NHEt***
Deslorelin	pGlu*	His	Trp	Ser	Tyr	**D-Trp**	Leu	Arg	Pro	**NHEt***
Leuprorelin	pGlu*	His	Trp	Ser	Tyr	**D-Leu**	Leu	Arg	Pro	**NHEt***
Nafarelin	pGlu*	His	Trp	Ser	Tyr	**D2Nal**	Leu	Arg	Pro	**Gly-NH_2**
Buserelin	pGlu*	His	Trp	Ser	Tyr	**Ser-tBu***	Leu	Arg	Pro	**NHEt***
Goserelin	pGlu*	His	Trp	Ser	Tyr	**Ser-tBu***	Leu	Arg	Pro	**aGly-NH_2***
Histerelin	pGlu*	His	Trp	Ser	Tyr	**His(Bzl)***	Leu	Arg	Pro	**NHEt***

*pGlu = pyroglutamic acid, D2Nal = (2-naphthyl)-D-alanine, Ser-tBu = serine-tert-butyl, His(Bzl) = N-benzyl-L-histidine, aGly-NH_2 = aza-glycine amine, NHEt = ethylamide

Radioligand Equilibrium Assays

Displacement experiments were performed as previously reported [32]. In short, membrane aliquots containing 15-20 µg protein were incubated in a total volume of 100 µL assay buffer (25 mM Tris HCl, pH 7.4 at 25 °C, supplemented with 2 mM $MgCl_2$, 0.1 % (w/v) BSA) at 25 °C for 2 hours. Ten concentrations of competing ligand were used in the presence of 30.000 cpm (~0.1 nM) ^{125}I-triptorelin. At this concentration, total radioligand binding did not exceed 10% of that added to prevent ligand depletion. Non-specific binding was determined in the presence of an excess amount of GnRH (1 µM). The reaction was terminated by the addition of 1 mL ice-cold wash buffer (25 mM Tris HCl, pH 7.4 at 25 °C, supplemented with 2 mM $MgCl_2$ and 0.05% (w/v) BSA). Separation of bound from free radioligand was performed by rapid filtration through Whatman GF/B filters saturated with 0.25% polyethylene imine (PEI) using a Brandel harvester. Filters were subsequently washed three times with 2 mL ice-cold wash buffer. Filter bound radioactivity was determined using a γ-counter (Wizard 1470, PerkinElmer).

Radioligand Kinetic Association and Dissociation Assays

Association experiments were carried out by incubating membrane aliquots containing 15-20 µg protein in a total volume of 100 µL assay buffer at 25 °C with 30.000 cpm (~0.1 nM) ^{125}I-triptorelin. The amount of radioligand bound to the receptor was determined at different time intervals for a total incubation time of 120 min.

Dissociation experiments were performed by preincubating membrane aliquots containing 15-20 µg protein in a total volume of 100 µL assay buffer at 25 °C for 45 min with 30.000 cpm (~0.1 nM) ^{125}I-triptorelin. After preincubation, dissociation was initiated by addition of an excess amount of GnRH (1 µM) in a total volume of 2.5 µL. The amount of radioligand still bound to the receptor was measured at various time intervals for a total incubation time of 120 min. The reaction was stopped and samples were harvested as described under *Radioligand Equilibrium Assays*.

Radioligand Kinetic Competition Association Assays

The binding kinetics of unlabeled ligands were quantified using the competition association assay based on the method by Motulsky and Mahan [33]. During optimization, three different concentrations of unlabeled triptorelin were tested; 0.3-, 1- and 3-fold its K_i value. The kinetic parameters of all other unlabeled ligands were determined at a concentration of 1-fold their K_i, unless stated otherwise. The competition association assay was initiated by adding membrane aliquots containing 15-20 µg protein in a total volume of 100 µL assay buffer at 25 °C with 50.000 cpm (~0.15 nM) ^{125}I-triptorelin in the absence or

presence of competing ligand. Of note, total radioligand binding did not exceed 10% of that added at this concentration to prevent ligand depletion. The amount of radioligand bound to the receptor was determined at different time intervals for a total incubation time of 120 min. The reaction was stopped and samples were harvested as described under *Radioligand Equilibrium Assays*.

TR-FRET Probe Equilibrium Assays

Unless otherwise specified, TR-FRET measurements were carried out using the conditions described in [34]. To determine the equilibrium affinity of the fluorescent probe, 5 µl Tag-lite™ GnRH cells (1400 cells μl^{-1}) were incubated for 1 h, to ensure signal stability, with increasing probe concentrations (ranging from 0 to 100 nM: Supplementary Figure S1) in a final volume of 10 µl. In parallel, a non-specific binding control was carried out in the presence of an excess amount of buserelin (100 µM). Binding signals were measured in a PHERAstar FS plate reader by exciting the Tb donor with 5 laser flashes at a wavelength of 337 nm and recording acceptor and donor emission fluorescence channels (A and B channels), at wavelengths of 520 nm and 490 nm respectively.

TR-FRET Equilibrium Probe Competition Assays

"Ready-to-use" assay plates containing serial dilutions of the test agonists were prepared as described in [34]. Subsequently 5 µl Tag-lite™ GnRH cells (1400 cells μl^{-1}) and 50 nM probe were added to the competitors and incubated at room temperature for 1 h, to ensure signal stability, in a final volume of 10 µl. Non-specific binding ("low signal") controls contained an excess amount of buserelin (100 µM), whereas in "high signal" controls, the test compounds were replaced by DMSO. Binding signals were recorded as described under *TR-FRET Probe Equilibrium Assays*.

TR-FRET Kinetic Probe Association and Dissociation Assays

Measurements were carried out in quadruplicate and in a final volume of 15 µl $well^{-1}$. First, a 5-point, 2-fold serial dilution of fluorescent probe (Supplementary Figure 2) was pre-dispensed on black 384 well low volume plates (Greiner) and the the PHERAstar FS injection system's syringes (previously washed with $NaOH/H_2O$) were either primed with 1500 µl solution of Tag-lite™ GnRH cells, (1000 cells μl^{-1}) or with 200 µM buserelin. Then, 4 µl of cells were quickly added to the probe with the first syringe and the association traces were recorded as described under *TR-FRET Probe Equilibrium Assays*, with kinetic intervals of 26 seconds. After 30 min, fluorescent probe dissociation was initiated by addition of 5 µl of an excess of unlabeled buserelin (final concentration 67 µM) with the second syringe and the

traces were recorded with kinetic intervals of 300 seconds in the same fashion. Alternatively a 1-point measurement was performed with 5 µL of probe (final concentration 25 nM) and 5 µL of Tag-lite™ GnRH cells (1400 cells/µL) and association was recorded with kinetic intervals of 120 seconds. After 24 min dissociation was initiated and recorded with the same kinetic interval.

TR-FRET Kinetic Probe Titration Assays

First, 5 µL of increasing concentrations of fluorescent probe was dispensed into 384 well plates, the injection system of the PHERAstar FS plate reader was primed with Tag-lite™ GnRH cells as described under *TR-FRET Probe Equilibrium Assays*. Then, 5 µl of cell solution was added with the syringe and the TR-FRET signals corresponding to probe association were recorded as described under *TR-FRET Probe Equilibrium Assays*.

TR-FRET Kinetic Probe Competition Assays (kPCA)

The basic principle of this assay is explained in [34]. Prior to each experiment, 6 µL of fluorescent probe (final concentration 15 nM) was dispensed to the "assay-ready" plates containing 100 nl of compound dilutions using a Multidrop Combi and the injection system of the PHERAstar FS plate reader was washed with $NaOH/H_20$ and primed with Tag-lite™ GnRH cells. Finally, the assay plates were introduced into the instrument, 4 µl of cells (1000 cells/µl) were rapidly dispensed with the syringe to each well and the TR-FRET signals corresponding to the competitive binding of probe and test compounds were recorded as described under *TR-FRET Probe Equilibrium Assays* with kinetic intervals of 78 seconds.

Data Analysis

All experimental data were analyzed using the nonlinear regression curve-fitting program GraphPad Prism v. 5.00 (GraphPad Software Inc., San Diego, CA). Further details on the handling of TR-FRET data are available in [34].

For radioligand binding assays, the previously reported K_D value of 0.35 nM for ^{125}I-triptorelin [32] was used to convert IC_{50} values obtained from competition curve analysis into K_i values with the help of the Cheng-Prusoff equation [35]:

$$K_i = IC_{50}/(1+[\text{radioligand}]/K_D)$$

Likewise, a K_D value of 0.8 nM obtained for the "red"-labeled buserelin by fitting the data from the TR-FRET Probe Equilibrium Binding Assay (Supplementary Figure S1) to the

model “One site – Specific binding”, was used to convert IC_{50} values from TR-FRET experiments to K_i values.

The observed association rates (k_{obs}) derived from both assays were obtained by fitting association data using one phase exponential association. The dissociation rates were obtained by fitting dissociation data to a one phase exponential decay model. The k_{obs} values were converted into association rate (k_{on}) values using the following equation:

$k_{on} = (k_{obs} – k_{off})/[radioligand]$

The association and dissociation rates were used to calculate the kinetic K_D using the following equation:

$K_D = k_{off}/k_{on}$

To further validate probe affinity and kinetic rate constants, association data from kinetic probe titration experiments were fitted to the ‘’Association kinetics – two or more concentrations of hot’’ model (Supplementary Figure S2). The obtained k_{on} from these experiments and K_D from equilibrium binding was used to calculate k_{off} as described above.

Association and dissociation rates for unlabeled ligands were calculated by fitting the data of the competition association assay using kinetics of competitive binding [33]:

$$K_A = k_1[L]\cdot 10^{-9} + k_2$$
$$K_B = k_3[I]\cdot 10^{-9} + k_4$$
$$S = \sqrt{(K_A - K_B)^2 + 4\cdot k_1 \cdot k_3 \cdot L \cdot I \cdot 10^{-18}}$$
$$K_F = 0.5(K_A + K_B + S)$$
$$K_S = 0.5(K_A + K_B - S)$$
$$Q = \frac{B_{\max} \cdot k_1 \cdot L \cdot 10^{-9}}{K_F - K_S}$$
$$Y = Q \cdot \left(\frac{k_4 \cdot (K_F - K_S)}{K_F \cdot K_S} + \frac{k_4 - K_F}{K_F} e^{(-K_F \cdot X)} - \frac{k_4 - K_S}{K_S} e^{(-K_S \cdot X)}\right)$$

Where k_1 is the k_{on} of the radioligand ($M^{-1}min^{-1}$), k_2 is the k_{off} of the radioligand (min^{-1}), L is the radioligand concentration (nM), I is the concentration of the unlabeled competitor (nM), X is the time (min) and Y is the specific binding of the radioligand (DPM). During a

competition association these parameters are set, obtaining k_1 from the control curve without competitor and k_2 from previously performed dissociation assays described under *Radioligand Association and Dissociation Assays*. With that the k_3, k_4 and B_{max} can be calculated, where k_3 represents the k_{on} ($M^{-1}min^{-1}$) of the unlabeled ligand, k_4 stands for the k_{off} of the unlabeled ligand and B_{max} equals the total binding (DPM). All competition association data were globally fitted.

In case of kPCA, the kinetics of the competitive binding model was enhanced with a mathematical term describing a mono-exponential decay that accounts for signal drift [34]. As stated for the radioligand binding assays, the kinetic rate constants of the fluorescent probe (k_1 and k_2) were determined in separate experiments and set constant in kPCA data analysis.

The residence time (RT) was calculated as in the following equation:

$$RT = 1/k_{off}$$

All values obtained from radioligand binding assays are means of at least three independent experiments performed in duplicate, unless stated otherwise. Values obtained from TR-FRET assays are means of two independent experiments performed in quadruplicate, unless stated otherwise.

Results

Determination of the association and dissociation rate constants of ^{125}I-triptorelin

The binding properties of ^{125}I-triptorelin to CHOhGnRH membranes were quantified with traditional kinetic radioligand binding assays. Association and dissociation experiments provided k_{on} and k_{off} values of 0.4 ± 0.1 $nM^{-1}min^{-1}$ and 0.05 ± 0.0004 min^{-1}, respectively (Figure 1A and Table 2). From these data the equilibrium dissociation constant (kinetic K_D) was calculated, which had a value of 0.2 nM.

Determination of the association and dissociation rate constants of the fluorescently labeled buserelin derivative probe

A fluorescently labeled buserelin derivative was used as a probe in all TR-FRET assays. The kinetic parameters of the fluorescent tracer were determined by performing association and dissociation experiments. Experiments yielded a k_{on} and k_{off} of 0.008 ± 0.001 $nM^{-1}min^{-1}$ and 0.01 ± 0.001 min^{-1}, respectively (Figure 1B, Table 3, Supplementary Figure 2). The kinetic K_D value calculated from these experiments was 1.2 nM.

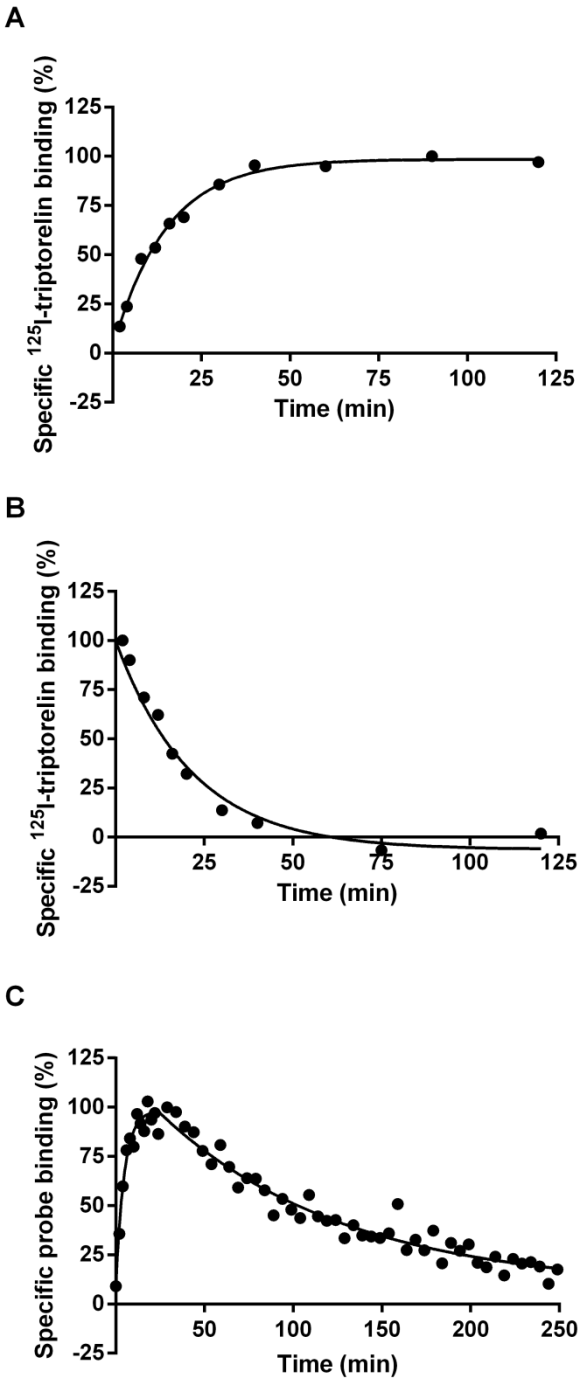

Figure 1: Association and dissociation kinetics of ^{125}I-triptorelin (A and B, respectively) or fluorescent probe (C) at the hGnRH receptor. Representative graphs from one experiment performed in duplicate (see Table 2 and 3 for kinetic parameters).

Table 2: Comparison of the affinity, dissociation constants and kinetic parameters of reference agonist triptorelin obtained with different radioligand binding assays

Assay	**pK_D[b] and (K_D (nM))**	**pK_i and (K_i (nM))**	**k_{on} (nM^{-1} min^{-1})**	**k_{off} (min^{-1})**
Displacement	N.A.	9.6 ± 0.09 (0.27)	N.A.	N.A.
Association and dissociation	9.9 ± 0.11 (0.13)	N.A.	0.40 ± 0.12	0.050 ± 0.0004
Competition association[a]	9.7 ± 0.12 (0.22)	N.A.	0.12 ± 0.014	0.026 ± 0.008

Values are means ± SEM of three separate experiments performed in duplicate. N.A., not applicable. [a]The binding kinetics of unlabeled triptorelin were determined by addition of 0.3-, 1- and 3-fold its K_i value. [b]$K_D = k_{off}/k_{on}$

Table 3: Comparison of the affinity, dissociation constants and kinetic parameters of the fluorescent buserelin probe obtained with different TR-FRET assays

Assay	**pK_D and (K_D (nM))**	**pK_i and (K_i (nM))**	**k_{on} (nM^{-1} min^{-1})**	**k_{off} (min^{-1})[b]**
Equilibrium association	9.1 ± 0.8 (0.8)	N.A.	N.A.	N.A.
Association and dissociation[a]	8.9 ± 0.9 (1.2)	N.A.	0.008 ± 0.001	0.010 ± 0.001
Multiple association and dissociation	8.7 ± 0.06 (2.1)	N.A.	0.008 ± 0.001	0.016 ± 0.002

Values are means ± SEM of three separate experiments. N.A., not applicable. [a]The dissociation kinetics of fluorescently labeled buserelin derivative were determined by addition of 10 µM buserelin. [b] $k_{off} = K_D$(equilibrium)$/k_{on}$

Determination of the binding affinity of hGnRHR agonists with ^{125}I-triptorelin

Equilibrium radioligand binding assays were performed to assess the ability of twelve GnRH analogues to displace ^{125}I-triptorelin from CHOhGnRH cell membranes. All ligands were able to fully displace ^{125}I-triptorelin in a concentration-dependent manner (Figure 2A and Table 4). All peptides had a Hill-coefficient close to unity in the ^{125}I-triptorelin displacement assay (data not shown), which indicated a competitive mode of inhibition with regard to the radioligand. Of all tested ligands nafarelin had the highest affinity for the

hGnRH receptor with a K_i value of 0.06 nM and GnRH had the lowest affinity of 13 nM. All other ligands had affinities in the low to sub-nanomolar range.

Determination of the binding affinity of hGnRHR agonists with TR-FRET

The binding affinity of twelve agonists was also determined using a fluorescently labeled buserelin derivative as a tracer and Tag-lite™ GnRH cells in a TR-FRET assay. In accordance with the radioligand binding results, all agonists were able to fully displace the fluorescent tracer from the hGnRH receptor in a concentration-dependent manner (Figure 2B and Table 4). The data were in fair agreement with the affinities determined in the radioligand displacement assay despite the inherent differences between the two assays (r^2=0.5 and p<0.05) (Figure 4C).

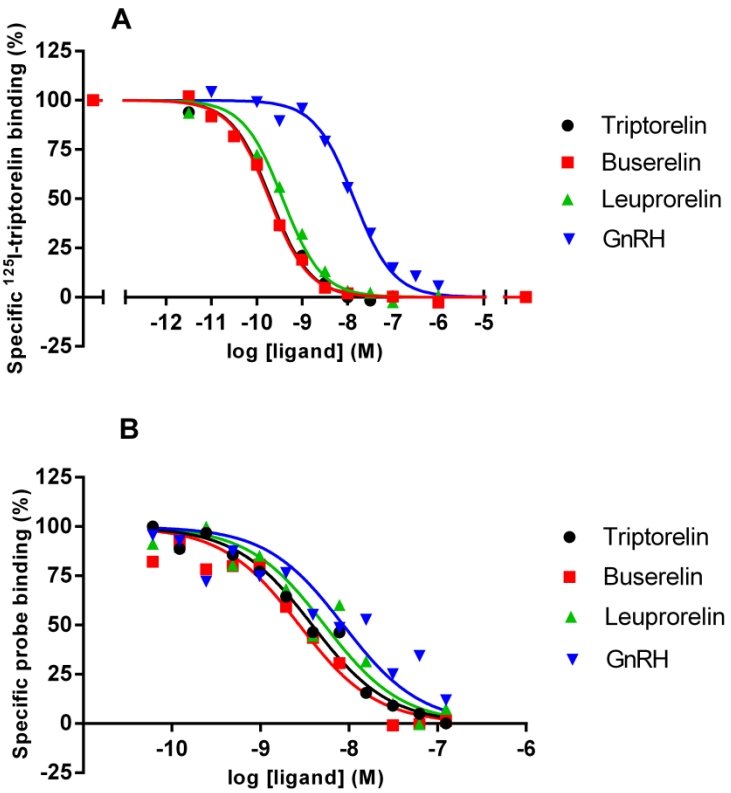

Figure 2: Displacement of ^{125}I-triptorelin (A) or fluorescent probe (B) from the hGnRH receptor by the twelve peptide agonists. Representative graphs from one experiment performed in duplicate (see Table 4 for affinity values)**.**

Validation and optimization of the competition association assay with ^{125}I-triptorelin

With the k_{on} and k_{off} values of ^{125}I-triptorelin obtained from traditional association and dissociation experiments, the k_{on} (k_3) and k_{off} (k_4) values of unlabeled triptorelin could be determined by fitting the kinetic parameters into the model of 'kinetics of competitive binding' as described under *'Material & Methods'*. Three different concentrations of unlabeled triptorelin were tested and presented a shared k_{on} (k_3) and k_{off} (k_4) value of 0.1 ± 0.01 $nM^{-1}min^{-1}$ and 0.03 ± 0.008 min^{-1}, respectively (Figure 3A). These values were in good agreement with the association and dissociation rates obtained with traditional kinetic experiments (Table 2). Additionally, a comparison of the affinity (0.3 nM) and dissociation

constants (0.1 nM and 0.2 nM), acquired from equilibrium and kinetic experiments respectively, further confirmed the competition association assay as a valid tool to determine the binding kinetics of unlabeled ligands at the hGnRH receptor (Table 2).

To improve the throughput of this assay, one concentration of competitor was selected that yielded an assay window discernable from both the baseline and control curve (i.e. specific binding approximately 40-60%). In this case, a concentration of competitor equal to 1-fold its K_i value presented the best assay window. Analysis of this single concentration showed similar kinetic rates for triptorelin in comparison to the three-concentration method, which were statistically indifferent (data not shown; $p>0.05$). Thus, this one-concentration method was used for subsequent determination of the binding kinetics of other unlabeled hGnRHR peptide agonists.

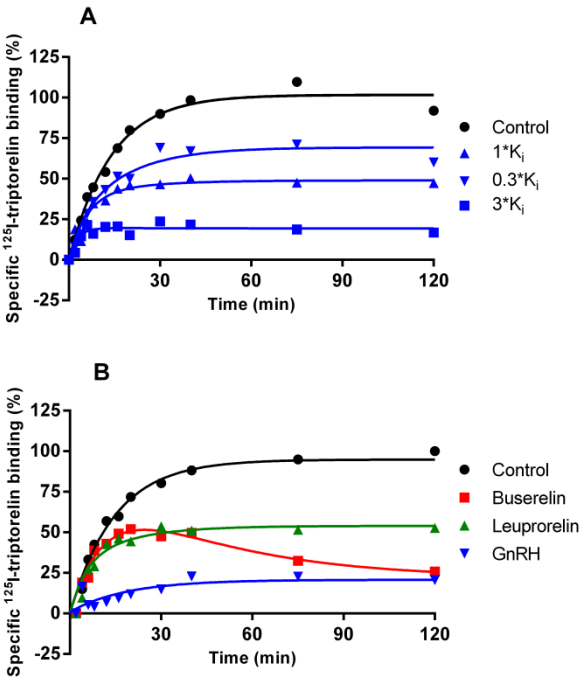

Figure 3: Competition association experiment with ^{125}I-triptorelin in the absence or presence of 0.3, 1 or 3*K_i value of unlabeled triptorelin (A) or 1*K_i value of buserelin, leuprorelin or GnRH (B). Representative graphs from one experiment performed in duplicate (See Table 2 for kinetic parameters).

Determination of the receptor binding kinetics of unlabeled hGnRHR agonists with ^{125}I-triptorelin

By use of the one-concentration competition association assay the binding kinetics of 11 other unlabeled hGnRHR agonists were quantified (Figure 3B, Table 5). Juxtaposing affinities (K_i values) and dissociation constants (K_D values) acquired from equilibrium and kinetic experiments resulted in a high correlation ($r^2 = 0.9$, $p<0.0001$). Firstly, this further confirmed that the competition association assay was a valid tool to determine the binding kinetics of unlabeled ligands for the hGnRH receptor (Figure 4A) and secondly, proved that equilibrium was reached for all agonists in the displacement experiments. The dissociation rates ranged from 0.2 ± 0.03 min^{-1} for goserelin to 0.01 ± 0.003 min^{-1} for buserelin, a variance of roughly 20-fold. Interestingly, three distinctive association patterns were obtained from the

competition association assays (Figure 3B). Firstly, an 'overshoot' in ^{125}I-triptorelin association was observed for slowly dissociating compounds, such as buserelin. Secondly, we noticed a shallow increase in ^{125}I-triptorelin association for rapidly dissociating compounds, such as GnRH, and lastly, no difference was observed in the shape of the ^{125}I-triptorelin association curve for equally fast-dissociating compounds, such as leuprorelin. The observed differences in dissociation kinetics were all in comparison to those of the radioligand ^{125}I-triptorelin (Figure 3B). Association rates ranged from 0.8 ± 0.2 $nM^{-1}min^{-1}$ for nafarelin to 0.02 ± 0.004 $nM^{-1}min^{-1}$ for fertirelin, a span of approximately 35-fold.

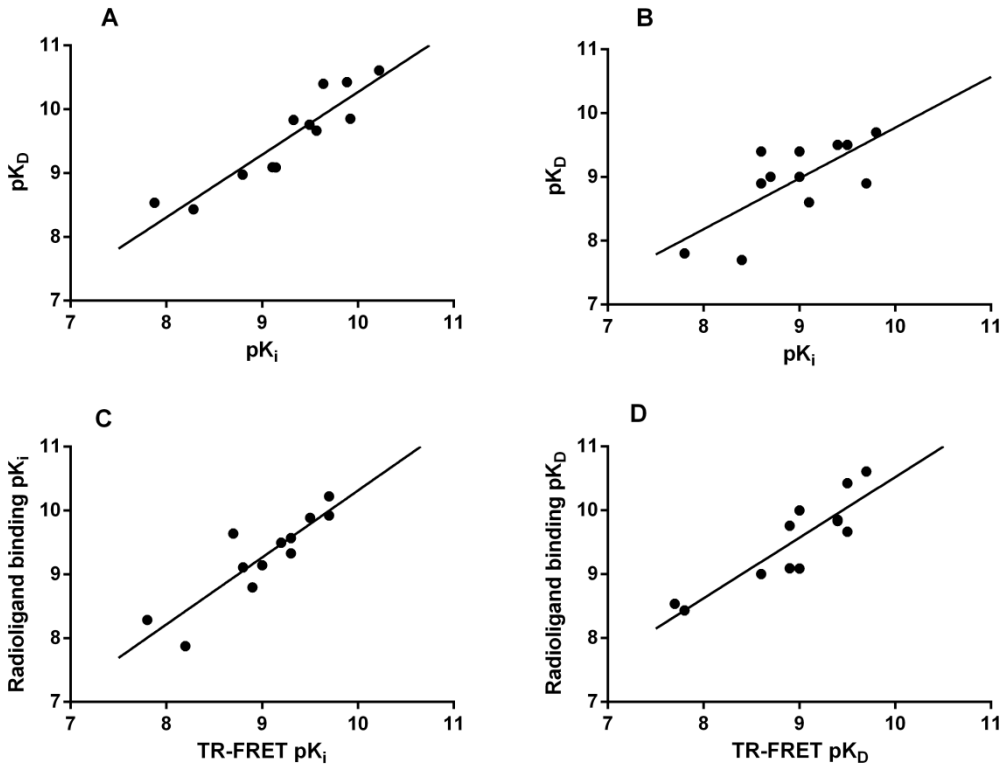

Figure 4: Correlation between affinities (pK_i) and dissociation constants (pK_D) derived from (A) radioligand binding (r^2= 0.9, P<0.0001) and (B) TR-FRET experiments (r^2=0.5, P<0.05). (C) Correlation between affinities (pK_i) derived from radioligand binding and HTRF experiments (r^2=0.5, P<0.05). (D) Correlation between dissociation constants (pK_D) derived from radioligand binding and TR-FRET experiments (r^2=0.8, P<0.001). In all cases, pK_i values were obtained from equilibrium displacement studies and pK_D values were determined with competition association experiments.

Determination of the receptor binding kinetics of unlabeled hGnRHR agonists with a fluorescently labeled buserelin derivative

Table 4: Binding parameters of GnRH peptide agonists derived from radioligand binding and TR-FRET experiments

	Radioligand binding		**TR-FRET**	
Agonist	**pK_i and (K_i (nM))**	**pK_D and (K_D (nM))**	**pK_i and (K_i (nM))**	**pK_D and (K_D (nM))**
GnRH	7.9 ± 0.05 (13)	8.5 ± 0.08 (2.9)	8.4 ± 0.6 (4.0)	7.7 ± 0.03 (22)
Triptorelin	9.6 ± 0.09 (0.3)	9.7 ± 0.1 (0.2)	9.5 ± 0.2 (0.4)	9.5 ± 0.03 (0.4)
[D-Ala^6]-GnRH	9.0 ± 0.05 (0.8)	9.1 ± 0.09 (0.8)	8.6 ± 0.4 (2.3)	8.9 ± 0.02 (1.3)
[D-Lys^6]-GnRH	8.3 ± 0.1 (5.2)	8.4 ± 0.2 (3.7)$^{\#}$	7.8 ± 0.3 (16)	7.8 ± 0.01 (15)
Fertirelin	9.2 ± 0.05 (0.7)	9.1 ± 0.08 (0.8)$^{\#}$	9.0 ± 0.3 (1.0)	9.0 ± 0.02 (0.9)
Alarelin	9.4 ± 0.1 (0.5)	9.8 ± 0.1 (0.2)	9.0 ± 0.3 (0.9)	9.4 ± 0.03 (0.4)
Deslorelin	10 ± 0.1 (0.1)	9.9 ± 0.1 (0.1) $^{\#}$	8.6 ± 0.6 (0.8)	9.4 ± 0.04 (0.4)
Leuprorelin	9.5 ± 0.09 (0.3)	9.8 ± 0.1 (0.2)	9.7 ± 0.3 (0.2)	8.9 ± 0.03 (1.2)
Nafarelin	10 ± 0.06 (0.06)	10.6 ± 0.1 (0.03)	9.8 ± 0.3 (0.2)	9.7 ± 0.06 (0.2)
Buserelin	9.9 ± 0.05 (0.1)	10.4 ± 0.2 (0.04)	9.4 ± 0.2 (0.4)	9.5 ± 0.04 (0.3)
Goserelin	8.8 ± 0.06 (1.6)	9.0 ± 0.08 (1.1)	9.1 ± 0.3 (0.9)	8.6 ± 0.02 (2.7)
Histerelin	9.8 ± 0.2 (0.2)	10 ± 0.08 (0.04)	8.7 ± 0.5 (1.9)	9.0 ± 0.04 (1.0)

Values are means ± SEM of at least three separate experiments performed in duplicate. $^{\#}$Values are means ± SEM of two separate experiments performed in duplicate. $K_D = k_{off}/k_{on}$

The kinetic parameters of the twelve GnRH agonists were also determined with TR-FRET experiments (Figure 5, Table 5 and Supplementary Figure 3). Association rates ranged from 0.1 ± 0.02 $nM^{-1}min^{-1}$ for triptorelin to 0.02 ± 0.002 $nM^{-1}min^{-1}$ for histerelin. Buserelin was again one of the slowest dissociating agonists with a dissociation rate of 0.02 ± 0.003 min^{-1}, while GnRH had the fastest dissociation rate of 0.4 ± 0.03 min^{-1}. The dissociation constants (K_D) calculated from k_{on} and k_{off} values were consistent with the affinities determined in HTRF displacement assays (Figure 4B) as well as with the K_D values obtained from the radioligand binding studies (Figure 4D). Dissociation rate constants (k_{off}) were in good agreement with the data obtained from radioligand binding experiments (r^2=0.7, p<0.0005) (Figure 6A), while the association rates (k_{on}) presented no correlation (r^2=0.03, p=0.6) (Figure 6B).

Discussion and Conclusions

Over the years several studies have indicated that long duration of action is an important feature contributing to improved efficacy of drugs designed to treat chronic illness. Moreover, increased target-residence time offers the potential for a once-daily dosage form

that increases patient compliance which is crucial for the management of diseases [1, 2, 5, 36-40].

The GnRH receptor is the target of multiple marketed peptide agonists, classified as functional antagonists, used to treat hormone-dependent diseases. Available patient information for the most commonly prescribed GnRH analogues suggests that the PK/PD profiles are very similar. Hence, knowledge of the *in vitro* binding kinetics could give extra insights into these well-known drugs. However, the potential impact of variable binding kinetics of these GnRH peptide derivatives on clinical efficacy has not been investigated. Aside from agonists, a few studies have detailed the effect of slow dissociation kinetics of

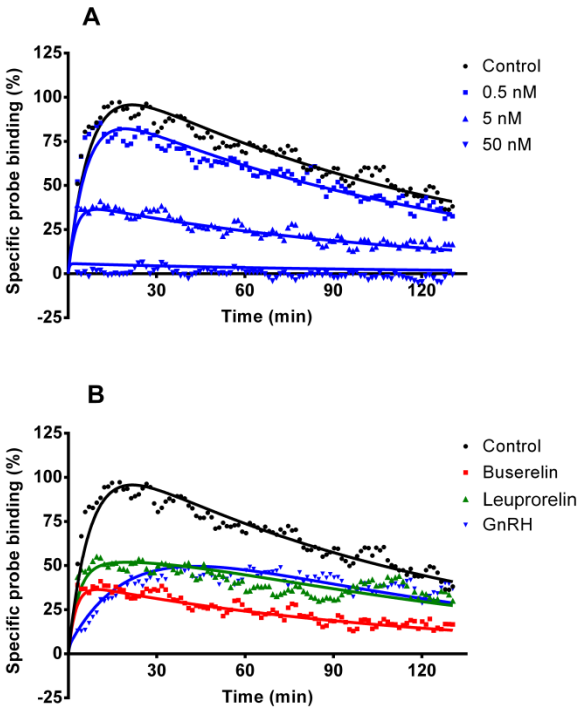

Figure 5: Competition association experiment with fluorescent probe in the absence or presence of increasing concentrations of buserelin (A) or one-concentration of unlabeled agonist that showed around 50% displacement (B). Representative graphs from one experiment performed in quadruplicate.

antagonists for the GnRH receptor to decrease the maximal response of an agonist (insurmountability) *in vitro* and to improve and prolong efficacy *in vivo*. A study of Kohout and coworkers [25] addressed the insurmountability of a small molecule GnRH antagonist, TAK-013. The authors examined the differences in antagonistic and kinetic properties of TAK-013 for hGnRHR, mouse GnRHR (mGnRHR) and mutated mGnRHR and found a good correlation between the degree of insurmountability in *in vitro* functional assays and the dissociation rate from the receptor. Therefore, they proposed slow receptor dissociation kinetics to be accountable for the mechanism of insurmountability of TAK-013. Similar findings were published [24] for another series of small molecule antagonists, i.e. uracils. Slowly dissociating ligands displayed insurmountable antagonism whereas faster dissociating ligands proved to be surmountable antagonists. To determine the dissociation rates of these uracil-series of antagonists the competition association method [33] was used with a proprietary small molecule radioligand as a tracer. Such a competition association assay has recently been applied to determine the receptor kinetics of ligands for several different GPCRs such as the adenosine A_{2A} receptor [41], the muscarinic M_3 receptor [42], the chemokine receptor CCR2 [43] and the

histamine H_1 and H_3 receptor [44]. We were able, for the first time, to determine the kinetic parameters of twelve GnRH peptide agonists, including many marketed drugs.

Two different techniques were applied, namely; radioligand binding studies and kinetic probe competition assays (kPCA) with a TR-FRET read-out. For the former, a comparison of the radioligand's kinetic parameters obtained from traditional radioligand binding experiments showed a good consistency with the kinetic parameters for triptorelin derived from the competition association assay (Table 2). Moreover, the kinetics of the 11 remaining GnRH agonists presented a good correlation between the kinetically derived K_D and the affinity obtained from equilibrium radioligand binding studies (Figure 4). Secondly, we also conducted these experiments with a fluorescently labeled buserelin probe in a TR-FRET assay. This technology has already been used for examining equilibrium GPCR ligand binding [45, 46] and more recently it was used to characterize the binding kinetics of the Histamine H1 receptor [34].

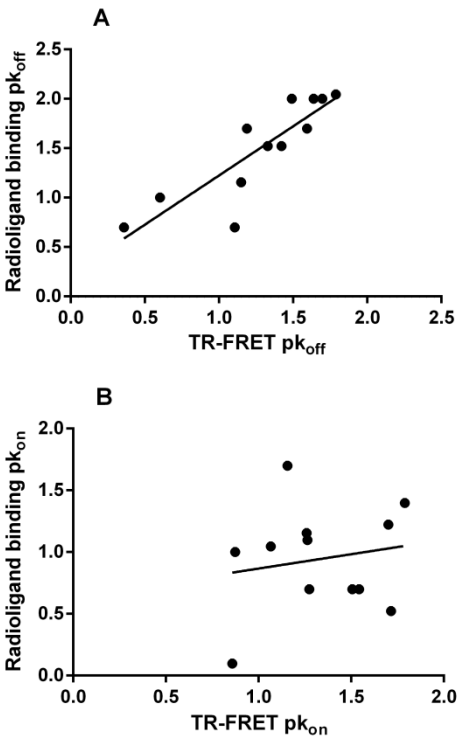

Figure 6: Correlation between the kinetic parameters obtained from radioligand binding assays and kPCA TR-FRET experiments. (A) Dissociation rate (k_{off}) (r^2=0.7, P<0.0005); (B) association rate (k_{on}) (r^2=0.03, P=0.6).

Comparing affinities and kinetic K_D values from both the radioligand binding and TR-FRET assays yielded significant correlations demonstrating a good reproducibility between both techniques. The two distinct assays also proved to be very amenable to the determination of the kinetic receptor binding parameters of (peptide) GnRH agonists. Dissociation rates, and thus residence times, between assays were in good accordance with p values of <0.0005, while the association rates were in less agreement between techniques. It should be noted that the experimental differences between both assays are considerable, which may have consequences for the kinetic parameters derived in the two assays. For example, the radioligand binding studies were manually dispensed while the TR-FRET assays were performed using automated dispensing devices. It has been reported that compound handling can be an important source of assay variability [47]. In addition, the kinetic binding parameters were determined using a one-concentration method for the

radioligand binding experiments whereas the kPCA studies used five different concentrations.

Table 5: Kinetic receptor binding parameters of GnRH peptide agonists derived from radioligand binding competition association assays and kPCA TR-FRET experiments

	Radioligand binding			**TR-FRET**		
Agonist	**k_{on} ($nM^{-1}min^{-1}$)[a]**	**k_{off} (min^{-1})[a]**	**RT (min)[c]**	**k_{on} ($nM^{-1}min^{-1}$)[b]**	**k_{off} (min^{-1})[b]**	**RT (min)[c]**
GnRH	0.06 ± 0.01	0.2 ± 0.02	6.3 ± 0.6	0.02 ± 0.01	0.44 ± 0.3	2.3 ± 1.6
Triptorelin	0.1 ± 0.01	0.03 ± 0.008	39 ± 12	0.1 ± 0.02	0.05 ± 0.008	21 ± 3.7
[D-Ala^6]-GnRH	0.08 ± 0.01	0.07 ± 0.01	15 ± 3.1	0.05 ± 0.007	0.07 ± 0.01	14 ± 2.3
[D-Lys^6]-GnRH	0.04 ± 0.02[#]	0.1 ± 0.04[#]	7.7 ± 2.3[#]	0.02 ± 0.01	0.25 ± 0.17	4 ± 2.6
Fertirelin	0.02 ± 0.004[#]	0.02 ± 0.001[#]	56 ± 3.1[#]	0.07 ± 0.009	0.06 ± 0.01	15 ± 2.4
Alarelin	0.09 ± 0.02	0.01 ± 0.002	77 ± 12	0.09 ± 0.009	0.03 ± 0.005	31 ± 4.8
Deslorelin	0.07 ± 0.01[#]	0.01 ± 0.002[#]	100 ± 20[#]	0.05 ± 0.005	0.02 ±0.004	44 ± 6.9
Leuprorelin	0.2 ± 0.04	0.03± 0.005	36 ± 6.4	0.03 ± 0.004	0.04 ± 0.006	26 ± 4.4
Nafarelin	0.8 ± 0.2	0.02 ± 0.003	50 ± 7.5	0.1 ± 0.02	0.03 ± 0.006	39 ± 9.8
Buserelin	0.2 ± 0.06	0.009 ± 0.003	111 ± 37	0.05 ± 0.004	0.02 ± 0.003	61 ± 10
Goserelin	0.2 ± 0.002	0.2 ± 0.03	5.6 ± 0.8	0.03 ± 0.005	0.08 ± 0.01	13 ± 2.4
Histerelin	0.3 ± 0.04	0.01 ± 0.002	83 ± 14	0.02 ± 0.002	0.02 ± 0.004	50 ± 8.8

Values are means ± SEM of at least three separate experiments performed in duplicate. [#]Values are means ± SEM of two separate experiments performed in duplicate. [a]k_{on} and k_{off} of unlabeled GnRH agonists were determined at 1-fold K_i concentrations. [b]k_{on} and k_{off} of unlabeled GnRH agonists were determined at 0.5, 5, 50 and 500 nM. [c]$RT = 1/k_{off}$

Another notable difference is that in the radioligand binding studies CHOhGnRH membranes were used whereas the TR-FRET assays were performed with Tag-lite™ HEK_{293} GnRH cells. Packeu *et al.* discussed the differences in membrane interactions of membrane preparations and whole cells and their effects on binding kinetics for the D_{2L}-dopamine receptors [48]. Moreover, the authors found slower dissociation rates from intact cells in comparison to membrane preparations and they proposed that an intact cellular environment could play a role in stabilizing the D_{2L}-dopamine receptors in a particular conformation. A similar reasoning might be applicable to the GnRH receptor, although in our case the receptor appears in a way that slows down the association rates of the peptides (Table 5). It

may also be that the peptides simply have more difficulty in reaching the receptor on intact cells than on membrane fragments.

It might be argued that the assay temperature of 25 °C is not representative for binding kinetics observed in vivo. For example, Sakai [49] examined the effect of temperature on the dissociation of ^{125}I-prolactin from the rabbit mammary gland prolactin receptor. They found a linear relationship between the dissociation rate and temperature with an increased dissociation rate at higher temperatures. Another study [50] also showed that the dissociation of [^{3}H]-QMDP from the histamine H_1 receptor was temperature-dependent, which was also true for the association rate but to a lesser extent. Arrhenius plots for both the association rate and dissociation rate of [^{3}H]-QMDP were linear between 6 °C and 37 °C. It should be noted that, although these studies show a linear increase in dissociation rates with higher temperatures the slope of this increase could be very different between targets and their ligands. Taken together, this indicates that the kinetic ranking of ligands for the same receptor can be expected to stay the same over different temperatures. Therefore, even though all our experiments were performed at 25 °C, the results are still of great value for translation to *in vivo* outcomes.

Numerous peptide GnRH derivatives have been synthesized and studied for their so-called structure-affinity relationships (SAR), with the aim to improve their affinity, potency and/or metabolic stability [20-22, 51-53] In summary, it was established that the NH_2-terminal domain (pGlu-His-Trp-Ser) of GnRH is important for receptor binding and activation with Trp^3 as a critical residue. In addition, the COOH-terminal domain (Pro-Gly-NH_2) is crucial for receptor binding where substitution of Pro^9 or removal of NH_2 results in very low affinity unless the COOH-terminal tail is substituted for an ethylamide which also improves metabolic stability. In contrast, the central domain of the peptide is less conserved and studies show that exchange of Tyr^5, Leu^7 or Arg^8 is mostly well tolerated. The most beneficial substitution is that of Gly^6 with a D-amino acid which provides a more favorable conformation and in turn results in increased potency. D-amino acids at the 6th position of the peptide are therefore incorporated in all marketed GnRH analogues. The amino acid sequences of the twelve GnRH peptides tested in this study are identical with the exception of the 6th amino acid and the carboxylic tail (Table 1). A tentative structure kinetic relationship (SKR) could be established for the carboxylic tail (i.e. substitution of the glycine-amide for an ethylamide). For instance, a comparison of triptorelin and deslorelin showed 2/3-fold changes in affinity (Table 4), which was also observed in residence time. This ethylamide-induced improvement in residence time was also true to a bigger extent for goserelin and buserelin, where the affinity was improved 2- or 16-fold (TR-FRET and radioligand binding, respectively), while the residence time was more significantly affected, witnessed by a 5-fold increase in the kPCA TR-FRET experiments and a 20-fold increase in the radioligand binding studies. This shows

that shortening the carboxylic tail of the peptide slightly increases the affinity, but results in a more significant improvement in residence time. Interestingly, three decades ago it was already speculated that buserelin has a longer residence time. In these studies, the authors proposed that the high potency and long duration of action of buserelin *in vivo* was a result of prolonged GnRH receptor binding [54-56]. Along similar lines, Flanagan and coworkers discussed slower dissociation rates of GnRH agonists with a more hydrophobic amino acid at position 6 [57]. However, no mechanism or kinetic binding data was reported at that time.

Previously published mutagenesis studies further strengthen our hypothesis indicating the importance of the ethylamide at the carboxylic tail. Davidson and coworkers showed that the $Asn^{2.65(102)}$ residue located near the extracellular end of TM2 plays a role in ligand binding, specifically with the carboxylic tail of GnRH analogs [58]. Mutations to alanine at this position significantly decreased the potency of GnRH analogs with Gly^{10}-NH_2, but had a lesser effect on GnRH analogs with an ethylamide tail [21, 59, 60]. It may be hypothesized that substitution of Gly^{10}-NH_2 with an ethylamide moiety creates less steric hindrance and increases hydrophobicity, thereby improving the fit of the agonist and thus elongating its residence time on the receptor.

In conclusion, two novel competition association assays were successfully developed and applied to determine the kinetic binding characteristics of twelve peptide agonists, including many marketed drugs targeting the GnRH receptor. All agonists proved to have high affinity for the GnRH receptor whereas significant differences were observed in their binding kinetics. These findings provide new insights and tools for the development of improved drugs targeting the GnRH receptor by incorporating optimized kinetic binding parameters. They also suggest that bringing this knowledge on kinetics to the clinic may help in improving or adjusting treatment protocols with better patient outcomes.

References

1. Zhang, R. and F. Monsma, *The importance of drug-target residence time.* Current opinion in drug discovery & development, 2009. **12**(4): p. 488-96.
2. Copeland, R.A., D.L. Pompliano, and T.D. Meek, *Drug-target residence time and its implications for lead optimization.* Nature reviews. Drug discovery, 2006. **5**(9): p. 730-9.
3. Swinney, D.C., *Biochemical mechanisms of drug action: what does it take for success?* Nature reviews. Drug discovery, 2004. **3**(9): p. 801-8.
4. Tummino, P.J. and R.A. Copeland, *Residence time of receptor-ligand complexes and its effect on biological function.* Biochemistry, 2008. **47**(20): p. 5481-92.
5. Guo, D., et al., *Drug-target residence time-a case for G protein-coupled receptors.* Medicinal research reviews, 2014. **34**(4): p. 856-92.
6. Anthes, J.C., et al., *Biochemical characterization of desloratadine, a potent antagonist of the human histamine H(1) receptor.* European journal of pharmacology, 2002. **449**(3): p. 229-37.
7. Maillard, M.P., et al., *In vitro and in vivo characterization of the activity of telmisartan: an insurmountable angiotensin II receptor antagonist.* The Journal of pharmacology and experimental therapeutics, 2002. **302**(3): p. 1089-95.
8. Kakar, S.S., W.E. Grizzle, and J.D. Neill, *The Nucleotide-Sequences of Human Gnrh Receptors in Breast and Ovarian-Tumors Are Identical with That Found in Pituitary.* Molecular and cellular endocrinology, 1994. **106**(1-2): p. 145-149.
9. von Alten, J., et al., *GnRH analogs reduce invasiveness of human breast cancer cells.* Breast Cancer Research and Treatment, 2006. **100**(1): p. 13-21.
10. Aguilar-Rojas, A., et al., *Gonadotropin-releasing hormone receptor activates GTPase RhoA and inhibits cell invasion in the breast cancer cell line MDA-MB-231.* BMC cancer, 2012. **12**: p. 550-561.
11. Angelucci, C., et al., *GnRH receptor expression in human prostate cancer cells is affected by hormones and growth factors.* Endocrine, 2009. **36**(1): p. 87-97.
12. Stojilkovic, S.S., J. Reinhart, and K.J. Catt, *Gonadotropin-releasing hormone receptors: structure and signal transduction pathways.* Endocrine reviews, 1994. **15**(4): p. 462-99.
13. Belchetz, P.E., et al., *Hypophysial responses to continuous and intermittent delivery of hypopthalamic gonadotropin-releasing hormone.* Science, 1978. **202**(4368): p. 631-3.
14. Lahlou, N., et al., *Gonadotropin and alpha-subunit secretion during long term pituitary suppression by D-Trp6-luteinizing hormone-releasing hormone microcapsules as treatment of precocious puberty.* The Journal of clinical endocrinology and metabolism, 1987. **65**(5): p. 946-53.
15. Labrie, F., *GnRH agonists and the rapidly increasing use of combined androgen blockade in prostate cancer.* Endocrine-related cancer, 2014: p. 301-317.
16. Leone Roberti Maggiore, U., et al., *Triptorelin for the treatment of endometriosis.* Expert Opin Pharmacother, 2014. **15**(8): p. 1153-79.
17. Depalo, R., et al., *GnRH agonist versus GnRH antagonist in in vitro fertilization and embryo transfer (IVF/ET).* Reprod Biol Endocrinol, 2012. **10**: p. 26.

18. Heitman, L.H. and A.P. IJzerman, *G protein-coupled receptors of the hypothalamic-pituitary-gonadal axis: a case for Gnrh, LH, FSH, and GPR54 receptor ligands.* Medicinal research reviews, 2008. **28**(6): p. 975-1011.
19. Millar, R.P. and C.L. Newton, *Current and future applications of GnRH, kisspeptin and neurokinin B analogues.* Nat Rev Endocrinol, 2013. **9**(8): p. 451-66.
20. Sealfon, S.C., H. Weinstein, and R.P. Millar, *Molecular mechanisms of ligand interaction with the gonadotropin-releasing hormone receptor.* Endocrine reviews, 1997. **18**(2): p. 180-205.
21. Millar, R.P., et al., *Gonadotropin-releasing hormone receptors.* Endocr rev, 2004. **25**(2): p. 235-275.
22. Karten, M.J. and J.E. Rivier, *Gonadotropin-Releasing-Hormone Analog Design - Structure-Function Studies toward the Development of Agonists and Antagonists - Rationale and Perspective.* Endocrine reviews, 1986. **7**(1): p. 44-66.
23. Heise, C.E., S.K. Sullivan, and P.D. Crowe, *Scintillation proximity assay as a high-throughput method to identify slowly dissociating nonpeptide ligand binding to the GnRH receptor.* Journal of biomolecular screening, 2007. **12**(2): p. 235-9.
24. Sullivan, S.K., et al., *Kinetics of nonpeptide antagonist binding to the human gonadotropin-releasing hormone receptor: Implications for structure-activity relationships and insurmountable antagonism.* Biochemical pharmacology, 2006. **72**(7): p. 838-49.
25. Kohout, T.A., et al., *Trapping of a nonpeptide ligand by the extracellular domains of the gonadotropin-releasing hormone receptor results in insurmountable antagonism.* Molecular pharmacology, 2007. **72**(2): p. 238-47.
26. Romero, E., et al., *Pharmacokinetic/pharmacodynamic model of the testosterone effects of triptorelin administered in sustained release formulations in patients with prostate cancer.* The Journal of pharmacology and experimental therapeutics, 2012. **342**(3): p. 788-98.
27. Lewis, K.A., et al., *A single histrelin implant is effective for 2 years for treatment of central precocious puberty.* The Journal of pediatrics, 2013. **163**(4): p. 1214-6.
28. Goericke-Pesch, S., et al., *Treatment of queens in estrus and after estrus with a GnRH-agonist implant containing 4.7 mg deslorelin; hormonal response, duration of efficacy, and reversibility.* Theriogenology, 2013. **79**(4): p. 640-6.
29. Aydiner, A., et al., *Two different formulations with equivalent effect? Comparison of serum estradiol suppression with monthly goserelin and trimonthly leuprolide in breast cancer patients.* Medical oncology, 2013. **30**(1): p. 354-362.
30. Alexander, S.P.H., et al., *The Concise Guide to Pharmacology 2013/14: G Protein-Coupled Receptors.* British Journal of Pharmacology, 2013. **170**(8): p. 1459-1581.
31. Smith, P.K., et al., *Measurement of protein using bicinchoninic acid.* Analytical biochemistry, 1985. **150**(1): p. 76-85.
32. Heitman, L.H., et al., *Amiloride derivatives and a nonpeptidic antagonist bind at two distinct allosteric sites in the human gonadotropin-releasing hormone receptor.* Molecular pharmacology, 2008. **73**(6): p. 1808-15.

33. Motulsky, H.J. and L.C. Mahan, *The kinetics of competitive radioligand binding predicted by the law of mass action.* Molecular pharmacology, 1984. **25**(1): p. 1-9.
34. Schiele, F., P. Ayaz, and A. Fernandez-Montalvan, *A universal, homogenous assay for high throughput determination of binding kinetics.* Analytical biochemistry, 2014. **486C**: p. 42-49.
35. Cheng, Y. and W.H. Prusoff, *Relationship between Inhibition Constant (K1) and Concentration of Inhibitor Which Causes 50 Per Cent Inhibition (I50) of an Enzymatic-Reaction.* Biochemical pharmacology, 1973. **22**(23): p. 3099-3108.
36. Smith, D.A., B.C. Jones, and D.K. Walker, *Design of drugs involving the concepts and theories of drug metabolism and pharmacokinetics.* Medicinal research reviews, 1996. **16**(3): p. 243-66.
37. Tashkin, D.P., *Is a long-acting inhaled bronchodilator the first agent to use in stable chronic obstructive pulmonary disease?* Current opinion in pulmonary medicine, 2005. **11**(2): p. 121-8.
38. Dowling, M.R. and S.J. Charlton, *Quantifying the association and dissociation rates of unlabelled antagonists at the muscarinic M3 receptor.* British journal of pharmacology, 2006. **148**(7): p. 927-37.
39. Swinney, D.C., *The role of binding kinetics in therapeutically useful drug action.* Current opinion in drug discovery & development, 2009. **12**(1): p. 31-9.
40. Vauquelin, G. and I. Van Liefde, *Slow antagonist dissociation and long-lasting in vivo receptor protection.* Trends in pharmacological sciences, 2006. **27**(7): p. 356-9.
41. Guo, D., et al., *Functional efficacy of adenosine A_{2A} receptor agonists is positively correlated to their receptor residence time.* Br J Pharmacol, 2012. **166**(6): p. 1846-1859.
42. Sykes, D.A., M.R. Dowling, and S.J. Charlton, *Exploring the mechanism of agonist efficacy: a relationship between efficacy and agonist dissociation rate at the muscarinic M3 receptor.* Molecular pharmacology, 2009. **76**(3): p. 543-51.
43. Zweemer, A.J., et al., *Multiple binding sites for small-molecule antagonists at the CC chemokine receptor 2.* Molecular pharmacology, 2013. **84**(4): p. 551-61.
44. Slack, R.J., et al., *Pharmacological characterization of GSK1004723, a novel, long-acting antagonist at histamine H(1) and H(3) receptors.* British journal of pharmacology, 2011. **164**(6): p. 1627-41.
45. Zhang, R. and X. Xie, *Tools for GPCR drug discovery.* Acta pharmacologica Sinica, 2012. **33**(3): p. 372-84.
46. Degorce, F., et al., *HTRF: A technology tailored for drug discovery - a review of theoretical aspects and recent applications.* Current chemical genomics, 2009. **3**: p. 22-32.
47. Gubler, H., U. Schopfer, and E. Jacoby, *Theoretical and experimental relationships between percent inhibition and IC50 data observed in high-throughput screening.* J Biomol Screen, 2013. **18**(1): p. 1-13.
48. Packeu, A., et al., *Antagonist-radioligand binding to D2L-receptors in intact cells.* Biochemical pharmacology, 2008. **75**(11): p. 2192-203.
49. Sakai, S., *Effect of hormones on dissociation of prolactin from the rabbit mammary gland prolactin receptor.* Biochem J, 1991. **279 (Pt 2)**: p. 461-5.

50. Treherne, J.M. and J.M. Young, *Temperature-dependence of the kinetics of the binding of [3H]-(+)-N-methyl-4-methyldiphenhydramine to the histamine H1-receptor: comparison with the kinetics of [3H]-mepyramine.* Br J Pharmacol, 1988. **94**(3): p. 811-22.
51. Fujino, M., et al., *Syntheses and Biological-Activities of Analogs of Luteinizing-Hormone Releasing Hormone (Lh-Rh).* Biochemical and biophysical research communications, 1972. **49**(3): p. 698-705.
52. Monahan, M.W., et al., *Synthetic Analogs of Hypothalamic Luteinizing-Hormone Releasing Factor with Increased Agonist or Antagonist Properties.* Biochemistry, 1973. **12**(23): p. 4616-4620.
53. Hovelmann, S., et al., *Impact of aromatic residues within transmembrane helix 6 of the human gonadotropin-releasing hormone receptor upon agonist and antagonist binding.* Biochemistry, 2002. **41**(4): p. 1129-1136.
54. Yeo, T., et al., *Response of luteinizing hormone from columns of dispersed rat pituitary cells to a highly potent analogue of luteinizing hormone releasing hormone.* The Journal of endocrinology, 1981. **91**(1): p. 33-41.
55. Koiter, T.R., et al., *A comparison of the LH-releasing activities of LH-RH and its agonistic analogue buserelin in the ovariectomized rat.* Life sciences, 1984. **34**(16): p. 1597-604.
56. Koiter, T.R., et al., *The prolonged action of the LHRH agonist buserelin (HOE 766) may be due to prolonged binding to the LHRH receptor.* Life sciences, 1986. **39**(5): p. 443-52.
57. Flanagan, C.A., et al., *A high affinity gonadotropin-releasing hormone (GnRH) tracer, radioiodinated at position 6, facilitates analysis of mutant GnRH receptors.* Endocrinology, 1998. **139**(10): p. 4115-9.
58. Davidson, J.S., et al., *Identification of N-glycosylation sites in the gonadotropin-releasing hormone receptor: role in receptor expression but not ligand binding.* Molecular and cellular endocrinology, 1995. **107**(2): p. 241-5.
59. Hoffmann, S.H., et al., *Residues within transmembrane helices 2 and 5 of the human gonadotropin-releasing hormone receptor contribute to agonist and antagonist binding.* Molecular endocrinology, 2000. **14**(7): p. 1099-1115.
60. Davidson, J.S., et al., *Asn102 of the gonadotropin-releasing hormone receptor is a critical determinant of potency for agonists containing C-terminal glycinamide.* J Biol Chem, 1996. **271**(26): p. 15510-4.

Supplemental Data

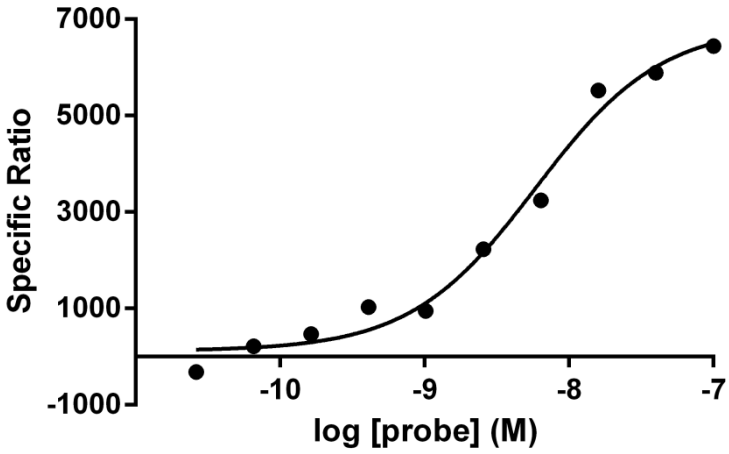

Supplementary Figure 1. Saturation equilibrium binding of fluorescent buserelin probe to Tag-lite™ GnRH cells (IC_{50} = 5.9 nM, r^2 = 0.99). Representative graph from one experiment performed in duplicate.

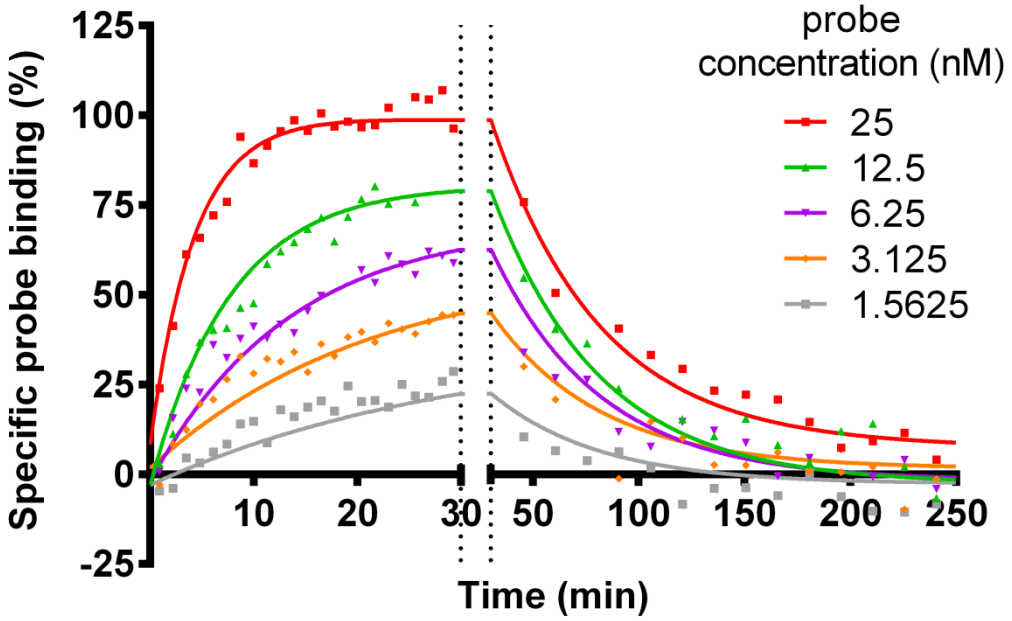

Supplementary Figure 2. Association and dissociation kinetics of five concentrations of fluorescent buserelin probe to Tag-lite™ GnRH cells. Representative graph from one experiment performed in duplicate.

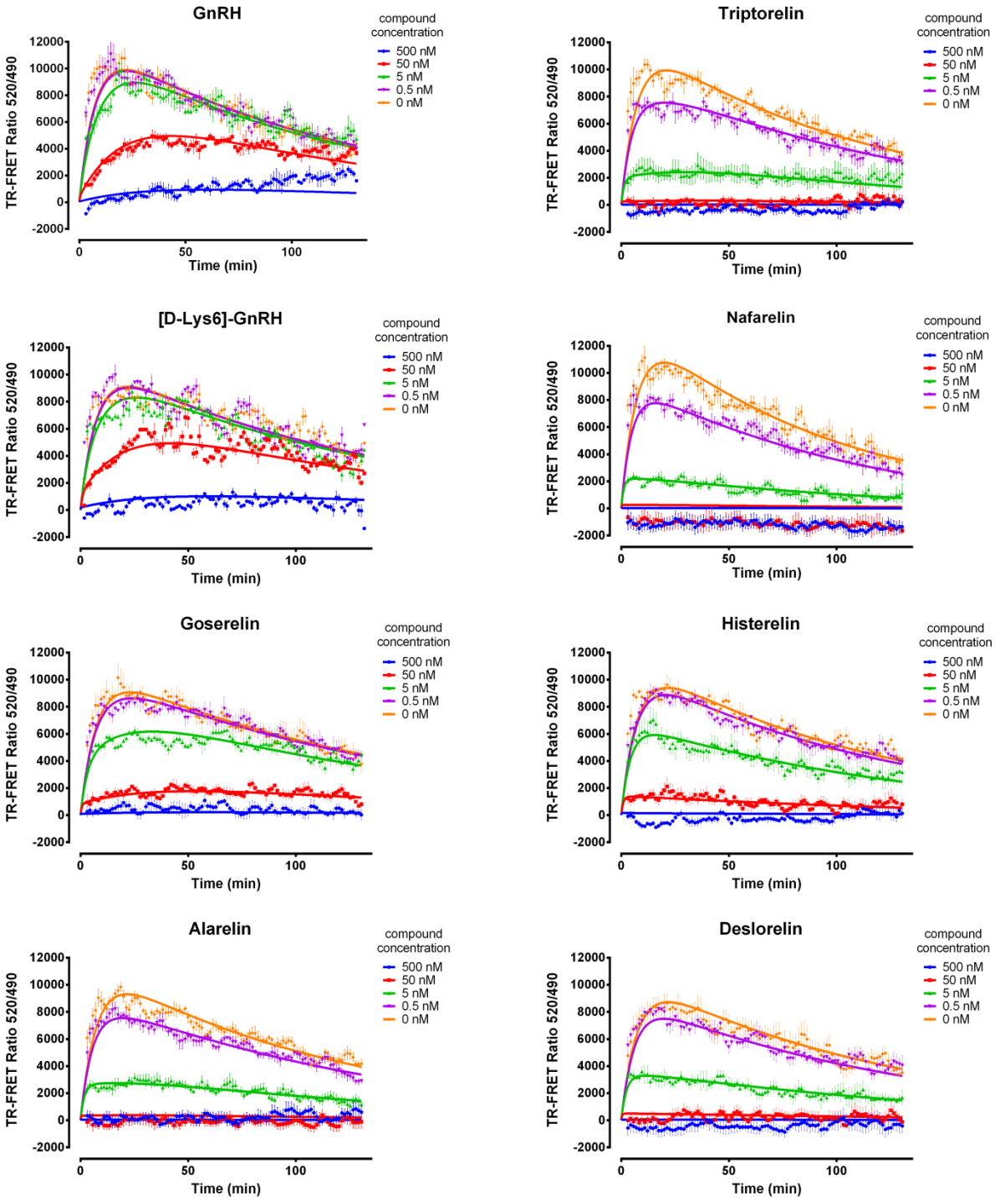

Supplementary Figure 3. kPCA traces of the GnRH peptide agonists analyzed. Four concentrations (0.5, 5, 50 and 500 nM) were examined. Representative graphs from one experiment performed in duplicate.

Chapter 4

Persistent GnRH receptor activation in pituitary αT3-1 cells analyzed with a label-free technology

Indira Nederpelt

Rochelle D. Vergroesen

Adriaan P. IJzerman

Laura H. Heitman

Biosensors & Bioelectronics **2016** *79: 721-727*

Abstract

The gonadotropin-releasing hormone (GnRH) receptor is a drug target for certain hormone-dependent diseases such as prostate cancer. In this study, we examined the activation profiles of the endogenous ligand, GnRH and a well-known marketed analog, buserelin using a label-free assay in pituitary αT3-1 cells with endogenous GnRH receptor expression. This whole cell impedance-based technology allows for the real-time measurement of morphological cellular changes. Both agonists dose-dependently decreased the impedance as a result of GnRH receptor activation with potencies of 9.37 ± 0.1 (pEC_{50} value, buserelin) and 7.87 ± 0.06 (pEC_{50} value, GnRH). Subsequently, GnRH receptor activation was completely abolished with a selective Gαq inhibitor, thereby confirming the $G\alpha_q$-coupling of the GnRH receptor in pituitary αT3-1 cells. Additionally, we observed continued responses after agonist stimulation of αT3-1 cells indicating long-lasting cellular effects. Wash-out experiments demonstrated that the long-lasting effects induced by GnRH were most likely caused by rebinding since over 70% of the original response was abolished after wash-out. In contrast, a long receptor residence time was responsible for the prolonged effects caused by buserelin, with over 70% of the original response remaining after wash-out. In summary, we validated that impedance-based label-free technology is suited for studying receptor-mediated activation in cell lines endogenously expressing the target of interest. Moreover, this real-time monitoring allows the examination of binding kinetics and its influence on receptor activation at a cellular level.

Introduction

Label-free technologies can noninvasively monitor real-time receptor-mediated phenotypic responses in living cells encompassing all involved signaling pathways [1, 2]. Label-free whole cell assays typically use a biosensor to detect a ligand-induced cellular response by ways of acoustic, electrical or other quantifiable signals [3, 4]. The main advantage of using biosensors and cell morphology as a readout is that cells can be assessed in their native and physiologically relevant environment bypassing the potentially negative effects of engineering on cell signaling [5, 6]. Additionally, label-free assays are highly sensitive therefore making them suitable for endogenous expression systems. Label-free studies are most commonly used to examine G protein-coupled receptor (GPCR) activation and G protein-signaling profiles [7-9], but also for investigating cytotoxicity, cell adhesion, proliferation, migration and invasion [6, 10, 11].

The gonadotropin-releasing hormone receptor (GnRHR) is part of the rhodopsin family of GPCRs and is sub-classified in the β-group where all endogenous ligands are peptides [12]. Its endogenous ligand, gonadotropin-releasing hormone (GnRH) is a decapeptide synthesized in hypothalamic neurons. GnRH regulates the synthesis and secretion of luteinizing hormone (LH) and follicle stimulation hormone (FSH) by selectively stimulating pituitary gonadotropes expressing the GnRH receptor [13]. The role of GnRHR in regulation of hormone levels in both males and females makes it an important target in hormone dependent diseases such as precocious puberty, fertility disorders and cancers of the prostate, mammary, ovary and endometrium [14, 15].

In the current study we investigated GnRHR-induced signaling in a heterologous CHOhGnRH-NFAT cell line as well as the αT3-1 cell line using a label-free whole cell impedance-based assay. The gonadotrope mouse pituitary αT3-1 cell line [16] is known to have high endogenous GnRHR expression [17]. In the present study, we established that both the heterologous CHOhGnRH-FNAT cell line and the endogenous αT3-1 cell line are suitable to study GnRHR-mediated signaling using a label-free technology. In addition, we were able to, for the first time, elucidate the functional effects of GnRHR agonists with different binding kinetics. Taken together, we demonstrated the importance of monitoring integrated cellular responses to gain knowledge in receptor signaling and binding kinetics that cannot be detected with traditional endpoint assays.

Methods

Materials and reagents

GnRH, buserelin and cetrorelix were purchased from Sigma-Aldrich Chemie B.V. (Zwijndrecht, the Netherlands), while UBO-QIC was purchased from the Institute of Pharmaceutical Biology (University of Bonn, Germany). [2-^{3}H(N)]-myoinositol (specific activity 10-25 Ci/mmol), isoplate-96™ white frame, clear well plates and YSi Poly-L-Lysine coated SPA beads were purchased from Perkin Elmer (Boston, MA). CHO cells stably expressing both the human GnRH receptor and an NFAT reporter gene (CHOhGnRH-NFAT) were obtained from Invitrogen (Carlsbad, CA). αT3-1 cells were a kind gift from Dr. Pamela L. Mellon (Salk Institute, San Diego, CA). xCELLigence E-plate 16 and 96 were obtained from Westburg (Leusden, the Netherlands). All other compounds and materials were obtained from standard commercial sources.

Cell culture

CHOhGnRH-NFAT cells were cultured in Dulbecco's Modified Eagle's Medium (DMEM) supplemented with 10% dialyzed fetal calf serum (FCS), 25 mM 4-(2-hydroxyethyl)-1-piperazineethanesulfonic acid (HEPES), 100 µg/ml zeocin, 600 µg/ml hygromycin, 100 IU/ml penicillin and 100 mg/ml streptomycin at 37 °C + 5% CO_2. αT3-1 cells were cultured in Dulbecco's Modified Eagle's Medium (DMEM) supplemented with 10% fetal calf serum (FCS), 4.5 g/L glucose, 548 mg/L L-glutamine, 110 mg/L pyruvate, 100 IU/ml penicillin and 100 mg/ml streptomycin at 37 °C + 5% CO_2. Cells were cultured as a monolayer and used for whole cell experiments when a confluency of ~75% was reached.

Label-free whole-cell assays

Label-free whole-cell assays were performed using the xCELLigence RTCA system [5, 6] as described previously [18].

CHOhGnRH-NFAT cells and αT3-1 cells were cultured as a monolayer on 10-cm ø culture plates and were harvested when confluency was around 75%. The experiment was started by adding 45 µl culture medium to each well to obtain background signal. Subsequently, 50 µl of cell suspension containing $1.6*10^{6}$ cells/ml was added to each well to obtain approximately 40.000 cells/well. After roughly 18 hours on the recording device station in a humidified atmosphere at 37°C + 5% CO_2, cells were stimulated with increasing concentrations of GnRH, buserelin or vehicle control. For antagonistic assays, background signal was obtained with 40 µl culture medium/well and cells were incubated with an excess of the antagonist cetrorelix (160 nM) or vehicle control 30 min prior to stimulation with submaximal (EC_{80}) concentrations of GnRH (31.6 nM) or buserelin (1 nM). For inhibition of the $G\alpha_q$ signaling pathway, αT3-1 cells were pretreated with 1 µM UBO-QIC or vehicle control 30 min prior to stimulation with submaximal (EC_{80}) concentrations of GnRH (31.6 nM)

or buserelin (1 nM). Submaximal (EC_{80}) concentrations of GnRH and buserelin were derived from concentration-response curves using Total Area Under the Curve (AUC) analysis (see section 'Data analysis').

Inositol phosphate accumulation assay

αT3-1 cells were seeded at a cell density of 100.000 cells/well with [^{3}H]-myoinositol (4 µCi/ml) overnight at 37°C and 5% CO_2. Subsequently, cells were washed twice with Buffer A containing 127 mM NaCl, 5 mM KCl, 2 mM $MgCl_2$, 0.5 mM NaH_2PO_4, 5 mM $NaHCO_3$, 1.8 mM $CaCl_2$, 10 mM HEPES and 0.1% BSA. Thereafter, cells were incubated for 20 minutes at 37 °C with Buffer A supplemented with 50 mM LiCl, followed by stimulation with increasing concentrations of GnRH or buserelin for 60 min at 37°C. Cells were lysed through 1 hour incubation with 10 mM formic acid at 4°C, after which 20 µL of solution was transferred to an isoplate™ 96 followed by addition of 80 µL YSi Poly-L-Lysine-coated SPA beads at 12 mg/ml. The mixture was shaken at room temperature for 60 min prior to a 5 min centrifuge step at 1500 rpm. Radioactivity of the extract/bead mixture was determined by scintillation spectrometry using the P-E 1450 Micobeta Wallac Trilux scintillation counter according to instruction manual (Perkin Elmer, Groningen, the Netherlands).

Data analysis

All experimental data were analyzed using GraphPad Prism 5.0 (GraphPad Software Inc., San Diego, CA). Cell index (CI) traces were normalized to time of agonist addition and then exported from RTCA Software 1.2 (Roche, Germany). Total AUC values up to 180 min after agonist addition were used for data analyses. Baseline was removed by subtracting vehicle, antagonist and inhibitor controls from corresponding normalized CI (NCI) traces.

Efficacy (E_{max}) and potency (pEC_{50}) values for GnRH and buserelin were obtained with non-linear regression of Total AUC data fitted by log(agonist) vs. response - Variable slope. Results were normalized to Total AUC induced by the maximal concentration of GnRH. Total AUC of agonist-induced cellular responses in presence of antagonist or pathway inhibitor were normalized to Total AUC obtained from αT3-1 cells responses treated with submaximal concentrations (EC_{80}) of corresponding agonist.

Efficacy (E_{max}) and potency (pEC_{50}) values for IP accumulation assay were obtained using non-linear regression of total counts upon GnRH or buserelin-induced $G\alpha_q$-activation fitted by log(agonist) vs. response - Variable slope. Results were normalized to total counts induced by the maximal concentration of GnRH.

All values obtained are means ± SEM of at least three independent experiments performed in duplicate.

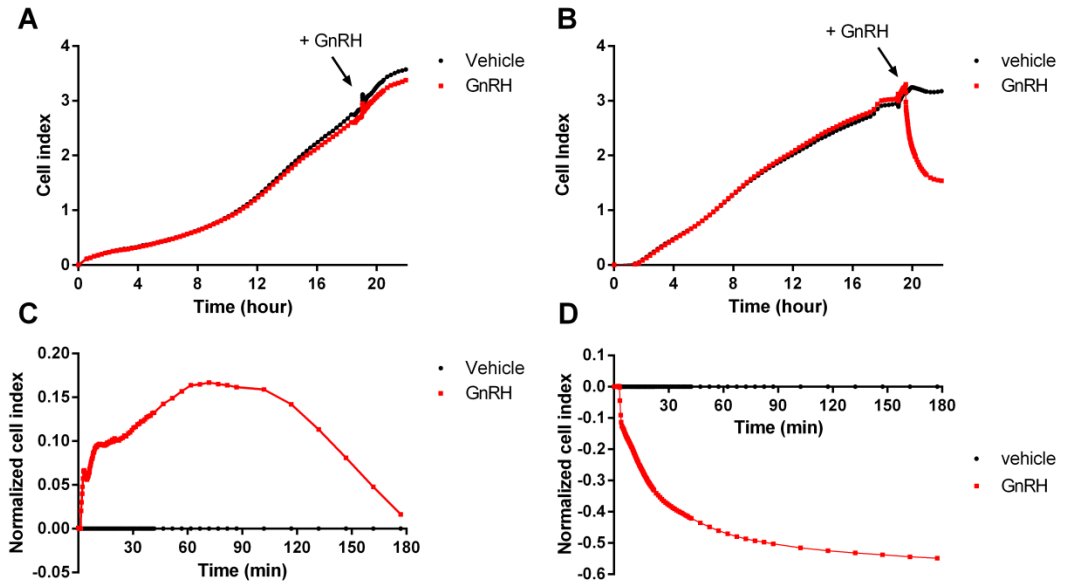

Figure 1: Real-time monitoring of the cell index as a measure of proliferation and adherence of CHOhGnRH-FNAT cells (A) and αT3-1 cells (B) before and after (18 h) addition of 1 µM GnRH. Zoom in on the effect of GnRH yielding the normalized cell index after addition of 1 µM GnRH to CHOhGnRH-NFAT cells (C) and αT3-1 cells (D).

Results

GnRHR signaling in heterologous and endogenous cells on the xCELLigence

Heterologous GnRH receptor-mediated signaling in CHOhGnRH-NFAT cells was monitored on the xCELLigence system. Overnight proliferation resulted in a cell index of approximately 4.0 (Figure 1A). Typically, the impedance increased upon agonist addition with a first peak around 10 min of approximately 0.075 NCI, followed by a second peak reaching approximately 0.15 NCI around 80 minutes. The signal decreased again back to baseline after approximately 180 min (Figure 1C).

Stimulation of CHOhGnRH-NFAT cells with increasing concentrations of GnRH and its analog buserelin resulted in a concentration-dependent increase in impedance (Figure 2A and 2C). From these impedance changes a concentration-response curve could be obtained providing pEC_{50} values of 10 ± 0.1 and 10.6 ± 0.2 for GnRH and buserelin, respectively (Figure 2E and Table 1). The efficacy of buserelin was similar to that of GnRH, namely 98 ± 4.5% (Table 1). To confirm that the observed changes in impedance are GnRHR-specific the

parental CHO cell line was used as a negative control. Treatment of these cells with 1 µM of GnRH did not result in a change in impedance (Figure 3A and 3D). Additionally, the selective GnRH peptide antagonist cetrorelix was able to block receptor activation by GnRH (Figure 3B and 3D).

Table 1: potency and efficacy of GnRH and buserelin obtained with xCELLigence and IP accumulation experiments performed with CHOhGnRH-NFAT and αT3-1 cells.

Agonist	CHOhGnRH-NFAT		αT3-1			
	(xCELLigence[#])		(xCELLigence[#])		(IP accumulation)	
	pEC_{50} (EC_{50} in nM)	E_{max} (%)	pEC_{50} (EC_{50} in nM)	E_{max} (%)	pEC_{50} (EC_{50} in nM)	E_{max} (%)
GnRH	10 ± 0.1 (0.1)	100 ± 3	7.8 ± 0.06 (17)	100 ± 1	7.9 ± 0.2 (12)	100 ± 0.9
Buserelin	10.6 ± 0.2 (0.03)	98 ± 5	9.3 ± 0.1 (0.46)	90 ± 3[*]	10 ± 0.1 (0.09)	115 ± 1[***]

Values are means ± SEM of three separate experiments performed in duplicate. [#] Values were calculated with total AUC analysis up to 180 min after agonist addition. Data were normalized to maximal response obtained for GnRH. [*]=p>0.05, [***]=p>0.0005, compared to E_{max} GnRH determined with Student's *t* test.

To examine if the GnRHR-mediated responses in the heterologous cell line could also be observed in the endogenous pituitary αT3-1 cell line, we studied GnRH signaling with the xCELLigence on this cell line. Overnight proliferation gave a cell index of roughly 3.0 (Figure 1B). In contrast to the effect on CHOhGnRH-NFAT cells, addition of 1 µM GnRH resulted in a decrease in impedance reaching and maintaining its plateau around 0.4 NCI within 1 hour up to but not limited to 180 min after stimulation (Figure 1D).

Addition of increasing concentrations of GnRH and buserelin resulted in a concentration-dependent decrease in impedance (Figure 2B and 2D). Interestingly, low concentrations of both GnRH and buserelin resulted in a positive NCI. The concentration-response curves gave an EC_{50} value of 17 nM for GnRH and a 37-fold lower EC_{50} value of 0.46 nM for buserelin (Figure 2F and Table 1). Buserelin had a slightly, yet significantly, lower efficacy than GnRH of 90 ± 3.1%. The GnRHR-mediated responses were selectively blocked by pretreatment with the GnRH peptide antagonist cetrorelix (3.8 ± 0.3%), supportive of a receptor-specific effect (Figure 3C, 3D). Since the xCELLigence detects morphological changes rather than one specific intracellular signaling pathway following GPCR activation we suppressed $G\alpha_q$-mediated signaling with inhibitor UBO-QIC prior to GnRH treatment. This selective inhibition of the $G\alpha_q$ pathway completely abolished GnRHR activation (3.8± 1.6%) (Figure 3D and 3E).

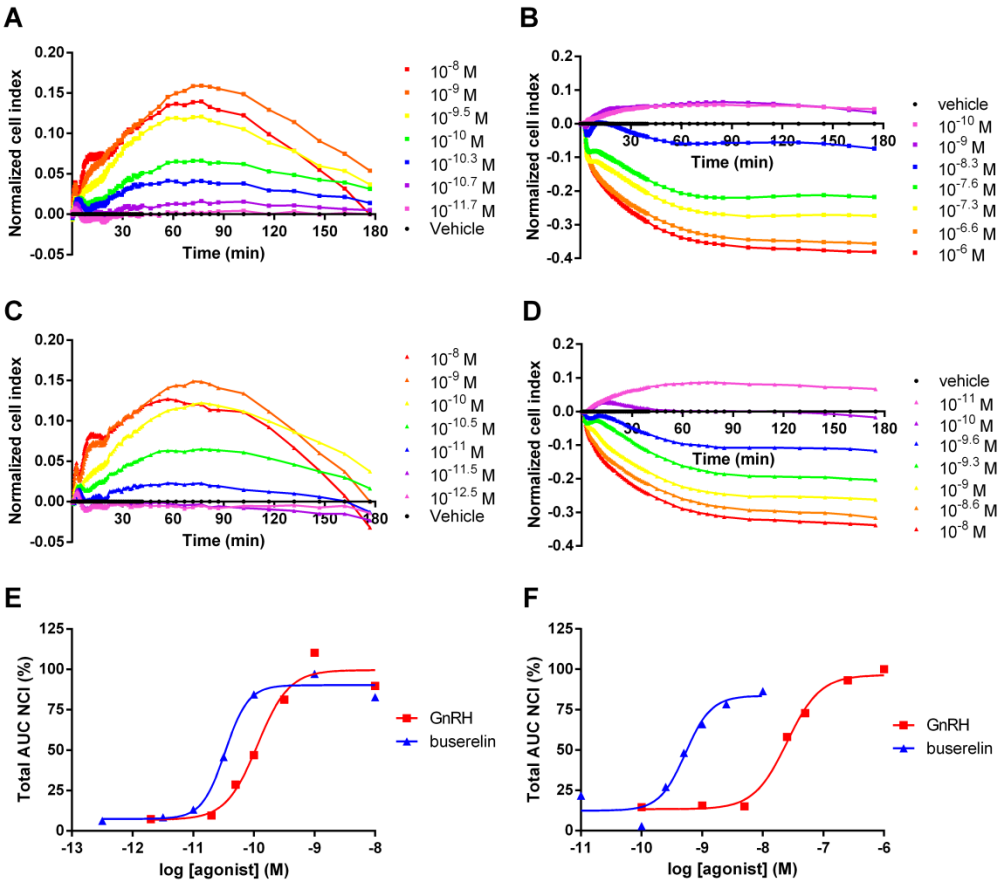

Figure 2: Concentration-dependent effects of GnRH and buserelin on CHOhGnRH-NFAT (left) and αT3-1 (right) cells. Representative graph of one experiment performed in duplicate of normalized cell index (NCI) after stimulation with increasing concentrations of GnRH (A; CHOhGnRH and B; αT3-1) or buserelin (C; CHOhGnRH and D; αT3-1). Representative concentration-effect curve of GnRH and buserelin derived from total AUC up to 180 min after agonist stimulation, data were normalized to maximal response after GnRH stimulation (E; CHOhGnRH and F; αT3-1).

GnRHR signaling in pituitary αT3-1 cells using second messenger assays

To compare our obtained potency and efficacy values for GnRH and buserelin to a more traditional second messenger assay we examined IP accumulation in αT3-1 cells upon GnRHR-activation which is a consequence of activating the $G\alpha_q$ pathway. Concentration-response curves of GnRH and buserelin yielded pEC_{50} values of 7.9 ± 0.2 and 10 ± 0.1, respectively (Supplementary Figure 1). In this assay, buserelin showed a significant increase in efficacy namely 115 ± 1% (Table 1).

Functional consequence of differential receptor binding kinetics in pituitary αT3-1 cells on the xCELLigence

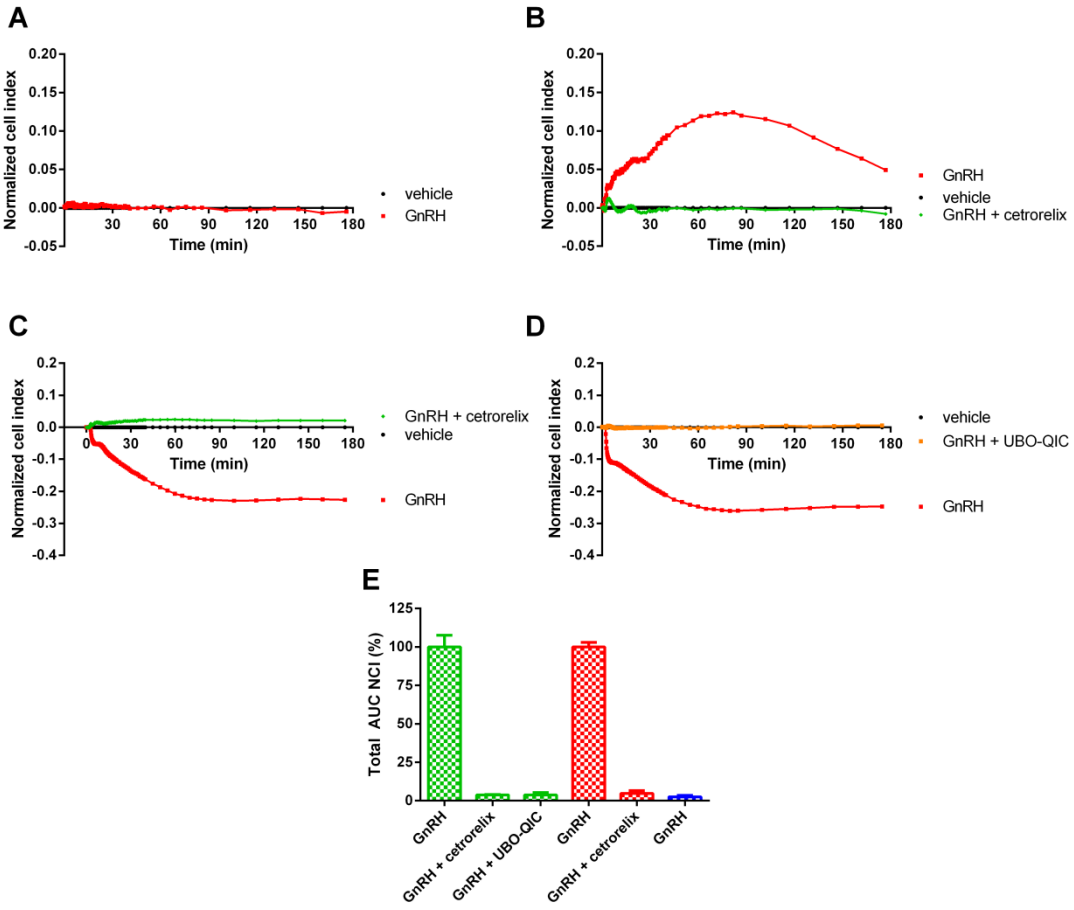

Figure 3: GnRHR mediated responses in parental CHO cells, CHOhGnRH-NFAT cells or αT3-1 cells. Representative graph of one experiment performed in duplicate of normalized cell index (NCI) after stimulation with GnRH of parental CHO cells (A), CHOhGnRH-NFAT cells (B) or αT3-1 cells (C) with or without pretreatment with cetrorelix or αT3-1 cells (D) with or without pretreatment with UBO-QIC. Bar graph of total AUC up to 180 min of cells stimulated with GnRH with or without 160 nM cetrorelix or 1 µM UBO-QIC pretreatment in αT3-1 cells (green), CHOhGnRH-NFAT cells (red) or parental CHO cells (blue), data were normalized to maximal response after GnRH stimulation without inhibitor (E).

GnRH and buserelin both showed sustained signaling on the xCELLigence, i.e. a decrease in impedance reaching and maintaining its plateau around 0.4 NCI within 1 hour up to but not limited to 180 min after stimulation, which indicates long-lasting functional effects. To examine whether these effects were due to a long drug-target residence time we performed a washout experiment. Thirty minutes after stimulating with EC_{80} concentrations of GnRH or buserelin, cells were washed followed by further label-free measurements (Figure 4A). Washout after stimulating the cells with GnRH or buserelin decreased the response relative to unwashed conditions to 43 ± 6% or 79 ± 5% after 30 min, respectively (Figure 4B

and Table 2). The response continued to decline after 120 minutes for GnRH (27 ± 7%) whereas buserelin remained active at approximately 80% of the control activation (Figure 4B and Table 2).

Discussion

Label-free impedance-based xCELLigence is suitable to study GnRHR activation

Label-free whole cell assays provide new perspectives in studying GPCR signaling by continuously measuring cell morphology changes upon receptor activation [2, 6, 8, 9]. These novel phenotypic functional assays have many advantages over traditional endpoint assays, as they measure integrated cellular responses rather than signals downstream one particular G protein pathway. Label-free whole cell assays thus encompass a complete overview of cellular function and responses after receptor activation. Here, we demonstrate for the first time signaling of the GnRH receptor using the label-free whole cell impedance-based xCELLigence system in heterologous CHOhGnRH-NFAT cells as well as endogenous gonadotrope pituitary αT3-1 cells.

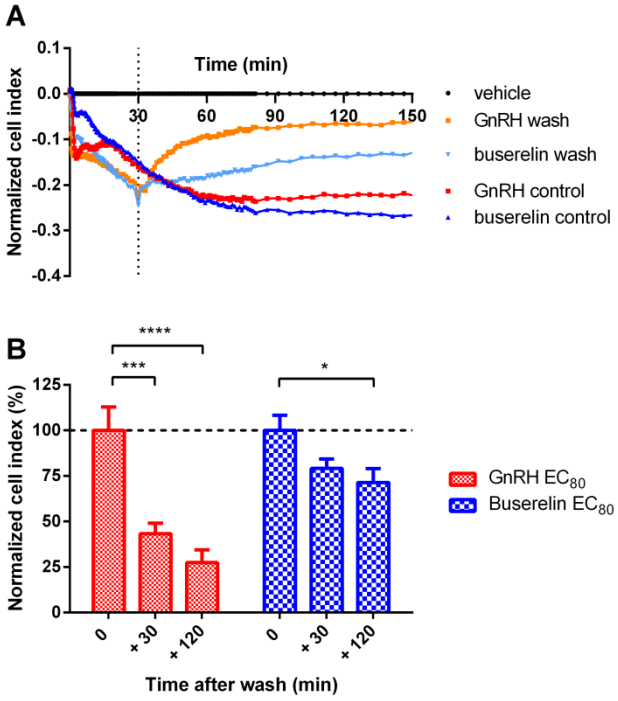

Figure 4: Wash out of αT3-1 cells stimulated with GnRH or buserelin. (A) Representative graphs of one experiment performed in duplicate after stimulation with either GnRH or buserelin (control) or followed by wash out at 30 min indicated by vertical dashed line (wash). (B) Bar graph of normalized cell index agonist induced effects 0 min, 30 min and 120 min after wash out (B). Data are mean ± SEM from three separate experiments performed in duplicate. Data were normalized to maximal response obtained before wash out, indicated as ‘’0’’, *= $p<0.05$, ***= $p<0.001$, ****= $p<0.0001$.

Initial experiments with CHOhGnRH-NFAT cells demonstrated that the xCELLigence system is suitable to study GnRHR-mediated responses in a heterologous expression system. Concentration-response curves provided a pEC50 value of 10 ± 0.1 for GnRH, which is comparable to previously reported data [19]. Control experiments with the parental CHO cell line and the selective GnRHR peptide antagonist cetrorelix showed

absence of GnRHR responses, further verifying that the observed responses were GnRHR-mediated.

Subsequent experiments established that the endogenous pituitary αT3-1 cell line is also well suited for studying GnRHR signaling on the xCELLigence. GnRH-mediated signals were selectively blocked by the peptide antagonist cetrorelix, confirming the agonist responses were GnRHR specific. Additionally, we observed that silencing of the $G\alpha_q$ pathway with the selective inhibitor UBO-QIC completely abrogated agonist-mediated αT3-1 cell responses. This illustrates that GnRH and buserelin signal through the $G\alpha_q$ pathway, which is in agreement with previously reported data [14, 20-22].

Considering that the endogenous mouse pituitary αT3-1 cell line is derived from immortalized anterior pituitary gonadotrope cells [16] and the mouse and human GnRHR are 99 % homologous, all further experiments were continued with the endogenous pituitary αT3-1 cell line.

Table 2: Receptor activation after wash out of EC_{80} concentrations of GnRH or buserelin

	EC_{80} response (%)	
Time after wash out	GnRH	Buserelin
0 min	100 ± 13	100 ± 8
+ 30 min	43 ± 6***	79 ± 5
+ 120 min	27 ± 7****	71 ± 8*

Values are means ± SEM of three separate experiments performed in duplicate. Cells were washed after 30 min agonist stimulation and values were calculated using normalized cell index at 0 min, 30 min and 120 min after wash out. Data were normalized to maximal response obtained before wash out, indicated as ''0 min''. *= p<0.05, ***= p<0.001, ****= p<0.0001, compared to 0 min determined using one-way ANOVA with Dunnett's post-test.

Two well-known GnRH receptor agonists were studied in this research; the endogenous ligand GnRH and buserelin a GnRHR agonist that slowly dissociates from the receptor [23]. In the label-free whole cell assays both agonists were able to activate the GnRH receptor in a concentration-dependent manner, albeit that buserelin had a 37-fold higher potency than GnRH (0.46 nM and 17 nM, respectively). Similar findings were observed in more traditional IP accumulation assays; here buserelin was 133-fold more potent than GnRH (0.09 nM and 12 nM, respectively). A much smaller (7-fold) potency shift between GnRH and buserelin has been reported before (3.4 nM and 0.47 nM) with total inositol phosphate production measurements using αT3-1 cells [24]. A possible explanation could be that the incubation time in their assay was only 30 min, which could result in an underestimated potency since buserelin might not yet have reached equilibrium. In our hands, the potency of GnRH was in the same range between the impedance-based and IP accumulation assays while buserelin was 5-fold more potent in the latter. Differences in

potency between label-free whole cell assays and traditional second messenger functional assays have been observed before [25-28].

Long-lasting residence time can be translated to a persistent activation profile in vitro

In contrast to previously published xCELLigence data on GPCR activation [25, 29], we observed long-lasting signaling events of GnRH and buserelin on αT3-1 cells implying persisted GnRHR activation. This finding might be explained by either rebinding of the agonist to the receptor or long-lasting target binding [30]. Long-lasting target residence time has already been reported for buserelin, however GnRH was found to have a shorter residence time [23]. It has been postulated that the *in vivo* high potency and long duration of action of buserelin was caused by long-lasting GnRH receptor binding [31-33]. Therefore, we hypothesized that the long-lasting effects caused by GnRH are due to rebinding of this molecule to the receptor while the long-lasting effects caused by buserelin are a result of this compound's prolonged target binding. To test this hypothesis we designed a washout experiment to minimize rebinding where we examined the remaining cellular response by GnRH and buserelin after washing. Wash out of GnRH or buserelin at EC_{80} concentrations showed a decreased signaling response for both agonists. Conversely, this decreased response in signaling was much more outspoken for GnRH than for buserelin. These results confirm our hypothesis, being that the observed persisted signaling profile of GnRH was due to rebinding while the persisted signaling profile of buserelin is a combination of both rebinding and prolonged drug-target occupancy caused by long drug-receptor residence time. Casarosa et al. [34], reported on a washout second messenger assay, examining cAMP production. In this assay the long residence time β_2 adrenoceptor (β_2-AR) agonist olodaterol remained associated with the receptor, while the short residence time β_2-AR agonist salbutamol was readily washed out. Lindstrom and coworkers performed washout experiments with U373MG cells endogenously expressing the Tachykinin 1 receptor (NK1R) measuring intracellular Ca^{2+} levels. They demonstrated that the response to the endogenous agonist Substance P was not restored after a 60 min wash out of the slowly dissociating NK1R antagonist aprepitant [35].

Conclusions

We have validated the label-free whole cell xCELLigence system as a valuable biosensor to investigate GnRHR-mediated signaling in endogenous pituitary αT3-1 cells. For the first time in a label-free assay environment we showed prolonged receptor signaling due to drug-target binding kinetics by wash out experiments. Our results illustrate the importance of monitoring phenotypic and integrative responses using label-free whole cell assays, since

traditional end-point assays are less suited to acquire information on drug-target binding kinetics in real-time. Incorporating whole cell label-free technologies in drug development will provide a more complete overview of the functional properties of a ligand and hopefully improve future drug discovery.

References

1. Scott, C.W. and M.F. Peters, *Label-free whole-cell assays: expanding the scope of GPCR screening.* Drug discovery today, 2010. **15**(17-18): p. 704-16.
2. Rocheville, M., et al., *Mining the potential of label-free biosensors for seven-transmembrane receptor drug discovery.* Progress in molecular biology and translational science, 2013. **115**: p. 123-42.
3. Zhang, R. and X. Xie, *Tools for GPCR drug discovery.* Acta pharmacologica Sinica, 2012. **33**(3): p. 372-84.
4. Fang, Y., *The development of label-free cellular assays for drug discovery.* Expert opinion on drug discovery, 2011. **6**(12): p. 1285-98.
5. Yu, N., et al., *Real-time monitoring of morphological changes in living cells by electronic cell sensor arrays: an approach to study G protein-coupled receptors.* Analytical chemistry, 2006. **78**(1): p. 35-43.
6. Xi, B., et al., *The application of cell-based label-free technology in drug discovery.* Biotechnology journal, 2008. **3**(4): p. 484-95.
7. Stallaert, W., et al., *Impedance responses reveal beta(2)-adrenergic receptor signaling pluridimensionality and allow classification of ligands with distinct signaling profiles.* PloS one, 2012. **7**(1): p. e29420.
8. Schroder, R., et al., *Deconvolution of complex G protein-coupled receptor signaling in live cells using dynamic mass redistribution measurements.* Nature biotechnology, 2010. **28**(9): p. 943-9.
9. Deng, H., H. Sun, and Y. Fang, *Label-free cell phenotypic assessment of the biased agonism and efficacy of agonists at the endogenous muscarinic M3 receptors.* Journal of pharmacological and toxicological methods, 2013. **68**(3): p. 323-33.
10. Leurs, U., et al., *GnRH-III based multifunctional drug delivery systems containing daunorubicin and methotrexate.* European journal of medicinal chemistry, 2012. **52**: p. 173-83.
11. Atienza, J.M., et al., *Dynamic and label-free cell-based assays using the real-time cell electronic sensing system.* Assay and drug development technologies, 2006. **4**(5): p. 597-607.
12. Fredriksson, R., et al., *The G-protein-coupled receptors in the human genome form five main families. Phylogenetic analysis, paralogon groups, and fingerprints.* Mol Pharmacol, 2003. **63**(6): p. 1256-72.
13. Stojilkovic, S.S., J. Reinhart, and K.J. Catt, *Gonadotropin-releasing hormone receptors: structure and signal transduction pathways.* Endocrine reviews, 1994. **15**(4): p. 462-99.
14. McArdle, C.A., *Gonadotropin-releasing hormone receptor signaling: biased and unbiased.* Mini Rev Med Chem, 2012. **12**(9): p. 841-850.
15. Labrie, F., *GnRH agonists and the rapidly increasing use of combined androgen blockade in prostate cancer.* Endocrine-related cancer, 2014: p. 301-317.

16. Windle, J.J., R.I. Weiner, and P.L. Mellon, *Cell lines of the pituitary gonadotrope lineage derived by targeted oncogenesis in transgenic mice.* Molecular endocrinology, 1990. **4**(4): p. 597-603.
17. Shah, B.H. and G. Milligan, *The gonadotrophin-releasing hormone receptor of alpha T3-1 pituitary cells regulates cellular levels of both of the phosphoinositidase C-linked G proteins, Gq alpha and G11 alpha, equally.* Molecular pharmacology, 1994. **46**(1): p. 1-7.
18. Hillger, J.M., et al., *Whole-cell biosensor for label-free detection of GPCR-mediated drug responses in personal cell lines.* Biosensors & Bioelectronics, 2015. **74**: p. 233-242.
19. Lu, Z.L., et al., *Structural determinants for ligand-receptor conformational selection in a peptide G protein-coupled receptor.* The Journal of biological chemistry, 2007. **282**(24): p. 17921-9.
20. Hsieh, K.P. and T.F. Martin, *Thyrotropin-releasing hormone and gonadotropin-releasing hormone receptors activate phospholipase C by coupling to the guanosine triphosphate-binding proteins Gq and G11.* Molecular endocrinology, 1992. **6**(10): p. 1673-81.
21. Naor, Z., *Signaling by G-protein-coupled receptor (GPCR): studies on the GnRH receptor.* Frontiers in neuroendocrinology, 2009. **30**(1): p. 10-29.
22. Grosse, R., et al., *Gonadotropin-releasing hormone receptor initiates multiple signaling pathways by exclusively coupling to G(q/11) proteins.* The Journal of biological chemistry, 2000. **275**(13): p. 9193-200.
23. Nederpelt, I., et al., *Characterization of 12 GnRH peptide agonists - a kinetic perspective.* Br J Pharmacol, 2016. **173**(1): p. 128-41.
24. Anderson, L., G. Milligan, and K.A. Eidne, *Characterization of the gonadotrophin-releasing hormone receptor in alpha T3-1 pituitary gonadotroph cells.* The Journal of endocrinology, 1993. **136**(1): p. 51-8.
25. Kammermann, M., et al., *Impedance measurement: a new method to detect ligand-biased receptor signaling.* Biochemical and biophysical research communications, 2011. **412**(3): p. 419-24.
26. Watts, A.O., et al., *Label-free impedance responses of endogenous and synthetic chemokine receptor CXCR3 agonists correlate with Gi-protein pathway activation.* Biochemical and biophysical research communications, 2012. **419**(2): p. 412-8.
27. Scandroglio, P., et al., *Evaluation of cannabinoid receptor 2 and metabotropic glutamate receptor 1 functional responses using a cell impedance-based technology.* Journal of biomolecular screening, 2010. **15**(10): p. 1238-47.
28. Guo, D., et al., *Functional efficacy of adenosine A_{2A} receptor agonists is positively correlated to their receptor residence time.* Br J Pharmacol, 2012. **166**(6): p. 1846-1859.
29. Zweemer, A.J., et al., *Multiple binding sites for small-molecule antagonists at the CC chemokine receptor 2.* Molecular pharmacology, 2013. **84**(4): p. 551-61.
30. Vauquelin, G. and S.J. Charlton, *Long-lasting target binding and rebinding as mechanisms to prolong in vivo drug action.* British journal of pharmacology, 2010. **161**(3): p. 488-508.

31. Yeo, T., et al., *Response of luteinizing hormone from columns of dispersed rat pituitary cells to a highly potent analogue of luteinizing hormone releasing hormone.* The Journal of endocrinology, 1981. **91**(1): p. 33-41.
32. Koiter, T.R., et al., *A comparison of the LH-releasing activities of LH-RH and its agonistic analogue buserelin in the ovariectomized rat.* Life sciences, 1984. **34**(16): p. 1597-604.
33. Koiter, T.R., et al., *The prolonged action of the LHRH agonist buserelin (HOE 766) may be due to prolonged binding to the LHRH receptor.* Life sciences, 1986. **39**(5): p. 443-52.
34. Casarosa, P., et al., *Functional and biochemical rationales for the 24-hour-long duration of action of olodaterol.* The Journal of pharmacology and experimental therapeutics, 2011. **337**(3): p. 600-9.
35. Lindstrom, E., et al., *Neurokinin 1 receptor antagonists: correlation between in vitro receptor interaction and in vivo efficacy.* The Journal of pharmacology and experimental therapeutics, 2007. **322**(3): p. 1286-93.

Supplemental Data

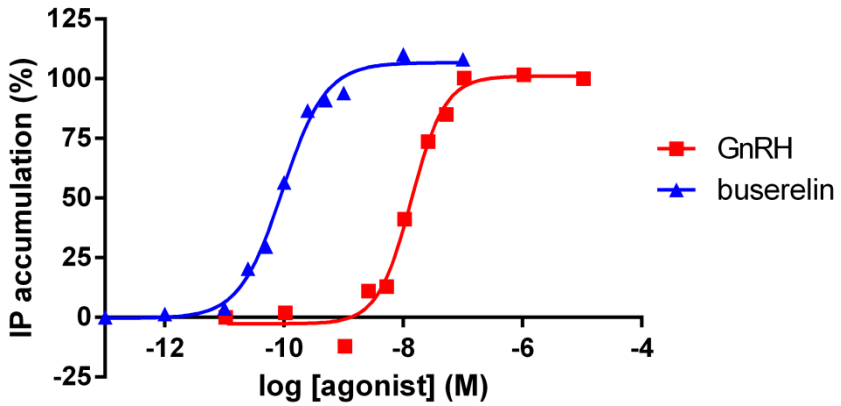

Supplementary Figure 1: Concentration-dependent effects of GnRHR agonists in αT3-1 cells. IP accumulation upon stimulation with increasing concentrations of GnRH (red) or buserelin (blue). A representative graph is shown of one experiment performed in duplicate, data were normalized to maximal response after GnRH stimulation.

Chapter 5

Kinetic binding and activation profiles of endogenous tachykinins targeting the NK1 receptor

Indira Nederpelt

Dave Bleeker

Bruno Tuijt

Adriaan P. IJzerman

Laura H. Heitman

Biochemical Pharmacology **2016** *118: 88-95*

Abstract

Ligand-receptor binding kinetics (i.e. association and dissociation rates) are emerging as important parameters for drug efficacy *in vivo*. Awareness of the kinetic behavior of endogenous ligands is pivotal, as drugs often have to compete with those. The binding kinetics of neurokinin 1 (NK1) receptor antagonists have been widely investigated while binding kinetics of endogenous tachykinins have hardly been reported, if at all. Therefore, the aim of this research was to investigate the binding kinetics of endogenous tachykinins and derivatives thereof and their role in the activation of the NK1 receptor.

We determined the binding kinetics of seven tachykinins targeting the NK1 receptor. Dissociation rate constants (k_{off}) ranged from 0.026 ± 0.0029 min^{-1} (Sar^9, $Met(O_2)^{11}$-SP) to 0.21 ± 0.015 min^{-1} (septide). Association rate constants (k_{on}) were more diverse: substance P (SP) associated the fastest with a k_{on} value of 0.24 ± 0.046 nM^{-1} min^{-1} while neurokinin A (NKA) had the slowest association rate constant of 0.001 ± 0.0002 nM^{-1} min^{-1}. Kinetic binding parameters were highly correlated with potency and maximal response values determined in label-free impedance-based experiments on U-251 MG cells.

Our research demonstrates large variations in binding kinetics of tachykinins which correlate to receptor activation. These findings provide new insights in the ligand-receptor interactions of tachykinins and underline the importance of measuring binding kinetics of both drug candidates and competing endogenous ligands.

Introduction

Ligand-receptor binding kinetics are reflected by the association and dissociation rates of a ligand to and from its receptor. These kinetic parameters are increasingly acknowledged as a key player in drug-target interactions and functional effects *in vivo* [1-5]. Understanding of desired binding kinetics of a drug for the target of interest is crucial for efficient and efficacious drug development. For example, for the muscarinic M_3 receptor a slow drug-target dissociation rate is desirable to achieve prolonged *in vivo* efficacy and better patient compliance [6]. In contrast, for the dopamine D_2 receptor a fast dissociation rate is desired to minimize on-target side effects [7]. Notably, the majority of successful drugs achieve their potency by competing with endogenous ligands for the same orthosteric binding site. Therefore, knowledge of the pharmacological behaviour of endogenous ligands could benefit the understanding of desirable binding kinetics of competing drugs for the target of interest.

The tachykinin receptor family consists of three neuropeptide G protein-coupled receptors (GPCRs), the neurokinin 1 receptor (NK_1R), neurokinin 2 receptor (NK_2R) and neurokinin 3 receptor (NK_3R). The endogenous ligands for these receptors are substance P (SP), neurokinin A (NKA), neurokinin B (NKB). Each endogenous tachykinin has a specific rank order to activate tachykinin receptors with regards to potency and affinity, namely SP>NKA>NKB for the NK_1 receptor, NKA>NKB>SP for the NK_2 receptor and NKB>NKA>SP for the NK_3 receptor. In 2000, a fourth endogenous tachykinin was discovered, namely hemokinin-1 [8]. Tachykinin receptors and their endogenous ligands are distributed throughout the central and peripheral nervous system and play an important role in e.g. nociception, cell proliferation, smooth muscle contraction and inflammation [9-11].

The neurokinin 1 receptor couples predominantly through the $G\alpha_q$ protein signaling pathway, but can also induce $G\alpha_s$ protein and β-arrestin signaling [12, 13]. Although a plethora of literature is available on G protein signaling of NK1 peptide agonists [14-16] and binding kinetics of NK1 antagonists [17-19], the kinetic binding parameters of the most well-known endogenous tachykinins (i.e. SP, NKA, NKB and Hemokinin-1) and their synthetic or truncated derivatives (i.e. septide, Pro^9-SP, SP(4-11) and Sar^9,$Met(O_2)^{11}$-SP) have rarely been reported, if at all. Therefore, our aim was to determine the binding kinetics of the afore mentioned tachykinins (Figure 1) by using a radiolabeled competition association assay. In an effort to correlate the binding kinetics to functional effects *in vitro* we used a label-free impedance-based assay to examine receptor activation in human astrocytoma U-251 MG cells endogenously expressing the NK1 receptor. This label-free system allows for the real-time monitoring of phenotypic receptor-mediated responses encompassing the entire

signaling cascade which makes it a very suitable system for this target that has been proven to activate multiple downstream signaling pathways [20, 21].

In summary, we have for the first time used a competition association assay to determine the binding kinetics of endogenous tachykinins and their most well-known derivatives. In addition, we were able to correlate the binding kinetics to functional effects *in vitro* using a whole-cell label-free technology. Our research illustrates the importance of knowledge of the association and dissociation rates of endogenous tachykinins and their role in receptor activation.

Figure 1: Amino acid sequences of the examined tachykinins. The differences between the peptides are expressed in green. Sar = methylated glycine, Met (O_2) = oxidized methionine and pGlu = pyro-glutamic acid.

Methods

Reagents and peptides

SP, hemokinin-1 and U-251 MG cells were purchased from Sigma-Aldrich (St. Louis, MO). NKA, NKB, septide, Pro^9-SP, SP (4-11), Sar^9,$Met(O_2)^{11}$-SP and antagonist SC203437 were obtained from Bio-Connect (Huissen, The Netherlands). Aprepitant was a kind gift from Roche Innovation Center Basel (Basel, Switzerland) and protease inhibitors (complete mini

cocktail) were purchased from Roche Diagnostics (Mannheim, Germany). [^{3}H][Sar^9,Met(O_2)^{11}]SP (specific activity 25-55 Ci/mmol) was obtained from Perkin Elmer (Boston, MA). Chinese Hamster Ovary (CHO) cells stably expressing the human neurokinin 1 receptor (CHOhNK1 cells) were kindly provided by AstraZeneca (Macclesfield, UK). xCELLigence E-plate 16 and 96 were purchased from Westburg (Leusden, the Netherlands). All other compounds and materials were obtained from standard commercial sources.

Cell culture

CHOhNK1 cells were cultured in Ham's F12 medium supplemented with 10% fetal calf serum (FCS), 2 mM glutamine and 1 mg/ml G418 at 37 °C + 5% CO_2. U-251 MG cells were cultured in Earle's Minimal Essential Medium (EMEM) supplemented with 10% FCS, 1 mM sodium pyruvate, 2 mM glutamine, 1% non-essential amino acids (NEAA), 100 IU/ml penicillin and 100 µg/ml streptomycin at 37 °C + 5% CO_2. Membranes were prepared as described previously [22]. In short, CHOhNK1 cells were collected in 50 mM Tris HCl buffer (pH 7.4 at 25°C) supplemented with 2 mM $MgCl_2$ and subsequently centrifuged twice at 100 000x *g* in an Optima LE-80 K ultracentrifuge (Beckman Coulter, Fullterton, CA, USA) for 20 min at 4°C.

Radioligand equilibrium displacement assays

Displacement experiments were carried out using CHOhNK1 membrane aliquots containing 5-15 µg protein in a total volume of 100 µL assay buffer (50 mM Tris HCl, pH 7.4 at 25 °C, supplemented with 5 mM $MgCl_2$ and protease inhibitor cocktail (1 tablet/10 ml)) at 4 °C for 90 minutes. Ten concentrations of competing ligand were used in the presence of one concentration [^{3}H][Sar^9,Met(O_2)^{11}]SP (25 000 dpm, ~2.5 nM). This concentration ensured that total radioligand binding did not exceed 10% of that added to prevent ligand depletion. Non-specific binding was determined in the presence of an excess amount of SC-203437 (10 µM).

Homologous displacement assays were performed using CHOhNK1 membrane aliquots containing 5-15 µg protein, incubating at 4 °C for 90 minutes. Ten concentrations of [Sar^9,Met(O_2)^{11}]SP were used in the presence of four different concentrations [^{3}H][Sar^9,Met(O_2)^{11}]SP (i.e. 4 nM, 3 nM, 2 nM and 1 nM).

The reactions were terminated by the addition of 1 mL ice-cold wash buffer (50 mM Tris HCl, pH 7.4 at 25 °C, supplemented with 5 mM $MgCl_2$). Separation of bound from free radioligand was performed by rapid filtration through Whatman GF/C filters saturated with 0.25% polyethylene imine (PEI) using a Brandel harvester. Filters were subsequently

washed three times with 2 mL ice-cold wash buffer. Filter bound radioactivity was determined using a liquid scintillation counter (Tri-Carb 2900 TR, PerkinElmer).

Radioligand kinetic association and dissociation assays

Association and dissociation experiments were performed similarly to Nederpelt *et al.* [22], using CHOhNK1 membrane aliquots containing 5-15 µg protein, incubating at 4 °C with one concentration [^{3}H][Sar^{9},Met(O_2)^{11}]SP (25 000 dpm, ~2.5 nM). Total incubation time of association experiments was 120 min with different time intervals. For dissociation experiments membrane aliquots were pre-incubated for 90 min and dissociation was initiated by addition of 10 µM SC-203437. The amount of radioligand still bound to the receptor was measured for 240 min at different time points.

Radioligand kinetic competition association assays

The binding kinetics of unlabeled peptides were quantified as described previously [22], using CHOhNK1 membrane aliquots containing 5-15 µg protein, incubating at 4 °C with one concentration [^{3}H][Sar^{9},Met(O_2)^{11}]SP (30 000 dpm, ~3 nM). Total incubation time of competition association experiments was 120 min with different time intervals. The assay was validated using three concentrations (0.3*IC_{50}, 1*IC_{50} and 3*IC_{50}) of [Sar^{9},Met(O_2)^{11}]SP while the binding kinetics of all remaining agonists were determined using a concentration where displacement of [^{3}H][Sar^{9},Met(O_2)^{11}]SP at 120 min was between 40 and 60%.

Label-free whole cell assays

Label-free whole-cell assays were performed using the xCELLigence a real-time cell analyzer (RTCA) system as described previously [23]. In short, this assay utilizes electrical impedance to measure changes in cell morphology. 20 000 U-251 MG cells/well were seeded in E-plates covered with golden electrodes on the bottom of each well, 18 hours prior to stimulation with increasing concentrations of agonist or vehicle control. For antagonistic assays, cells were incubated for 30 min with an excess of selective NK1 antagonist aprepitant (1 µM) prior to stimulation with submaximal (EC_{80}) concentrations of agonist.

Data analysis

All experimental data were analyzed using the nonlinear regression curve-fitting program GraphPad Prism v. 6.00 (GraphPad Software Inc., San Diego, CA). Radioligand binding assays were analyzed as described previously [22]. In short, association and dissociation rates of unlabeled ligands were calculated by fitting the data of the competition association assay using non-linear regression - kinetics of competitive binding [24] using equation 1.

Equation 1:

$$K_A = k_1[L]\cdot 10^{-9} + k_2$$

$$K_B = k_3[I]\cdot 10^{-9} + k_4$$

$$S = \sqrt{(K_A - K_B)^2 + 4\cdot k_1 \cdot k_3 \cdot L \cdot I \cdot 10^{-18}}$$

$$K_F = 0.5(K_A + K_B + S)$$

$$K_S = 0.5(K_A + K_B - S)$$

$$Q = \frac{B_{\max} \cdot k_1 \cdot L \cdot 10^{-9}}{K_F - K_S}$$

$$Y = Q \cdot \left(\frac{k_4 \cdot (K_F - K_S)}{K_F \cdot K_S} + \frac{k_4 - K_F}{K_F} e^{(-K_F \cdot X)} - \frac{k_4 - K_S}{K_S} e^{(-K_S \cdot X)}\right)$$

Where k_1 is the k_{on} of the radioligand ($M^{-1}min^{-1}$), k_2 is the k_{off} of the radioligand (min^{-1}), L is the radioligand concentration (nM), I is the concentration of the unlabeled competitor (nM), X is the time (min) and Y is the specific binding of the radioligand (DPM). These parameters are set during a competition association, obtaining k_1 from the control curve without competitor and k_2 from previously performed dissociation assays described under *2.4 Radioligand kinetic association and dissociation assays*. With that the k_3, k_4 and B_{max} can be calculated, where k_3 represents the k_{on} ($M^{-1}min^{-1}$) of the unlabeled ligand, k_4 stands for the k_{off} of the unlabeled ligand and B_{max} equals the total binding (DPM). All competition association data were globally fitted. Data were normalized to maximal specific binding of [^{3}H][Sar^9,Met(O_2)^{11}]SP in absence of competitor.

Data from xCELLigence experiments were exported from RTCA Software 1.2 (Roche, Germany) after normalizing the cell index (CI) traces to the time of agonist addition. Baseline was removed by subtracting vehicle or antagonist traces from corresponding normalized CI (NCI) traces. The maximal NCI response of each concentration (peak) was used for data analyses.

Maximal response (E_{max}) and potency (pEC_{50}) values for all agonists were analyzed with non-linear regression of peak analysis fitted by log(agonist) vs. response - Variable slope. Results were normalized to the maximal NCI response induced by SP. The peak of agonist-induced cellular responses in presence of antagonist were normalized to the peak obtained from treatment with submaximal concentrations of the corresponding agonist.

Results

Characterization of [^{3}H][Sar^9,Met(O_2)^{11}]SP

The kinetic binding parameters of [^{3}H][Sar^9,Met(O_2)^{11}]SP interacting with CHOhNK1 membranes were determined with traditional kinetic radioligand binding studies. Association and dissociation assays supplied k_{on} and k_{off} values of 0.17 ± 0.028 nM^{-1} min^{-1} and 0.016 ±

0.0015 min^{-1}, respectively (Figure 2A and 2B). The kinetic K_D (k_{off}/k_{on}) calculated from these experiments was 0.093 ± 0.018 nM. The dissociation constant was determined with homologous displacement experiments (Figure 2C) and yielded a K_D of 2.5 ± 0.7 and this value was used to convert IC_{50} values to K_i values in the equilibrium binding studies.

Binding affinity of hNK1R peptide agonists

The binding affinity of seven hNK1R peptide agonists was determined with equilibrium radioligand displacement studies. With the exception of NKB (no significant displacement at 10 µM, data not shown), all peptides were able to completely displace [^{3}H][Sar^9,Met(O$_2$)^{11}]SP in a concentration-dependent manner (Figure 3). Unlabeled Sar^9,Met(O$_2$)^{11}-SP, SP, Pro^9, hemokinin-1 and SP(4-11) all had nanomolar affinities, ranging from 2.1 nM for SP to 37 nM for SP(4-11). NKA and septide showed a much lower affinity in the micromolar range of 1933 nM and 2417 nM, respectively (Table 1).

Competition association assay optimization and validation with [^{3}H][Sar^9,Met(O$_2$)^{11}]SP

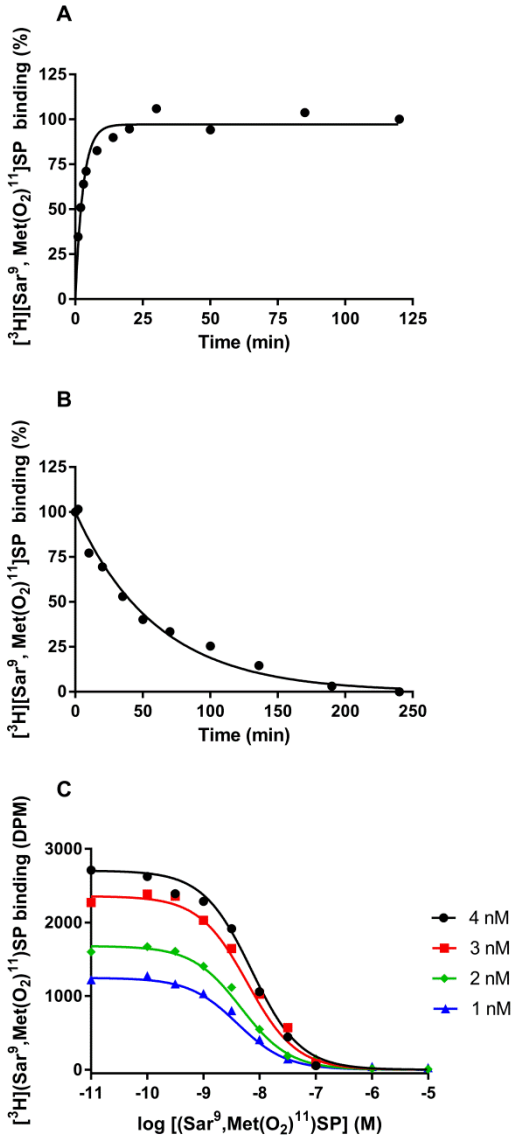

Figure 2: Association (A) and dissociation (B) kinetics of one concentration [^{3}H][Sar^9,Met(O$_2$)^{11}]SP (25 000 dpm, ~2.5 nM) and homologous displacement (C) of four concentrations [^{3}H][Sar^9,Met(O$_2$)^{11}]SP (i.e. 4 nM, 3 nM, 2 nM and 1 nM) by [Sar^9,Met(O$_2$)^{11}]SP on CHOhNK1 membranes at 4 °C. Representative graphs are shown from one experiment performed in duplicate.

The k_{on} (k_3) and k_{off} (k_4) values of unlabeled Sar^9,Met(O$_2$)^{11}-SP were quantified by fitting the k_{on} (k_1) and k_{off} (k_2) values of [^{3}H][Sar^9,Met(O$_2$)^{11}]SP into the model of 'kinetics of competitive binding' as described in Materials & Methods. Three different concentrations of Sar^9,Met(O$_2$)^{11}-SP, i.e. 0.3-fold, 1-fold and 3-fold its IC_{50} value, were tested and resulted in a shared k_{on} (k_3) and k_{off} (k_4) value of 0.094 ± 0.011 nM^{-1} min^{-1} and 0.026 ± 0.0029 min^{-1}, respectively (Figure 4A and Table 1). The association and dissociation rates obtained with this assay agreed fairly well with those obtained in traditional binding assays (Table 1). Kinetic dissociation constants and affinity values were also in good agreement, validating the competition association as a valuable tool for the determination of binding kinetics of unlabeled hNK1 ligands. To improve the throughput of this assay it was examined if using a single concentration (i.e. 1-fold their IC_{50} value) yielded similar binding

kinetics parameters. The k_{on} and k_{off} values of the single concentration method proved to be not significantly different, i.e. 0.078 ± 0.012 nM^{-1} min^{-1} and 0.024 ± 0.0038 min^{-1} respectively. Therefore, the remaining peptides were tested using this single concentration method.

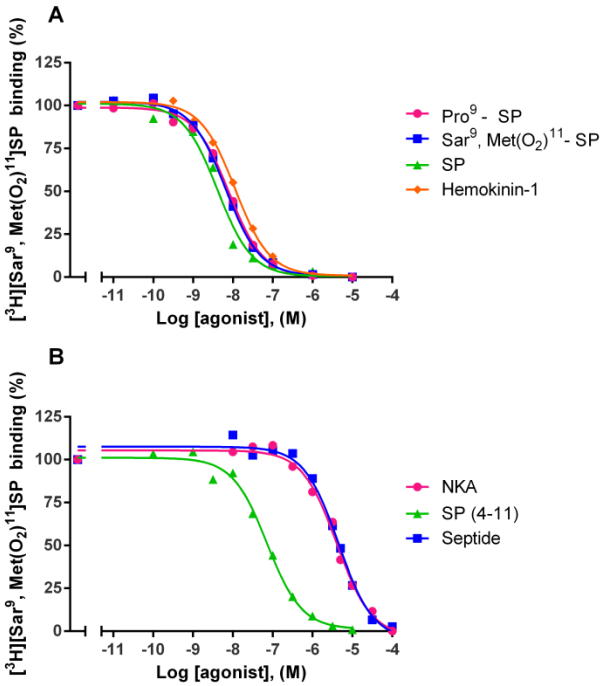

Figure 3: Displacement of one concentration [^{3}H][Sar^9,Met(O$_2$)^{11}]SP (25 000 dpm, ~2.5 nM) by NK1 peptide agonists on CHOhNK1 membranes at 4 °C. Representative graphs are shown from one experiment performed in duplicate (See Table 1 for affinity values).

Binding kinetics of hNK1R peptide agonists

The one-concentration competition association assay was used to determine the binding kinetics of the remaining agonists (Figure 4B and 4C). K_i values and kinetic K_D values of all peptides were highly correlated (r^2 = 0.99 and p<0.0001; data not shown), although kinetic K_D values were around 10-fold lower than K_i values. Dissociation rates varied approximately 9-fold, ranging from 0.026 ± 0.0029 min^{-1} for Sar^9,Met(O$_2$)^{11}-SP and 0.21 ± 0.015 min^{-1} for septide (Table 1). Interestingly, a 240-fold difference was observed in association rates for the peptide agonists. SP had the fastest association rate of 0.24 ± 0.046 nM^{-1} min^{-1} and NKA showed the slowest association rate of 0.001 ± 0.0002 nM^{-1} min^{-1} (Table 1).

NK1 receptor activation in human astrocytoma U-251 MG cells

To examine receptor activation we used a cell line that endogenously expresses the human NK1 receptor, i.e. astrocytoma U-251 MG cells. Stimulation of the cells with agonist resulted in a rapid transient (~2 min) negative effect on the impedance followed by a positive response for all agonists (Figure 5A, representative trace of SP). Potency values (EC_{50}) ranged from 0.04 ± 0.01 nM for Sar^9, $Met(O_2)^{11}$-SP to 3.9 ± 1.8 nM for NKA while only NKA showed a significant increase in E_{max} in comparison to SP (Figure 5B, 5C and Table 1). Pre-incubation with 1 µM aprepitant, a selective non-peptide NK1 receptor antagonist, completely abolished receptor signaling for all agonists (Figure 5D).

Correlation plots of binding and receptor activation parameters of hNK1R peptide agonists

Lastly, we investigated the correlation between the kinetic binding parameters (pk_{on} and pk_{off}) and the receptor activation parameters (pEC_{50} and E_{max}). The dissociation rate constants correlated well with association rate constants (R^2=0.73, P=0.014), potency (R^2=0.67, P=0.025), maximal response values (R^2=0.70, P=0.018) and a good correlation was obtained with affinity values (R^2=0.84, P=0.0039). In contrast, the association rate constants did not show any significant correlation with the *in vitro* maximal response (R^2=0.45, P=0.10). Finally, an excellent correlation was

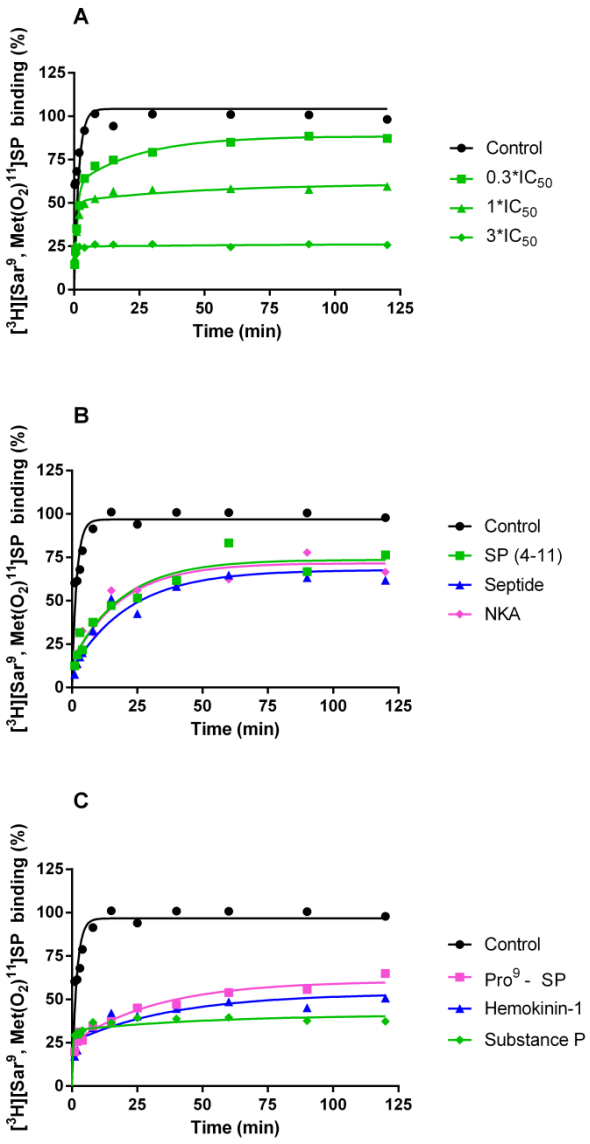

Figure 4: Competition association assay at 4 °C with one concentration [^{3}H][Sar^9,$Met(O_2)^{11}$]SP (30 000 dpm, ~3 nM) in the absence or presence of 0.3, 1 or 3*IC_{50} value of unlabeled [Sar^9,$Met(O_2)^{11}$]SP (A) or 1*IC_{50} value of SP (4-11), septide and NKA (B) or SP, Pro^9 and hemokinin-1 (C). Representative graphs are shown from one experiment performed in duplicate (See Table 1 for kinetic parameters).

observed between the association rate constants and the affinity (R^2=0.99, P<0.0001) and potency values (R^2=0.90, P=0.0012).

Discussion

Binding kinetics of endogenous tachykinins and their derivatives vary greatly

Ligand-receptor binding kinetics are defined by the association and dissociation rates of a ligand to and from its receptor. These parameters are increasingly recognized to be important in the understanding of a drugs mechanism of action [5, 25, 26]. Many successful drugs achieve their effects by competing with endogenous ligands, therefore insights into the kinetics of endogenous ligands could provide clues for the desired binding kinetics of potential drugs. In this study we focused on determining the binding kinetics of endogenous tachykinins and their derivatives targeting the NK1 receptor, including but not limited to Substance P, NKA and hemokinin-1 (Figure 1) using a competition association assay. This assay was first described in 1984 [24] and has to date been used to investigate the binding kinetics of ligands for quite a number of GPCRs [22, 27, 28]. Here, we validated the competition association assay as a reliable method to determine the binding kinetics of unlabeled NK1 peptide agonists. This was demonstrated by the similar k_{on} and k_{off} values in comparison to the traditional association and dissociation assays, as well as the excellent correlation between the affinity and kinetic K_D values. Notably, K_i values were consistently 10-fold higher in comparison to kinetic K_D values. It should be noted that there were some experimental differences between equilibrium displacement and competition association assays. For instance, equilibrium experiments were performed with 90 minutes incubation while the kinetic K_D from the competition association is not (or less) time dependent. Moreover, to improve the assay window for competition association assays the concentration radioligand and membranes was increased. Additionally, membrane batches differed between assays. These differences can add up to the 10-fold discrepancy between equilibrium K_i and kinetic K_D values reported in this study. Of note, literature K_i and K_D values of NK1 agonists are also quite variable and even differ up to 20-fold [16, 29-31]. Investigation of the correlations between the kinetic binding parameters (k_{on} and k_{off}) and the affinity values of all agonists showed a significant correlation between pK_i and pk_{off} values (R^2=0.84, P<0.005) and an excellent correlation between pK_i and pk_{on} values (R^2=0.99, P<0.0001). Since the association rate is often thought to be diffusion rate limited (10^8 ~ 10^9 M^{-1} s^{-1} [32]) and the affinity is calculated by dividing the dissociation rate by the association rate, it is commonly assumed that changes in affinity are directly derived from changes in dissociation rates.

Significant correlations between pK_i and pk_{off} values are often reported [5, 25, 33], while a correlation between the association rate and affinity is less prevalent. However, in this study it was demonstrated that for the most well-known tachykinins the association rates ranged 240-fold while dissociation rates only differed 8-fold. Takeda *et al.* also reported over 100-fold differences between the association rate of SP versus NKA while the dissociation rates only differed 3-fold [34]. Similar to synthetic ligands for the β2-adrenoceptor, orexin-2 receptor and Kv11.1 potassium channel [35-37], our findings illustrate that association rates are the main incentive that dictate the affinity of endogenous tachykinins targeting the NK1 receptor. It should be noted that in addition to binding kinetics, other parameters such as rebinding, ligand elimination, degradation and target vulnerability also play an important role in the mechanism of action of the ligand of interest [38].

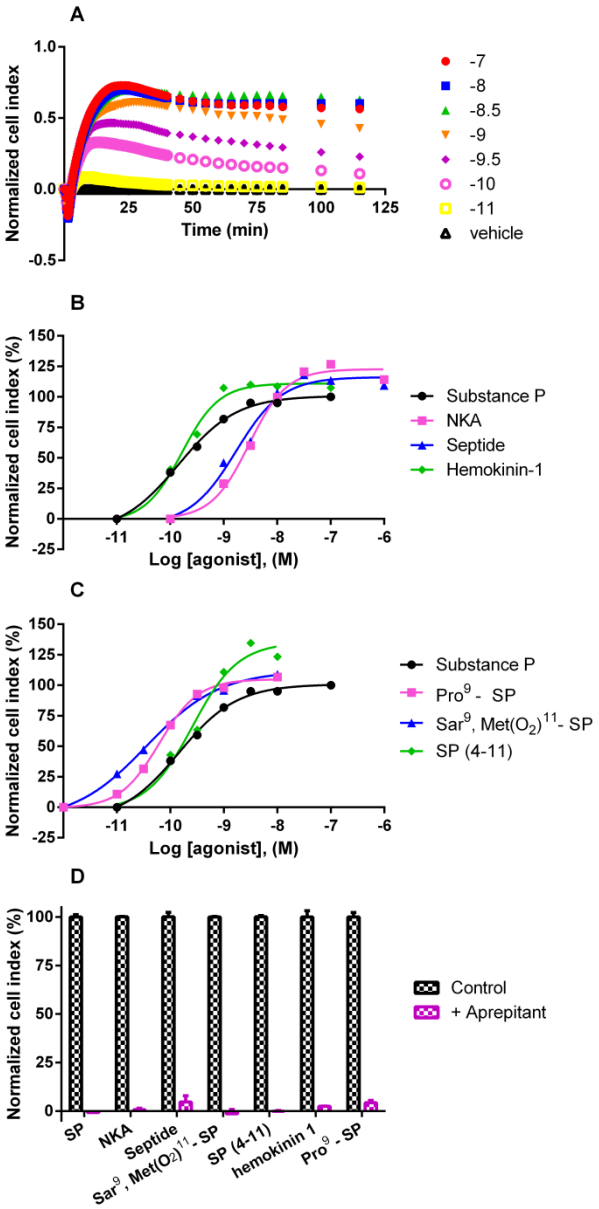

Figure 5: Concentration-dependent effects of NK1 agonists on U-251 MG cells. Representative xCELLigence traces of one experiment performed in duplicate of normalized cell index (NCI) after stimulation with increasing concentrations of SP (A) and representative concentration-effect curves of all agonists derived from peak analysis, data were normalized to maximal response after SP stimulation (B and C). Representative bar graph of one experiment performed in duplicate of peak analysis after stimulation with EC_{80} concentrations of agonist in presence or absence of 1 µM aprepitant (D).

Diversity in NK1 receptor potency but not activation profiles on label-free impedance-based system

In addition to the binding parameters we also investigated the receptor activation profiles of all tested tachykinins, except NKB. Most of the NK1 receptor signaling studies have been performed with G protein pathway-specific assays such as cAMP and IP turnover assays [14-16]. However, an assay that measures the whole cellular response over time overcomes the limitations of pathway-specific end-point assays and is thus more suitable to study NK1 receptor activation and its correlation to binding kinetics. Therefore we used a label-free impedance-based assay to study NK1 receptor activation in human astrocytoma U-251 MG cells that endogenously express the NK1 receptor. Addition of increasing concentrations of agonist resulted in a concentration-dependent increase in impedance for all tested tachykinins. These responses were selectively inhibited by the small molecule antagonist aprepitant, supporting a NK1 receptor specific response. All tachykinins had much higher potencies in comparison to literature values that used endpoint assays [16, 39], which is often observed in label-free assays that monitor cell morphology rather than one downstream signaling pathway [40, 41]. Of note, the cell index trace was identical for fastly and slowly associating agonists. It could be argued that numerous factors are involved in receptor activation kinetics, such as the rate of G protein-coupling and kinetics of production of second messengers. These factors could prove it difficult to selectively measure the effects of agonist-receptor association rates on receptor activation kinetics.

N-terminal domain of tachykinins is important for association rate and potency

The N-terminus of tachykinins is believed to be important for receptor affinity and selectivity, albeit indirectly by regulating peptide conformations that are crucial in peptide-receptor binding and activation [42, 43]. Valentin-Hansen *et al.* recently mapped SP binding sites on the NK1 receptor and reported that the first 6 C-terminal amino acids of SP are specifically organized fitting onto the surface of the receptor while the remaining N-terminal amino acids are forming a cone-shaped entity that could accommodate interactions with multiple residues of the N-terminal tail of the receptor [44]. Interestingly, in our study we found that tachykinins with shorter N-terminal domains such as NKA and septide not only had significantly reduced affinities and potencies but also had a more than 200-fold decrease in association rates (Table 1). It could be postulated that the slower association rates are due to a less optimal peptide conformation in consequence of a lack of interactions with the N-terminal tail of the receptor resulting in a decreased affinity and potency.

Binding kinetics correlate with in vitro activation profiles

A good correlation was observed between the dissociation rate and *in vitro* maximal response (Table 1). Correlations between *in vitro* maximal response and dissociation rates have been reported before. In example, Guo *et al.* [45] examined binding kinetics and efficacies of adenosine A_{2A} agonists and found that slower dissociation correlated with increased efficacies in a label-free assay. Moreover, a study investigating dissociation rates and functional effects of muscarinic M3 receptor agonists proved that high maximal response values were positively correlated with slow dissociation rates [46]. Collectively, these findings support our observation that receptor dissociation rates can be a good predictor of *in vitro* efficacies at the NK1 receptor. Moreover, a very good correlation was observed between the association rate and potency values. We found that tachykinins with faster dissociation rates and slower association rates (i.e. lower affinities) have lower potencies in comparison with SP. Interestingly, these agonists are known to only activate the $G\alpha_q$ pathway [16, 39, 47, 48]. A correlation between binding kinetics and biased signaling has been discussed before for the NK2 receptor. Specifically, an allosteric modulator for the NK2 receptor (i.e. LPI805), was investigated for its effects on the binding kinetics and signaling profile of NKA [14]. It was demonstrated that addition of LPI805 resulted in faster dissociation and slower association rates of NKA, as well as abolishing $G\alpha_s$ signaling.

In conclusion, the competition association assay was validated as a valuable tool to study the binding kinetics of tachykinins targeting the NK1 receptor. We have, for the first time, elucidated the binding kinetics of endogenous tachykinins and their most well-known derivatives and found small differences in their dissociation rates (8-fold difference) and large differences in their association rates (240-fold difference). Dissociation rates correlated well with *in vitro* efficacies, while association rates correlated highly with potency values obtained with a label-free assay. Taken together, these results indicate that diverging binding kinetics can play a significant role in differentially activating the NK1 receptor. Our research underlines the importance of knowledge of binding kinetics of endogenous ligands, as it was demonstrated that for endogenous tachykinins both dissociation and association rate constants differed significantly which in turn had differential effects in receptor activation. Moreover, these kinetic values should be considered when designing novel competing drugs targeting the NK1 receptor.

Table 1: Binding (affinity, association rate and dissociation rate) and activation (*in vitro* potency and maximal response) parameters of **the examined tachykinins.**

Ligand	**pK_i (and K_i in nM)**	**pK_D (and K_D in nM)**	**k_{on} ($nM^{-1}min^{-1}$)**	**k_{off} (min^{-1})**	**RT (min)**	**pEC_{50} # (and EC_{50} in nM)**	**E_{max} (%)##**
Substance P	8.7 ± 0.01 (2.1)	10 ± 0.09 (0.11)	0.24 ± 0.046	0.027 ± 0.0025	37 ± 3.4	9.9 ± 0.1 (0.07)	100 ± 3
Sar^9, $Met(O_2)^{11}$-SP #	8.5 ± 0.03 (3.5)	9.6 ± 0.07 (0.27)	0.094 ± 0.011	0.026 ± 0.0029	39 ± 4.4	10 ± 0.1 (0.04)	110 ± 1
Pro^9 - SP	8.4 ± 0.02 (3.8)	9.5 ± 0.05 (0.32)	0.18 ± 0.021	0.059 ± 0.0024	17 ± 0.67	10 ± 0.08 (0.06)	116 ± 8
Hemokinin-1	8.1 ± 0.08 (8.1)	9.1 ± 0.05 (0.79)	0.064 ± 0.013	0.048 ± 0.0065	21 ± 2.9	10 ± 0.1 (0.1)	135 ± 22
NKA	5.7 ± 0.04 (1933)	6.7 ± 0.1 (180)	0.0010 ± 0.00018	0.19 ± 0.036	5.3 ± 1.0	8.4 ± 0.16 (3.9)	145 ± 10*
SP(4-11)	7.4 ± 0.04 (37)	8.4 ± 0.06 (3.8)	0.037 ± 0.0025	0.14 ± 0.018	7.1 ± 0.89	9.9 ± 0.19 (0.25)	129 ± 10
Septide	5.6 ± 0.03 (2418)	6.8 ± 0.03 (171)	0.0012 ± 0.000042	0.21 ± 0.015	4.6 ± 0.4	8.7 ± 0.06 (1.8)	134 ± 11

Values are means ± SEM of three separate experiments performed in duplicate, #3-concentration competition association, # #Values were calculated with peak analysis and data were normalized to maximal response obtained for Substance P. Of note, NKB was unable to displace [^{3}H]-Sar^9, $Met(O_2)^{11}$-SP (-3% and -10% displacement at 10 µM). * $p < 0.05$, compared to E_{max} SP determined using one-way ANOVA with Dunnett's post-test.

References

1. Zhang, R. and F. Monsma, *The importance of drug-target residence time.* Current opinion in drug discovery & development, 2009. **12**(4): p. 488-96.
2. Vauquelin, G. and S.J. Charlton, *Long-lasting target binding and rebinding as mechanisms to prolong in vivo drug action.* British journal of pharmacology, 2010. **161**(3): p. 488-508.
3. Tummino, P.J. and R.A. Copeland, *Residence time of receptor-ligand complexes and its effect on biological function.* Biochemistry, 2008. **47**(20): p. 5481-92.
4. Swinney, D.C., *The role of binding kinetics in therapeutically useful drug action.* Current opinion in drug discovery & development, 2009. **12**(1): p. 31-9.
5. Guo, D., et al., *Drug-target residence time-a case for G protein-coupled receptors.* Medicinal research reviews, 2014. **34**(4): p. 856-92.
6. Tashkin, D.P., *Is a long-acting inhaled bronchodilator the first agent to use in stable chronic obstructive pulmonary disease?* Current opinion in pulmonary medicine, 2005. **11**(2): p. 121-8.
7. Kapur, S. and P. Seeman, *Antipsychotic agents differ in how fast they come off the dopamine D2 receptors. Implications for atypical antipsychotic action.* J Psychiatry Neurosci, 2000. **25**(2): p. 161-6.
8. Zhang, Y., et al., *Hemokinin is a hematopoietic-specific tachykinin that regulates B lymphopoiesis.* Nat Immunol, 2000. **1**(5): p. 392-7.
9. Steinhoff, M.S., et al., *Tachykinins and their receptors: contributions to physiological control and the mechanisms of disease.* Physiol Rev, 2014. **94**(1): p. 265-301.
10. Pantaleo, N., et al., *The mammalian tachykinin ligand-receptor system: an emerging target for central neurological disorders.* CNS Neurol Disord Drug Targets, 2010. **9**(5): p. 627-35.
11. Pennefather, J.N., et al., *Tachykinins and tachykinin receptors: a growing family.* Life Sci, 2004. **74**(12): p. 1445-63.
12. Quartara, L. and C.A. Maggi, *The tachykinin NK1 receptor. Part I: ligands and mechanisms of cellular activation.* Neuropeptides, 1997. **31**(6): p. 537-63.
13. Valentin-Hansen, L., et al., *Biased Gs Versus Gq Proteins and beta-Arrestin Signaling in the NK1 Receptor Determined by Interactions in the Water Hydrogen Bond Network.* J Biol Chem, 2015. **290**(40): p. 24495-508.
14. Maillet, E.L., et al., *A novel, conformation-specific allosteric inhibitor of the tachykinin NK2 receptor (NK2R) with functionally selective properties.* FASEB J, 2007. **21**(9): p. 2124-34.
15. Palma, C., F. Nardelli, and S. Manzini, *Correlation between binding characteristics and functional antagonism in human glioma cells by tachykinin NK1 receptor antagonists.* Eur J Pharmacol, 1999. **374**(3): p. 435-43.
16. Sagan, S., et al., *Tachykinin peptides affect differently the second messenger pathways after binding to CHO-expressed human NK-1 receptors.* J Pharmacol Exp Ther, 1996. **276**(3): p. 1039-48.
17. Rizzi, A., et al., *In vitro and in vivo pharmacological characterization of the novel NK(1) receptor selective antagonist Netupitant.* Peptides, 2012. **37**(1): p. 86-97.

18. Lindstrom, E., et al., *Neurokinin 1 receptor antagonists: Correlation between in vitro receptor interaction and in vivo efficacy.* Journal of Pharmacology and Experimental Therapeutics, 2007. **322**(3): p. 1286-1293.
19. Hale, J.J., et al., *Structural optimization affording 2-(R)-(1-(R)-3,5-bis(trifluoromethyl)phenylethoxy)-3-(S)-(4-fluoro)phenyl-4-(3-oxo-1,2,4-triazol-5-yl)methylmorpholine, a potent, orally active, long-acting morpholine acetal human NK-1 receptor antagonist.* Journal of Medicinal Chemistry, 1998. **41**(23): p. 4607-4614.
20. Scott, C.W. and M.F. Peters, *Label-free whole-cell assays: expanding the scope of GPCR screening.* Drug discovery today, 2010. **15**(17-18): p. 704-16.
21. Rocheville, M., et al., *Mining the potential of label-free biosensors for seven-transmembrane receptor drug discovery.* Progress in molecular biology and translational science, 2013. **115**: p. 123-42.
22. Nederpelt, I., et al., *Characterization of 12 GnRH peptide agonists - a kinetic perspective.* Br J Pharmacol, 2016. **173**(1): p. 128-41.
23. Nederpelt, I., et al., *Persistent GnRH receptor activation in pituitary alphaT3-1 cells analyzed with a label-free technology.* Biosens Bioelectron, 2016. **79**: p. 721-7.
24. Motulsky, H.J. and L.C. Mahan, *The kinetics of competitive radioligand binding predicted by the law of mass action.* Molecular pharmacology, 1984. **25**(1): p. 1-9.
25. Copeland, R.A., D.L. Pompliano, and T.D. Meek, *Drug-target residence time and its implications for lead optimization.* Nature reviews. Drug discovery, 2006. **5**(9): p. 730-9.
26. Swinney, D.C., et al., *The Role of Binding Kinetics in GPCR Drug Discovery.* Curr Top Med Chem, 2015. **15**(24): p. 2504-22.
27. Sullivan, S.K., et al., *Kinetics of nonpeptide antagonist binding to the human gonadotropin-releasing hormone receptor: Implications for structure-activity relationships and insurmountable antagonism.* Biochemical pharmacology, 2006. **72**(7): p. 838-49.
28. Slack, R.J., et al., *Pharmacological characterization of GSK1004723, a novel, long-acting antagonist at histamine H(1) and H(3) receptors.* British journal of pharmacology, 2011. **164**(6): p. 1627-41.
29. Torrens, Y., et al., *Further evidence for the presence of "septide-sensitive" tachykinin binding sites in tissues possessing solely NK(1) tachykinin receptors.* Biochem Biophys Res Commun, 2000. **270**(2): p. 668-72.
30. Tian, Y., et al., *The unpredicted high affinities of a large number of naturally occurring tachykinins for chimeric NK1/NK3 receptors suggest a role for an inhibitory domain in determining receptor specificity.* J Biol Chem, 1996. **271**(34): p. 20250-7.
31. Cascieri, M.A., et al., *Characterization of the binding of a potent, selective, radioiodinated antagonist to the human neurokinin-1 receptor.* Mol Pharmacol, 1992. **42**(3): p. 458-63.
32. Smith, G.F., *Medicinal chemistry by the numbers: the physicochemistry, thermodynamics and kinetics of modern drug design.* Prog Med Chem, 2009. **48**: p. 1-29.
33. Lu, H. and P.J. Tonge, *Drug-target residence time: critical information for lead optimization.* Curr Opin Chem Biol, 2010. **14**(4): p. 467-74.

34. Takeda, Y., et al., *Ligand binding kinetics of substance P and neurokinin A receptors stably expressed in Chinese hamster ovary cells and evidence for differential stimulation of inositol 1,4,5-trisphosphate and cyclic AMP second messenger responses.* J Neurochem, 1992. **59**(2): p. 740-5.
35. Mould, R., et al., *Binding kinetics differentiates functional antagonism of orexin-2 receptor ligands.* Br J Pharmacol, 2014. **171**(2): p. 351-63.
36. Sykes, D.A. and S.J. Charlton, *Slow receptor dissociation is not a key factor in the duration of action of inhaled long-acting beta2-adrenoceptor agonists.* Br J Pharmacol, 2012. **165**(8): p. 2672-83.
37. Yu, Z., A.P. IJzerman, and L.H. Heitman, *Kv 11.1 (hERG)-induced cardiotoxicity: a molecular insight from a binding kinetics study of prototypical Kv 11.1 (hERG) inhibitors.* Br J Pharmacol, 2015. **172**(3): p. 940-55.
38. de Witte, W.E., et al., *In vivo Target Residence Time and Kinetic Selectivity: The Association Rate Constant as Determinant.* Trends Pharmacol Sci, 2016.
39. Torrens, Y., et al., *Substance P(6-11) and natural tachykinins interact with septide-sensitive tachykinin receptors coupled to a phospholipase C in the rat urinary bladder.* Neuropeptides, 1997. **31**(3): p. 243-51.
40. Kammermann, M., et al., *Impedance measurement: a new method to detect ligand-biased receptor signaling.* Biochemical and biophysical research communications, 2011. **412**(3): p. 419-24.
41. Scandroglio, P., et al., *Evaluation of cannabinoid receptor 2 and metabotropic glutamate receptor 1 functional responses using a cell impedance-based technology.* Journal of biomolecular screening, 2010. **15**(10): p. 1238-47.
42. Vigna, S.R., *The N-terminal domain of substance P is required for complete homologous desensitization but not phosphorylation of the rat neurokinin-1 receptor.* Neuropeptides, 2001. **35**(1): p. 24-31.
43. Huang, R.R., et al., *Interaction of substance P with the second and seventh transmembrane domains of the neurokinin-1 receptor.* Biochemistry, 1994. **33**(10): p. 3007-13.
44. Valentin-Hansen, L., et al., *Mapping substance P binding sites on the neurokinin-1 receptor using genetic incorporation of a photoreactive amino acid.* J Biol Chem, 2014. **289**(26): p. 18045-54.
45. Guo, D., et al., *Functional efficacy of adenosine A_{2A} receptor agonists is positively correlated to their receptor residence time.* Br J Pharmacol, 2012. **166**(6): p. 1846-1859.
46. Sykes, D.A., M.R. Dowling, and S.J. Charlton, *Exploring the mechanism of agonist efficacy: a relationship between efficacy and agonist dissociation rate at the muscarinic M3 receptor.* Molecular pharmacology, 2009. **76**(3): p. 543-51.
47. Wijkhuisen, A., et al., *Identification in the NK1 tachykinin receptor of a domain involved in recognition of neurokinin A and septide but not of substance P.* FEBS Lett, 1999. **447**(2-3): p. 155-9.

48. Pradier, L., et al., *Septide - an Agonist of the Nk(1) Receptor Acting at a Site Distinct from Substance-P.* British Journal of Pharmacology, 1993. **110**: p. P57-P57.

Chapter 6

From receptor binding kinetics to signal transduction; a missing link in predicting *in vivo* drug-action

Indira Nederpelt

Maria Kuzikov

Patrick Schnider

Bruno Tuijt

Adriaan P. IJzerman

Elizabeth C. M. de Lange

Laura H. Heitman

Manuscript in preparation

Abstract

An important question in drug discovery is how to overcome the serious challenge of high drug attrition rates due to lack of efficacy. A missing link in the understanding of determinants for drug efficacy is the relation between drug-target binding kinetics and signal transduction, particularly in the physiological context of (multiple) endogenous ligands. In this study we show, for the first time, how differences in drug-target binding kinetics lead to different cellular responses induced by endogenous agonists. Our findings were consistent throughout different kinetic assays and cellular backgrounds. We conclude that knowledge of the relationship between *in vitro* drug-target binding kinetics and cellular responses is important to ultimately improve the understanding of drug efficacy *in vivo*.

Introduction

Drug discovery is challenged with overcoming high attrition rates due to lack of efficacy in clinical trials. In the past decade, numerous researchers have proposed drug-target binding kinetics (i.e. association and dissociation rates) as important *in vitro* parameters and have suggested including these early in the drug discovery paradigm [1-4]. While plasma pharmacokinetic profiles are relatively well understood, and progress is made in understanding and predicting target tissue distribution and target occupancy [5-7], the crucial step from drug-target binding kinetics to the *in vivo* cellular effects that precede the whole body's response is typically missing (Figure 1). Since these responses cannot yet be measured in the living body, we have to use *in vitro* systems that reflect the *in vivo* conditions as closely as possible. So far numerous receptor binding assays, such as radioligand binding [8], surface plasmon resonance (SPR), surface acoustic wave (SAW) [9], and time-resolved fluorescence resonance energy transfer (TR-FRET) assays [10], have been designed and validated to study binding kinetics at the receptor level. However, there is a need for kinetic functional assays to better predict *in vivo* cellular responses of kinetically diverse compounds. Functional assays that are well suited for this purpose include the real-time GloSensor™ cAMP assay [11, 12], measuring cAMP production, and the real-time impedance-based xCELLigence™ assay [13, 14], that measures changes in cell morphology as a more integral cellular response.

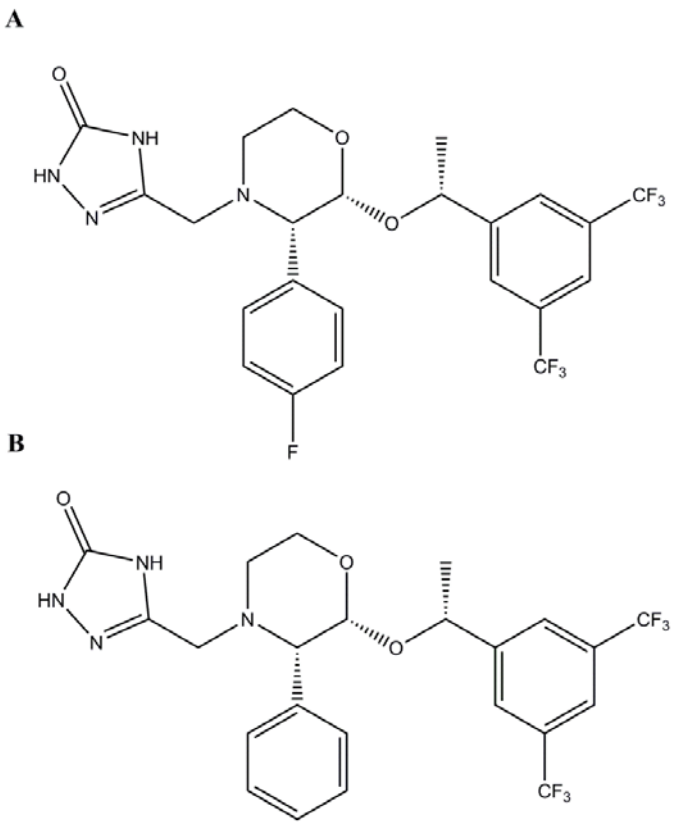

Supplemental Figure 1: Chemical structure of aprepitant (A) and desfluoro aprepitant (DFA) (B).

The neurokinin 1 (NK1) receptor is an example of a target for which drugs with optimal binding kinetics are reported. It is mainly expressed in the central nervous system (CNS) and plays a role in the regulation of affective behavior and emesis in the brain, as well as nociception in the spinal cord [15, 16]. While a plethora of NK1 antagonists have been synthesized [17-19], most antagonists have failed in the clinic due to a reported lack of efficacy [20, 21]. Currently, two small molecule NK1 antagonists are marketed to treat

chemotherapy-induced emesis and nausea, namely aprepitant and netupitant. A study of Hale *et al.* indicated that aprepitant is superior to other NK1 receptor antagonists due to its slow receptor dissociation rate [22]. These results were confirmed in a later study in which the long-lasting *in vivo* effects of aprepitant were directly related to its slow dissociation rate rather than a long half-life [23]. More recently, the highly selective NK1 antagonist netupitant, in combination with a serotonin 5-HT_3 receptor antagonist, was approved by the FDA [24]. Similar to aprepitant, netupitant's effects were considered insurmountable, i.e. able to depress the maximal agonist-induced response by preventing agonist rebinding, and shown resistant to wash-out experiments, i.e. during wash-out netupitant was still tightly bound to the receptor [25]. The authors proposed slow receptor dissociation kinetics as the mechanism hereof.

Another important aspect in *in vivo* receptor binding is competition of the drug with endogenous ligands. It is therefore crucial to study the binding kinetics and subsequent cellular responses of drug candidates in the presence of such endogenous ligands, as the binding kinetics of these competing endogenous ligands can be substantially different [26]. For example, the binding kinetics of endogenous NK1 receptor ligands, called tachykinins, such as substance P (SP) and neurokinin A (NKA) have been found to be very divergent [27]. The necessity of slow receptor binding kinetics of NK1 receptor antagonists to achieve high *in vivo* efficacy in addition to the varying binding kinetics of the endogenous tachykinins, i.e. NKA and SP, makes the NK1 receptor a good model system to examine distinct kinetic interactions of antagonist and agonist binding and their effects on signal transduction.

In short, in this study the *in vitro* functional effects of receptor binding kinetics were examined for kinetically divergent agonists and antagonists using the NK1 receptor as a model system. We report differential signal transduction profiles for differential kinetic binding profiles of antagonists and endogenous agonists and these results were congruous throughout varying assay temperatures, cellular backgrounds and kinetic assays. Moreover, a novel approach studying the onset of receptor activation was designed. We provide, for the first time, a qualitative translation of binding kinetics into kinetic cellular responses enabling better predictions of *in vivo* drug effects.

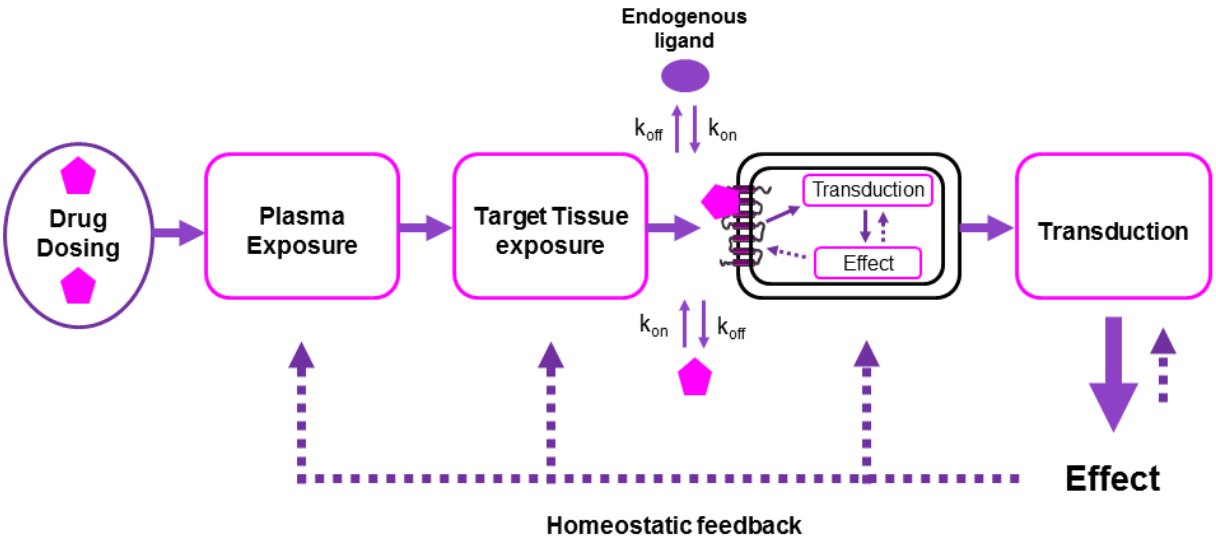

Figure 1: Schematic overview of factors involved between drug dosing and body responses, i.e. drug effects. While drug dosing, plasma pharmacokinetics, target tissue distribution, intra-tissue or target site distribution, cellular signal transduction and body responses are often examined drug-target binding kinetics are often disregarded. More importantly, elucidation of the pivotal step, i.e. effects of binding kinetics on signal transduction, from drug-target binding kinetics to in vivo drug responses is highly desirable.

Methods

Reagents and compounds

SP and NKA were purchased from Sigma-Aldrich (St. Louis, MO) and Bio-Connect (Huissen, The Netherlands), respectively. All NK1 antagonists were synthesized in-house as described previously[22]. Chinese Hamster Ovary (CHO) cells stably expressing the human neurokinin 1 receptor (CHOhNK1 cells) were kindly provided by AstraZeneca (Macclesfield, UK) and U-251 MG cells were purchased from Sigma-Aldrich (St. Louis, MO). xCELLigence E-plate 16 and 96 were purchased from Westburg (Leusden, the Netherlands). pGloSensor™-22F cAMP plasmid, GloSensor™ cAMP reagent and FuGENE HD transfection reagent were obtained from Promega GmbH (Mannheim, Germany). CELLSTAR® 384-Well Plates, Tissue Culture Treated were purchased from Greiner Bio-One (Frickenhausen, Germany). [^{3}H][Sar^{9},Met(O$_2$)^{11}]SP (specific activity 25-55 Ci/mmol) was obtained from Perkin Elmer (Boston, MA). All other reagents and materials were obtained from commercial resources.

Cell culture

U-251 MG cells were cultured in Earle's Minimal Essential Medium (EMEM) supplemented with 10% FCS, 1 mM sodium pyruvate, 2 mM glutamine, 1% non-essential amino acids (NEAA), 100 IU/ml penicillin and 100 µg/ml streptomycin at 37 °C + 5% CO_2. CHOhNK1 cells were cultured in Ham's F12 medium supplemented with 10% fetal calf serum (FCS), 2 mM glutamine and 1 mg/ml G418 at 37 °C + 5% CO_2.

Dual-point competition association assays

Dual-point competition association assays were performed as prescribed previously [28], following the radioligand binding protocol of Nederpelt *et al.[27]*. In short, CHOhNK1 membrane aliquots containing 5-15 µg protein were incubated at 4 °C with 25 000 dpm (~2.5 nM) [^{3}H][Sar^9,Met(O_2)^{11}]SP and one concentration of competing antagonist (i.e. concentration at which approximately 50% (30-70%) [^{3}H][Sar^9,Met(O_2)^{11}]SP binding was achieved). Specific binding of [^{3}H][Sar^9,Met(O_2)^{11}]SP was determined at two time-points; 30 min (t1), which is the time-point at which equilibrium of [^{3}H][Sar^9,Met(O_2)^{11}]SP binding was achieved, and 120 min (t2) at which all competing antagonists reached equilibrium.

Impedance-based morphology assays

Label-free morphology assays were performed using the xCELLigence RTCA system as described previously [27, 29]. U-251 MG cells were treated with three different concentrations (0.07 nM, 0.21 nM and 0.7 nM) of aprepitant or DFA for 30 min prior to stimulation with increasing concentrations of SP or NKA.

Real-time cAMP accumulation assay

Real-time cAMP production was measured using the life cell cAMP GloSensor™ assay [11, 12]. The technology is based on a cAMP-biosensor, which undergoes a conformational change upon cAMP binding, followed by the turnover of Luciferin.

CHOhNK1 cells were transiently transfected with the pGloSensor™-22F cAMP (i.e. 6 ng/µL) plasmid using FuGene HD (3 µL:1 µg DNA plasmid) as a transfection reagent. Accordingly, cells were harvested and reconstituted to 0.5 x 10^6 cells/ml (10.000 cells/well) in DMEM/F-12/ HEPES supplemented with 1% FCS, 2 mM glutamine and 1 mg/ml G418. The diluted plasmid solution was combined with the transfection reagent and incubated for 20 min at room temperature. Subsequently, the transfection mixture and cell solution were mixed for additional 5 min before plating in 384-well plates. The transfected cells were incubated for 24 h at 37 °C + 5 % CO_2 followed by treatment with Glo-substrate (i.e. 3% v/v) for 2 h at room temperature. Subsequently, three different concentrations (0.07 nM, 0.21 nM and 0.7 nM) of Aprepitant or DFA were added to cells for 30 min (pre-incubation) using Echo™ 550 Liquid

Handler (Labcyte), followed by addition of increasing concentrations of SP or NKA. Real-time changes in the level of cAMP were detected using an Envision HTS microplate reader 2103 (PerkinElmer).

Data analysis

All experimental data were analyzed using the curve-fitting program GraphPad Prism v. 6.00 (GraphPad Software Inc., San Diego, CA).

Data from dual-point competition association assays were analyzed by dividing the specific binding at t1 (B_{t1}) with the specific binding at t2 (B_{t2}).

$$KRI = B_{t1} / B_{t2}$$

Data from morphology and cAMP experiments were analyzed as described previously [27]. Efficacy (E_{max}) and potency (pEC_{50}) values for SP and NKA were analyzed with non-linear regression of peak analysis fitted by log(agonist) vs. response - Variable slope. Results were normalized to the maximal response induced by agonist without antagonist.

The onset of receptor activation was analyzed by calculating the slope with linear regression of the first 8 minutes of the cellular response.

$$\text{onset} = \frac{\Delta \text{ cellular response}}{\Delta \text{ time}}$$

All data are means of at least three separate experiments performed in duplicate or triplicate. Statistical analysis was performed using one-way ANOVA with Dunnett's post-test.

Results

Aprepitant and DFA have very divergent binding kinetics at the NK1 receptor

The kinetic binding parameters of 87 small molecule NK1 receptor antagonists were determined using a qualitative kinetic screening method, namely a dual-point competition association assay (data not shown). These experiments yielded KRI values ranging from 0.7 ± 0.18, to 2.0 ± 0.18, i.e. indicating faster and slower dissociation kinetics in comparison to the radioligand [^{3}H][Sar^{9},Met(O_2)^{11}]SP, respectively. Aprepitant (KRI of 1.8 ± 0.10) and DFA (KRI of 1.0 ± 0.13) were selected for further studies as they had the highest chemical similarity combined with the most divergent binding kinetics (Supplemental Figure 1).

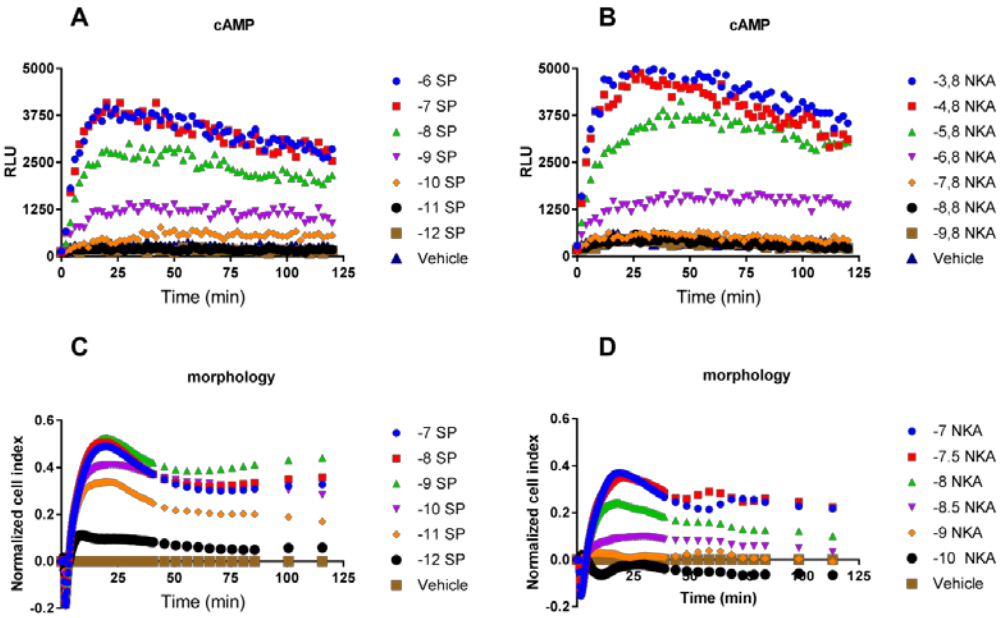

Figure 2: Real-time NK1 receptor-mediated responses monitored with cAMP (A and B) or morphology (C and D) experiments induced by addition of increasing concentrations of endogenous agonist SP (A and C) or NKA (B and D). Representative graph of at least three experiments performed in duplicate (morphology assays) or triplicate (cAMP assays). RLU stands for relative light units and NCI stands for normalized cell index.

Real-time functional effects of NK1 receptor activation by SP and NKA are comparable between kinetic assays

The cellular response to NK1 receptor activation was monitored using two real-time assays, namely a cAMP assay (GloSensor) and a morphology-based assay (xCELLigence). A time-dependent and concentration-dependent increase in cAMP production was observed with the GloSensor assay for both endogenous agonists SP and NKA with a maximal cAMP value around 20 to 30 minutes after stimulation (Figure 2A and B). These experiments yielded EC_{50} values for SP and NKA of 2.2 ± 0.5 nM and 483 ± 142 nM, respectively (Table 1 and 2). Similarly, upon SP or NKA stimulation cellular impedance was increased time- and concentration-dependently with a peak response around 20-30 minutes (Figure 2C and D), with EC_{50} values of 0.026 ± 0.004 nM for SP and 3.9 ± 1.1 nM for NKA (Table 1). Potencies obtained in the morphology assay were systematically higher in comparison to the cAMP assay.

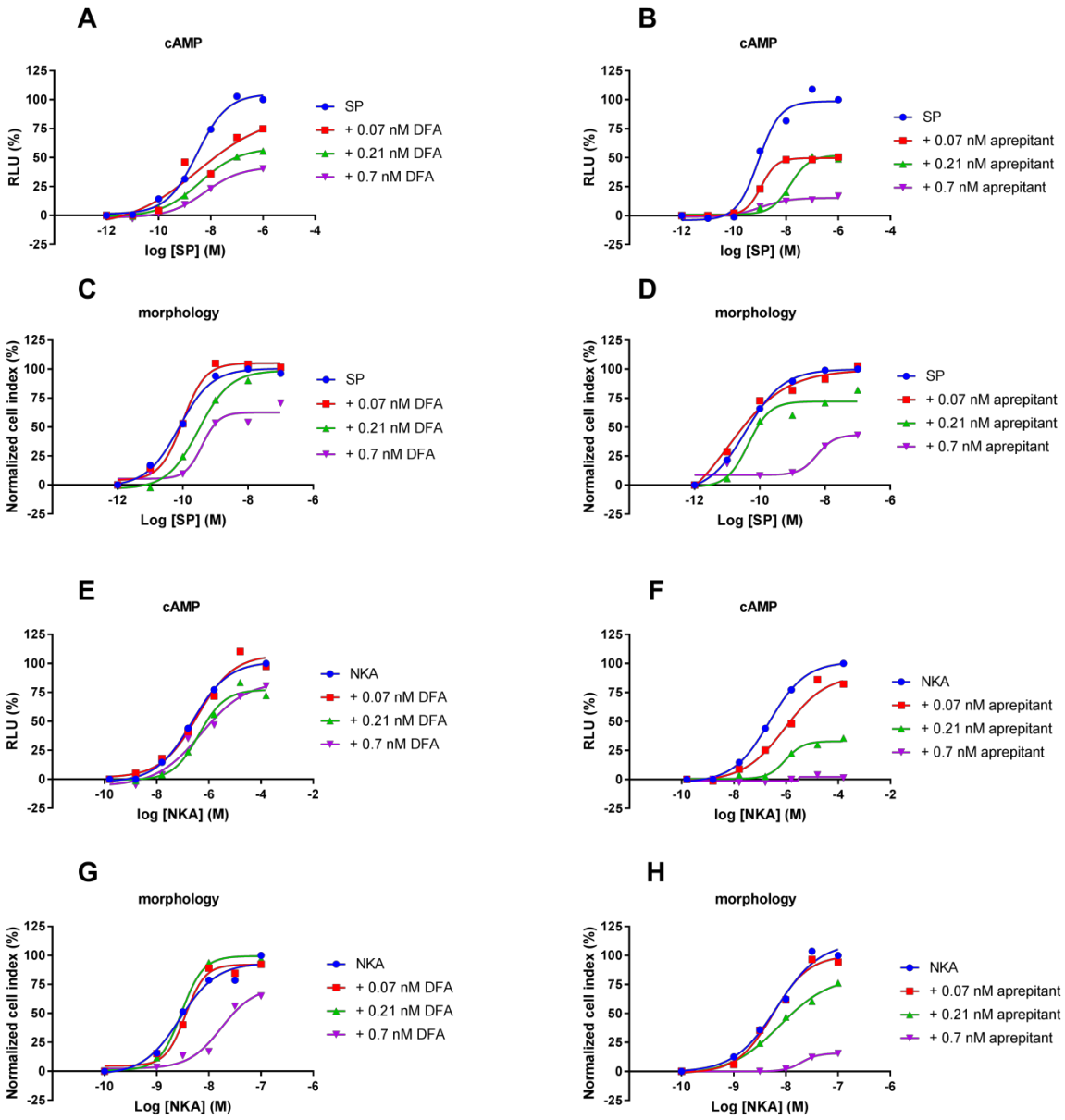

Figure 3: Concentration-dependent effects induced by endogenous agonist SP pre-incubated with vehicle (control), DFA or aprepitant determined with cAMP (A and B) or morphology (C and D) experiments. Concentration-dependent effects induced by endogenous agonist NKA pre-incubated with vehicle (control) DFA or aprepitant determined with cAMP (E and F) or morphology (G and H) experiments. Representative graph of at least three experiments performed in duplicate (morphology assays) or triplicate (cAMP assays). RLU stands for relative light units and NCI stands for normalized cell index.

Aprepitant is more effective in decreasing SP-mediated maximal response

To investigate the antagonistic effects of aprepitant and DFA on SP-mediated NK1 receptor activation, cells were pre-incubated with varying concentrations of antagonist prior to stimulation with SP. In the cAMP assay both antagonists were unable to significantly shift the EC_{50} of SP, however the E_{max} of SP was significantly decreased (Figure 3A and B, Table 1). At the highest concentrations aprepitant was more efficacious in lowering the E_{max} than DFA abolishing over 80% in comparison to control while DFA only decreased the E_{max} by 39% (Table 1). Interestingly, in the morphology assay both antagonists increased the EC_{50} values of SP to 3.0 ± 1.3 nM for DFA and 0.23 ± 0.08 nM for aprepitant (Figure 3C and D, Table 1). Similar to the cAMP assay, the E_{max} of SP was significantly reduced by the antagonists to 82 ± 6.9% of control in the presence of DFA and to a larger extent for aprepitant, i.e. to 53 ± 8.5% (Table 1). Moreover, IC_{50} values were examined by pre-incubating increasing concentrations of antagonist prior to addition of EC_{80} concentrations of agonist (Figure 4). This resulted in IC_{50} values of 0.15 ± 0.02 nM (cAMP assay) and 0.22 ± 0.1 nM (morphology assay) for DFA. IC_{50} values for aprepitant were comparable to DFA with 0.19 ± 0.07 nM and 0.58 ± 0.22 nM from the cAMP and morphology assay, respectively.

Antagonistic effects were more pronounced upon NKA-mediated receptor activation

The inhibitory effects of both antagonists were also investigated for NKA-mediated NK1 receptor activation. In the cAMP assay, aprepitant was able to decrease the potency of NKA by 10-fold, while DFA did not affect the agonist potency (Figure 3E and F, Table 1). This is markedly different from the results observed with SP-mediated receptor activation. Conversely, both antagonists lowered the maximal effect of NKA, while aprepitant was most effective and lowered the E_{max} to 7.8 ± 4.2% (Table 1). On the xCELLigence, the highest concentrations of both antagonists increased the EC_{50} values by 2-fold for DFA and 7-fold for aprepitant (Figure 3G and H, Table 1). Similar to the cAMP assay, both antagonists decreased the maximal effect of NKA while aprepitant was more efficacious (30 ± 6.2%) than DFA (81 ± 8.9%) (Table 1). Furthermore, pretreatment of increasing concentrations of antagonist prior to addition of EC_{80} concentrations of agonist resulted in IC_{50} values ranging from 0.26 ± 0.08 nM (cAMP) to 0.12 ± 0.006 nM (morphology) for DFA while IC_{50} values for aprepitant ranged from 0.23 ± 0.09 nM (cAMP) to 0.43 ± 0.07 nM (morphology) (Figure 4). IC_{50} values of aprepitant and DFA obtained from the two assays were similar.

Aprepitant caused a reduced rate of NK1 receptor activation induced by NKA and SP

To examine the real-time effects of DFA and aprepitant on the inhibition of the cellular response to NK1 receptor activation, a novel analysis method was designed to examine the onset of receptor activation. The increase in cAMP production within the first 8 minutes after

addition of the endogenous agonist was compared in the presence and absence (control) of an antagonist. The onset of SP-induced cAMP production was significantly decreased (i.e. up to 6-fold) upon pre-incubation with aprepitant but not with DFA (Figure 5A, B and C, Table 2). Similarly, the onset of SP-induced impedance changes was significantly decreased 5-fold upon aprepitant pretreatment, while pretreatment with DFA was less significant (Figure 5D and E, Table 2). Moreover, the ability of aprepitant to reduce the onset of receptor activation was more pronounced for NKA, where a significant 15-fold decrease in onset was observed in cAMP production and a significant 8-fold decrease for morphological changes (Figure 6F, G, H and I Table 2). Conversely, DFA did not significantly decrease the onset of receptor activation in both cAMP and morphology assays.

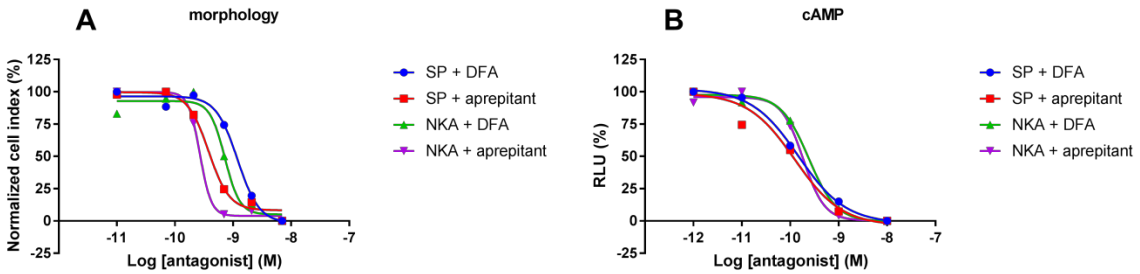

Figure 4: Concentration-dependent inhibition by DFA or aprepitant of EC_{80} concentrations of SP- or NKA- mediated receptor activation measured with morphology (A) or cAMP (B) experiments. Representative graph of at least three experiments performed in duplicate (morphology assays) or triplicate (cAMP assays). RLU stands for relative light units and NCI stands for normalized cell index.

Discussion

To our knowledge, we are the first to provide an extensive investigation on *in vitro* cellular responses in relation to receptor binding kinetics of antagonists and endogenous agonists. This research has significant implications for the understanding of signal transduction induced by kinetically diverse ligand-receptor interactions and the interplay between endogenous agonists and drugs targeting the receptor of interest.

The NK1 receptor is an interesting target for the treatment of neurological disorders and currently two drugs, aprepitant and netupitant, are approved for the treatment of chemotherapy induced emesis [30]. While the high *in vivo* efficacy of aprepitant is attributed to its slow dissociation kinetics [23], a mechanistic interpretation of the translation of binding kinetics to functional effects is lacking. Therefore, this study was designed to bridge the gap

between receptor binding kinetics and functional effects *in vitro*, which is important for the understanding of the translation of *in vitro* to *in vivo* data.

We hypothesized that the slowly dissociating antagonist aprepitant would be more effective in antagonizing the receptor than its fast dissociating analogue DFA. The rightward-shift in potency of SP and NKA was most discernable at the highest concentration of antagonist, where aprepitant increased the EC_{50} value and decreased the E_{max} value more significantly than DFA (Table 1, Figure 3). While aprepitant was fully insurmountable, DFA was only partially insurmountable. The latter can be explained by the fact that although DFA is a faster dissociating compound when compared to aprepitant, DFA is still a slower dissociating compound in comparison to the endogenous agonists SP and NKA. Hence, pre-incubation with DFA resulted in partially insurmountable antagonism as opposed to surmountable antagonism with an even faster dissociating antagonist. Our results for aprepitant are in line with its previously reported insurmountable effects [22]. In the same study the ID_{50} values of aprepitant and DFA were determined in an animal model for CNS activity (gerbil foot tapping), where aprepitant was 3-fold more potent than its analogue DFA [22]. Another study examined the insurmountable effects of a close analogue of aprepitant and DFA, namely L-742,694. A clear decrease in E_{max} of SP after pre-incubation with L-742,694 was reported and this effect was associated with the slow dissociation rate of this antagonist from the NK1 receptor [31]. Altogether, these findings support our hypothesis that slowly dissociating antagonists are important for achieving a high *in vivo* efficacy by insurmountable antagonism at the NK1 receptor.

While both antagonists aprepitant and DFA were able to increase the EC_{50} and decrease E_{max} values for both NKA and SP, NKA was overall more sensitive to antagonism than SP. This supposed “probe-dependency”, i.e. observed effects are dependent on the probe (e.g. agonist) used, is already widely acknowledged in the field of allosteric modulation [32, 33], while this concept is rarely considered for orthosteric interactions. Interestingly, we have previously determined the binding kinetics of SP and NKA and found large differences in the association rates of both agonists, i.e. NKA associates 240-fold slower to the NK1 receptor than SP [27]. This slow association could be an explanation as to why NKA is more sensitive to antagonism, considering that both antagonists have more time to intervene with NKA target binding due to their assumed faster association rates, slower dissociation rates and pre-incubation time. The differential kinetics (and therefore sensitivity) of both endogenous agonists should be taken into account for further research towards the NK1 receptor and other GPCRs that have multiple endogenous ligands [26].

A comparison between EC_{50} values obtained with the cAMP or morphology assays showed lower potency values for the latter. This is in line with other observations, namely that potency values acquired from label-free assays such as the xCELLigence are often reported to be much lower and may be attributed to the fact that these assays encompass the entire cellular response thereby accumulating multiple signaling pathways instead of only one [34-36]. Moreover, it appeared that the morphology assay was more sensitive to pick up shifts in potency upon antagonist treatment while the cAMP assay was most sensitive in detecting insurmountability, i.e. a decrease in maximal effect. A possible explanation could be the differences in assay set-up that can alter the assay sensitivity. For instance, morphology experiments are typically performed at 37 °C while cAMP assays were carried out at 25 °C. Lower assay temperatures result in slower dissociation rates which could explain the higher sensitivity of the cAMP assay to detect insurmountability. Moreover, the cAMP assay was carried out with CHOhNK1 cells while the morphology assay was performed with U-251 MG cells. Multiple studies have previously discussed the concept of receptor reserve, i.e. high receptor coupling efficiency and/or high-receptor density [37, 38]. It was proposed that tissue with essentially no receptor reserve treated with an insurmountable antagonist could present a decrease in maximal response with only a marginal rightward shift in potency. Heterologous cell lines are often reported to have higher receptor reserves in comparison to cell lines with endogenous expressions. Our results suggest that U-251 MG cells may have a higher receptor reserve than CHOhNK1 cells and U-251 MG cells might therefore be better suited to detect a shift in potency. These findings demonstrate the importance of choosing the appropriate assay and cell type for the aim of the research.

The functional effects of antagonist binding kinetics are often examined with insurmountability assays using end-point measurements [39] but also real-time experiments [40]. Although a few studies have paid some attention to the real-time changes in cellular effects [13, 14, 41, 42], we are the first to report a quantitative analysis method for the real-time cellular responses induced by agonists with antagonist pre-incubations. In this study, we were able to correlate the kinetics of receptor activation (i.e. rate of onset) to receptor binding kinetics of antagonists. The slowly dissociating antagonist aprepitant was effective in not only significantly decreasing the maximal effect of SP and NKA but also in significantly reducing the onset of receptor activation, which would have been missed using a traditional end-point assay. Hence, this novel analysis provides a robust and time-efficient screening method to detect slowly dissociating antagonists using a real-time functional assay.

In conclusion, in this research the effects of kinetically diverse agonists and antagonists on receptor responses were extensively studied. We demonstrated that the binding kinetics of both antagonists and endogenous agonists have significantly different

effects on signal transduction profiles, i.e. potency values, *in vitro* efficacy values and onset rate of signal transduction. Moreover, these findings were consistent throughout different kinetic assays, assay temperatures and cellular backgrounds. We propose that incorporating real-time functional assays early in the drug discovery program will enable the detection of kinetically interesting compounds. Moreover, combining knowledge of binding kinetics and functional kinetics of drugs and endogenous ligands could improve predictions of *in vivo* drug action and thereby the success rate of drug discovery.

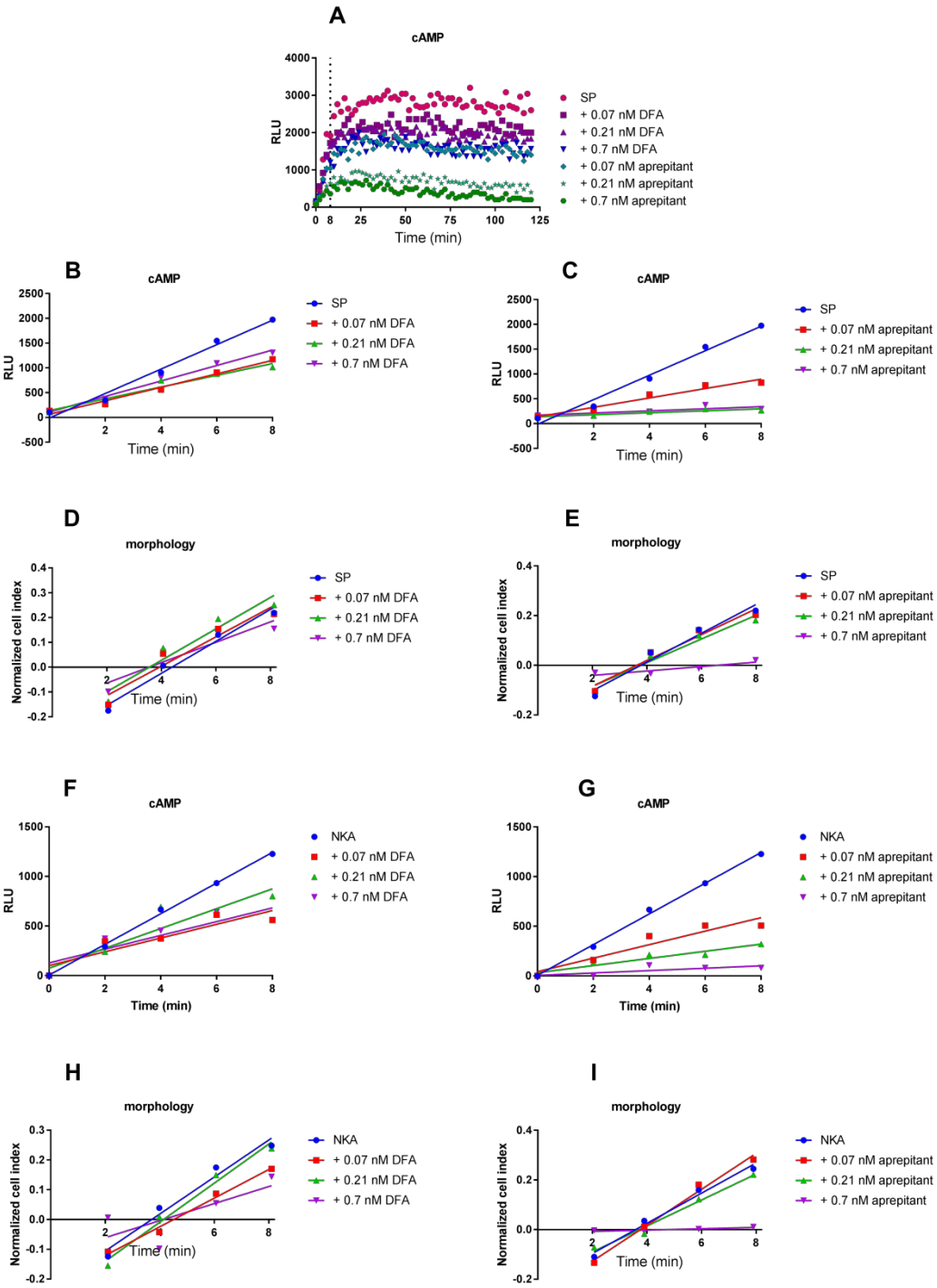

Figure 5: Time-dependent effects induced by EC_{80} concentration of SP after pre-incubation with DFA or aprepitant observed with cAMP assay (A). Zoom-in on first 8 minutes of time-dependent effects induced by EC_{80} concentration of SP (B and C) or NKA (F and G) after pre-incubation with DFA or aprepitant determined with cAMP experiments. Representative graph of at least three experiments performed in triplicate. RLU stands for relative light units. Zoom-in on first 8 minutes of time-dependent effects induced by EC_{80} concentration of SP (D and E) or NKA (H and I) after pre-incubation with DFA or aprepitant determined with morphology experiments. Representative graph of at least three experiments performed in duplicate. NCI stands for normalized cell index**.**

Table 1: Potency and maximal effect values of SP with or without antagonist pre-incubation determined with cAMP or morphology assays

	EC_{50} (nM)				E_{max} (%)			
	cAMP		morphology		cAMP		morphology	
	SP	NKA	SP	NKA	SP	NKA	SP	NKA
Agonist	2.2 ± 0.5	483 ± 142	0.026 ± 0.004	3.9 ± 1.1	100 ± 5.1	100 ± 7.7	100 ± 0.95	100 ± 0.44
+ 0.07 nM DFA	1.9 ± 0.5 ^{NS}	399 ± 19 ^{NS}	0.053 ± 0.020^{NS}	3.0 ± 0.52 ^{NS}	78 ± 4.5*	84 ± 18 ^{NS}	97 ± 5.6 ^{NS}	109 ± 7.6 ^{NS}
+ 0.21 nM DFA	2.7 ± 0.8 ^{NS}	304 ± 89 ^{NS}	0.06 ± 0.015*	3.3 ± 0.45 ^{NS}	75 ± 7.7*	67 ± 10*	104 ± 4.2^{NS}	108 ± 6.7 ^{NS}
+ 0.7 nM DFA	2.3 ± 0.7 ^{NS}	1080 ± 356 ^{NS}	3.0 ± 1.3*	8.5 ± 0.46*	61 ± 10**	61 ± 15*	82 ± 6.9**	81 ± 8.9**
+ 0.07 nM aprepitant	1.6 ± 0.2 ^{NS}	1008 ± 165 ^{NS}	0.022 ± 0.008^{NS}	5.0 ± 1.7 ^{NS}	62 ± 5.7**	71 ± 13 ^{NS}	96 ± 7.6^{NS}	97 ± 2.3^{NS}
+ 0.21 nM aprepitant	8.8 + 5.4 ^{NS}	1051 ± 170*	0.11 ± 0.01****	8.0 ± 2.8 ^{NS}	55 ± 15**	43 ± 19**	79 ± 5.0***	79 ± 10**
+ 0.7 nM aprepitant	1.3 ± 0.3 ^{NS}	4370 ± 524***	0.23 ± 0.08**	26 ± 6.8**	19 ± 5.5****	7.8 ± 4.2****	53 ± 8.5****	30 ± 6.2****

Values are means ± SEM of at least three separate experiments performed in duplicate (morphology) or triplicate (cAMP). Values were calculated with peak analysis and data were normalized to maximal response obtained for SP or NKA only. * $p < 0.05$, ** $p < 0.01$, *** $p < 0.001$, **** $p < 0.0001$ compared to SP or NKA, determined using one-way ANOVA with Dunnett's post-test.

Table 2: Onset of SP- or NKA-induced receptor activation after pretreatment with DFA or aprepitant determined with cAMP or morphology assays.

	cAMP (RLU min^{-1})[#]		Morphology (NCI min^{-1}) [#]	
	SP	**NKA**	**SP**	**NKA**
Agonist	215 ± 37	147 ± 35	0.05 ± 0.004	0.05 ± 0.004
+ 0.07 nM DFA	125 ± 31^{NS}	98 ± 29^{NS}	0.06 ± 0.006^{NS}	0.06 ± 0.005^{NS}
+ 0.21 nM DFA	120 ± 27^{NS}	98 ± 33^{NS}	0.05 ± 0.006^{NS}	0.05 ± 0.007^{NS}
+ 0.7 nM DFA	158 ± 26^{NS}	71 ± 22^{NS}	0.03 ± 0.005*	0.04 ± 0.014^{NS}
+ 0.07 nM aprepitant	94 ± 13*	75 ± 13^{NS}	0.05 ± 0.002^{NS}	0.05 ± 0.011^{NS}
+ 0.21 nM aprepitant	63 ± 17**	43 ± 7.7*	0.04 ± 0.006^{NS}	0.03 ± 0.007^{NS}
+ 0.7 nM aprepitant	36 ± 7**	9.7 ± 1.6**	0.009 ± 0.003****	0.006 ± 0.003**

Values are means ± SEM of at least three separate experiments performed in duplicates (morphology) or triplicates (cAMP). The onset of receptor activation was calculated on the first 8 min after agonist stimulation. [#] RLU stands for relative light units and NCI stands for normalized cell index. * $p < 0.05$, ** $p < 0.01$, *** $p < 0.001$, **** $p < 0.0001$ compared to agonist only, determined using one-way ANOVA with Dunnett's post-test.

References

1. Zhang, R. and F. Monsma, *The importance of drug-target residence time.* Current opinion in drug discovery & development, 2009. **12**(4): p. 488-96.
2. Swinney, D.C., et al., *The Role of Binding Kinetics in GPCR Drug Discovery.* Curr Top Med Chem, 2015. **15**(24): p. 2504-22.
3. Guo, D., et al., *Drug-target residence time-a case for G protein-coupled receptors.* Medicinal research reviews, 2014. **34**(4): p. 856-92.
4. Copeland, R.A., *The drug-target residence time model: a 10-year retrospective.* Nat Rev Drug Discov, 2016. **15**(2): p. 87-95.
5. de Witte, W.E., et al., *In vivo Target Residence Time and Kinetic Selectivity: The Association Rate Constant as Determinant.* Trends Pharmacol Sci, 2016. **37**(10): p. 831-42.
6. Danhof, M., et al., *Mechanism-based pharmacokinetic-pharmacodynamic modeling: biophase distribution, receptor theory, and dynamical systems analysis.* Annu Rev Pharmacol Toxicol, 2007. **47**: p. 357-400.
7. Yamamoto, Y., et al., *A Generic Multi-Compartmental CNS Distribution Model Structure for 9 Drugs Allows Prediction of Human Brain Target Site Concentrations.* Pharm Res, 2016.
8. Guo, D., et al., *Equilibrium and kinetic selectivity profiling on the human adenosine receptors.* Biochem Pharmacol, 2016. **105**: p. 34-41.
9. Heym, R.G., et al., *Label-free detection of small-molecule binding to a GPCR in the membrane environment.* Biochim Biophys Acta, 2015. **1854**(8): p. 979-86.
10. Schiele, F., P. Ayaz, and A. Fernandez-Montalvan, *A universal homogeneous assay for high-throughput determination of binding kinetics.* Anal Biochem, 2015. **468**: p. 42-9.
11. DiRaddo, J.O., et al., *A real-time method for measuring cAMP production modulated by Galphai/o-coupled metabotropic glutamate receptors.* J Pharmacol Exp Ther, 2014. **349**(3): p. 373-82.
12. Buccioni, M., et al., *Innovative functional cAMP assay for studying G protein-coupled receptors: application to the pharmacological characterization of GPR17.* Purinergic Signal, 2011. **7**(4): p. 463-8.
13. Stallaert, W., et al., *Impedance responses reveal beta(2)-adrenergic receptor signaling pluridimensionality and allow classification of ligands with distinct signaling profiles.* PloS one, 2012. **7**(1): p. e29420.
14. Schroder, R., et al., *Deconvolution of complex G protein-coupled receptor signaling in live cells using dynamic mass redistribution measurements.* Nature biotechnology, 2010. **28**(9): p. 943-9.
15. Garcia-Recio, S. and P. Gascon, *Biological and Pharmacological Aspects of the NK1-Receptor.* Biomed Res Int, 2015. **2015**: p. 495704.
16. Munoz, M. and R. Covenas, *Involvement of substance P and the NK-1 receptor in human pathology.* Amino Acids, 2014. **46**(7): p. 1727-50.

17. Ballet, S., et al., *Design of novel neurokinin 1 receptor antagonists based on conformationally constrained aromatic amino acids and discovery of a potent chimeric opioid agonist-neurokinin 1 receptor antagonist.* J Med Chem, 2011. **54**(7): p. 2467-76.
18. Di Fabio, R., et al., *Identification, biological characterization and pharmacophoric analysis of a new potent and selective NK1 receptor antagonist clinical candidate.* Bioorg Med Chem, 2013. **21**(21): p. 6264-73.
19. Hanessian, S., et al., *Design, Synthesis, and Optimization of Balanced Dual NK1/NK3 Receptor Antagonists.* ACS Med Chem Lett, 2014. **5**(5): p. 550-5.
20. Goldstein, D.J., et al., *Lanepitant, an NK-1 antagonist, in migraine prevention.* Cephalalgia, 2001. **21**(2): p. 102-6.
21. Fahy, J.V., et al., *Effect of an NK1 receptor antagonist (CP-99,994) on hypertonic saline-induced bronchoconstriction and cough in male asthmatic subjects.* Am J Respir Crit Care Med, 1995. **152**(3): p. 879-84.
22. Hale, J.J., et al., *Structural optimization affording 2-(R)-(1-(R)-3,5-bis(trifluoromethyl)phenylethoxy)-3-(S)-(4-fluoro)phenyl-4-(3-oxo-1,2,4-triazol-5-yl)methylmorpholine, a potent, orally active, long-acting morpholine acetal human NK-1 receptor antagonist.* Journal of Medicinal Chemistry, 1998. **41**(23): p. 4607-4614.
23. Lindstrom, E., et al., *Neurokinin 1 receptor antagonists: Correlation between in vitro receptor interaction and in vivo efficacy.* Journal of Pharmacology and Experimental Therapeutics, 2007. **322**(3): p. 1286-1293.
24. Thompson, C.A., *Netupitant-palonosetron combination approved by FDA.* Am J Health Syst Pharm, 2014. **71**(23): p. 2000.
25. Rizzi, A., et al., *In vitro and in vivo pharmacological characterization of the novel NK(1) receptor selective antagonist Netupitant.* Peptides, 2012. **37**(1): p. 86-97.
26. Nederpelt, I., et al., *Kinetic Profile of Neuropeptide-Receptor Interactions.* Trends Neurosci, 2016.
27. Nederpelt, I., et al., *Kinetic binding and activation profiles of endogenous tachykinins targeting the NK1 receptor.* Biochem Pharmacol, 2016.
28. Guo, D., et al., *Dual-point competition association assay: a fast and high-throughput kinetic screening method for assessing ligand-receptor binding kinetics.* J Biomol Screen, 2013. **18**(3): p. 309-20.
29. Yu, N., et al., *Real-time monitoring of morphological changes in living cells by electronic cell sensor arrays: an approach to study G protein-coupled receptors.* Analytical chemistry, 2006. **78**(1): p. 35-43.
30. Rojas, C. and B.S. Slusher, *Mechanisms and latest clinical studies of new NK1 receptor antagonists for chemotherapy-induced nausea and vomiting: Rolapitant and NEPA (netupitant/palonosetron).* Cancer Treat Rev, 2015. **41**(10): p. 904-13.
31. Cascieri, M.A., et al., *Characterization of the binding and activity of a high affinity, pseudoirreversible morpholino tachykinin NK1 receptor antagonist.* Eur J Pharmacol, 1997. **325**(2-3): p. 253-61.

32. Wootten, D., A. Christopoulos, and P.M. Sexton, *Emerging paradigms in GPCR allostery: implications for drug discovery.* Nat Rev Drug Discov, 2013. **12**(8): p. 630-44.
33. Lindsley, C.W., et al., *Practical Strategies and Concepts in GPCR Allosteric Modulator Discovery: Recent Advances with Metabotropic Glutamate Receptors.* Chem Rev, 2016. **116**(11): p. 6707-41.
34. Scandroglio, P., et al., *Evaluation of cannabinoid receptor 2 and metabotropic glutamate receptor 1 functional responses using a cell impedance-based technology.* Journal of biomolecular screening, 2010. **15**(10): p. 1238-47.
35. Kammermann, M., et al., *Impedance measurement: a new method to detect ligand-biased receptor signaling.* Biochemical and biophysical research communications, 2011. **412**(3): p. 419-24.
36. Nederpelt, I., et al., *Persistent GnRH receptor activation in pituitary alphaT3-1 cells analyzed with a label-free technology.* Biosens Bioelectron, 2016. **79**: p. 721-7.
37. Kenakin, T., S. Jenkinson, and C. Watson, *Determining the potency and molecular mechanism of action of insurmountable antagonists.* J Pharmacol Exp Ther, 2006. **319**(2): p. 710-23.
38. Charlton, S.J. and G. Vauquelin, *Elusive equilibrium: the challenge of interpreting receptor pharmacology using calcium assays.* Br J Pharmacol, 2010. **161**(6): p. 1250-65.
39. Malherbe, P., et al., *Mapping the binding pocket of a novel, high-affinity, slow dissociating tachykinin NK3 receptor antagonist: biochemical and electrophysiological characterization.* Neuropharmacology, 2014. **86**: p. 259-72.
40. Nicholls, D.J., et al., *Pharmacological characterization of AZD5069, a slowly reversible CXC chemokine receptor 2 antagonist.* J Pharmacol Exp Ther, 2015. **353**(2): p. 340-50.
41. Hothersall, J.D., et al., *Structure-activity relationships of the sustained effects of adenosine A2A receptor agonists driven by slow dissociation kinetics.* Mol Pharmacol, 2016.
42. Bosma, R., et al., *BRET-based beta-arrestin2 recruitment to the histamine H1 receptor for investigating antihistamine binding kinetics.* Pharmacol Res, 2016. **111**: p. 679-87.

Chapter 7

Conclusions and future perspectives

In this thesis the binding kinetics of endogenous neuropeptides and drugs targeting two well-known neuropeptide receptors (i.e. the GnRH receptor and NK1 receptor) have been investigated. Kinetic binding and functional assays have been designed and validated to examine the differences in binding kinetics of the above-mentioned ligands. This final chapter focusses on providing a conclusion to the previous chapters while highlighting ongoing challenges with regard to binding kinetics. Moreover, opportunities for further research toward binding kinetics and neuropeptide receptors are discussed.

Conclusions

Kinetic assays contribute to a more complete pharmacological profile of ligands

Assays applied in current drug discovery are mainly used for equilibrium assessments of drug candidates. However, since kinetic binding parameters are increasingly recognized as important considerations in drug discovery a need for kinetic assays is imminent. Throughout all the chapters of this thesis, several binding and functional assays have been designed to serve kinetic binding assessments of various ligands. In Chapter 3 kinetic radioligand binding studies were compared to kinetic time-resolved fluorescence resonance energy transfer (TR-FRET) studies. For both assays a competition association assay was developed and validated and results obtained from the two methods were highly correlated. In Chapter 4 a functional wash-out experiment using the label-free real-time xCELLigence was performed with the two most kinetically diverse agonists from Chapter 3. The results from these experiments were in agreement with the kinetic data obtained with the kinetic radioligand and TR-FRET binding assays. Moreover, in Chapter 6 a medium-throughput kinetic screening assay was used to qualitatively examine the dissociation rates of a library of antagonists. Two exemplary antagonists with contrasting dissociation rates were further examined with two kinetic functional assays. Kinetic functional data from a real-time impedance-based morphology assay and a novel real-time cAMP assay corresponded well with the kinetic screening assay. Furthermore, data from both kinetic functional assays were highly correlated. In conclusion, kinetic binding and kinetic functional assays are very suitable and transferable for the investigation of kinetic ligand-receptor interactions.

Binding kinetics of endogenous neuropeptides are very diverse

Neuropeptides are 3-100 amino acid long polypeptides and are synthesized by neurons. They can bind neuropeptide receptors and together they are involved in many physiological and behavioral functions, making neuropeptides and their cognate receptors an attractive target to treat a wide range of diseases. While drug discovery programs predominantly focus on characterizing the drug candidate, knowledge of the pharmacological profile of the endogenous ligand and its target is essential when orthosteric drugs are desired. Chapter 2 reviews the kinetic profile of three exemplary neuropeptide receptors and their endogenous ligands (i.e. GnRH receptor, CRF1 receptor and NPY receptor). The neuropeptide binding kinetics, release rate and receptor internalization rates were very different for all three receptor-neuropeptide pairs emphasizing the importance and variability of kinetic profiles. Moreover, in Chapter 5 the binding kinetics of multiple endogenous ligands

targeting the NK1 receptor were determined. These ligands proved to have very different binding kinetics, particularly association rates were very variable.

Differential binding kinetics can have differential functional effects in vitro

While binding kinetics are progressively acknowledged as pivotal pharmacological parameters of a drug candidate, understanding of the translation of binding kinetics to *in vitro* and *in vivo* functional effects is still largely absent. The *in vitro* functional effects of neuropeptide agonists with variable dissociation rates were examined in Chapter 4. Long lasting receptor activation was evident for a slowly dissociating agonist while a fastly dissociating analog failed to show persistent receptor activation. Additionally, Chapter 5 demonstrated that differences in association rates lead to altered potency and efficacy values *in vitro*. Moreover, differential binding kinetics of endogenous ligands and their competing antagonists play an important role in the interaction of the ligands with the receptor. In Chapter 6, it was illustrated that slowly dissociating antagonists can have superior efficacy to its fastly dissociating counterpart. Additionally, slowly dissociating antagonists can cause a reduced rate of signal transduction. Moreover, the binding kinetics of the competing endogenous ligands also proved to be of importance. Antagonistic effects were significantly bigger in the presence of a slowly associating in comparison to a fastly associating endogenous ligand.

In summary, this thesis provides a large variety of kinetic assays that can be used to qualitatively and quantitatively determine receptor binding kinetics of ligands of interest. Additionally, the binding kinetics of endogenous neuropeptides can be very different and should therefore be considered when designing orthosteric drugs. Moreover, the combination of endogenous ligands and competitive drugs with differential binding kinetics can have significantly different functional effects *in vitro*. Finally, a wide range of kinetic assays, improved knowledge of endogenous ligand binding kinetics and a good understanding of the translational effects of binding kinetics could improve drug discovery today and decrease drug attrition rates in the future.

Lessons learned

Assay considerations

The search for optimal assay conditions is particularly challenging when designing an assay to study binding kinetics for neuropeptide ligands. Firstly, kinetic binding assays that utilize a tracer ligand are heavily reliant on the binding kinetics of the tracer. If the aim of the project is to find slowly dissociating ligands and the binding kinetics of tracer are very fast,

the mathematical model to evaluate the results is unable to provide quantitative data. To acquire quantitative parameters, the binding kinetics of the tracer ligands and unlabeled ligands should ideally be in the same time range (i.e. seconds, minutes, hours). Secondly, kinetic binding assays are often carried out at room temperature or sometimes at even lower temperatures. In these cases, the obtained kinetic binding parameters are not measured at physiological temperature (37 °C). It should be taken into account that binding kinetics will be significantly faster at higher temperatures [1-3]. Lastly, the type of kinetic assay can also be of influence. For instance, functional assays are often implemented as endpoint measurements, e.g. accumulation of a protein or 2nd messenger measured after a certain incubation time. Consequently an over- or underestimation of pharmacological parameters can occur due to inadequate incubation times. Conversion of endpoint assays into real-time measurements could circumvent this limitation.

Pharmacological profile of the drug, receptor and its endogenous ligands in the human body

The need for fast or slow binding kinetics of a drug candidate is always relative to its target system and therefore understanding of the pharmacological profile of the entire system is crucial. Firstly, the pharmacokinetic (PK) half-life of the drug candidate needs to be considered. For example, if the PK half-life is slower than the residence time (RT) of the drug the latter becomes less relevant. Conversely, if the RT of the drug is slower than the PK half-life, binding kinetics play a pivotal role in dictating the duration of action of the drug, assuming target engagement *in vivo*. Secondly, the internalization and desensitization rate of the targeted receptor should be taken into account. For instance, if the internalization rate of the receptor is faster than the dissociation rate of the drug the latter becomes trivial for agonist (and arguably antagonist) drugs. Correspondingly, if the receptor internalizes slowly, binding kinetics of agonist (and arguably antagonist) drugs can be very pertinent as the drug effect is hardly limited by receptor internalization. Finally, the kinetic profiles of both the drug and the endogenous ligands should be deliberated. Since the majority of drugs target the orthosteric binding site of the receptor, they are in constant competition with endogenous ligands. Concentrations of endogenous ligands in the human body often fluctuate significantly and binding kinetics can also be quite variable. Consequently, the binding kinetics and release rate of endogenous ligands should be determined in anticipation of achieving optimal binding kinetics of the drug candidate.

Future perspectives

This thesis predominantly focused on binding kinetics, ranging from designing and comparing kinetic assays to determining kinetic parameters of well-known drugs and endogenous ligands and translating binding kinetics to *in vitro* functional effects. The following paragraphs will discuss some future perspectives for neuropeptide receptors and GPCRs in general.

Increasing the output of kinetic assays

Within this thesis we have discussed multiple assays suitable for qualitative and quantitative measurements of ligand-receptor binding kinetics. Additional, more high-throughput screening methods could aid in the applicability of kinetic assays in drug discovery programs. Guo *et al.* have developed a medium-throughput screening assay to qualitatively estimate dissociation rates of ligands [4]. To date this screening assay has been successfully applied to multiple GPCRs [5-7], including the NK1 receptor in this thesis. However, a screening assay suitable for the estimation of association rates is still lacking. Additionally, while some binding assays can be transformed in high-throughput formats, radioligand binding assays are often performed in very low throughput formats. Glickman *et al* have reviewed the potential of using scintillation proximity assays (SPA) in high-throughput screening and kinetic measurements [8]. To date only a few research groups have used this SPA assay to study binding kinetics of GPCR ligands. In 2007, the kinetics of small molecule GnRH antagonists were qualitatively assessed in a high-throughput format [9] and more recently, a quantitative determination of the binding kinetics of human adenosine A_1 receptor ligands was reported [10].

When researchers are interested in examining binding kinetics of antagonists in functional assays, insurmountability assays are typically the assay of choice. However, this assay is heavily reliant on assay conditions. For instance, a recent study of Vauquelin *et al* demonstrated the importance of pre-incubation times, where too short a pre-incubation of antagonist might not be sufficient for decreasing the maximal response [11]. Importantly, ‘’too short’’ pre-incubation times are dependent on the association rate of the antagonist and assay temperatures and might therefore be different per ligand and assay. Moreover, the time at which measurements are terminated could result in skewed results depending on the equilibrium between receptor, agonist and antagonist. Additionally, the kinetic data from functional assays such as the real-time cAMP assay and the real-time impedance-based morphology assay are often disregarded, as results from only one time-point are considered. Chapters 4 and 6 demonstrate the value of acknowledging functional kinetics and further studies of this concept on other targets would be beneficial.

Beyond binding kinetics, what happens after a ligand binds to its target?

Throughout the chapters in this thesis the *in vitro* translational effects of binding kinetics have been explored, including the kinetics of cellular responses. To gain more insights into these receptor activation kinetics more information should be gathered about the individual kinetics of all proteins and enzymes involved in the final response. To illustrate the kinetic information available to date, the kinetics of the $G\alpha_q$ pathway are reviewed here (Figure 1). The $G\alpha_q$ pathway is initiated by binding of an agonist to the $G\alpha_q$ coupled receptor leading to a conformational change which results in the exchange of GDP for GTP and activation of the G protein. Consequently, phospholipase C (PLC) is activated and induces hydrolysis of phosphoinositol 4,5-biphosphate (PIP_2) into inositol 1,4,5-triphosphate (IP_3). IP_3 subsequently binds to IP_3 receptors resulting in the release of Ca^{2+} into the cytosol, which induces the activation of myosin light chain kinases (MLCKs). Finally, upon activation of MLCKs actin filaments are contracted. All these processes together occur within seconds but information on the kinetic parameters of components of the $G\alpha_q$ pathway is limited and the representation is not consistent throughout the literature (e.g. *rate* constants versus *time* constants). It should be noted that these (rare) reports of kinetics of the activation and production of these downstream proteins could be receptor and pathway specific. For instance, G protein coupling and activation could be different for all G protein subtypes, i.e. $G\alpha_s$ protein coupling being faster or slower than $G\alpha_q$ coupling. Another important factor to consider is the kinetic differences in G protein and β-arrestin coupling. A study of Nuber *et al.*, reported a tau value (time constant) of 2.2 s for β-arrestin coupling to the β_2-adrenergic receptor [12], versus 0.05-25 s for G protein coupling. Arguably, the GPCR under investigation could also influence the kinetics of G protein coupling. Moreover, it should be noted that ligand-receptor binding kinetics could influence the rate of G protein or β-arrestin coupling and activation.

Furthermore, the chapters in this thesis have demonstrated that varying binding kinetics can have divergent functional effects. For example, in Chapter 4 persistent signaling responses were observed for a slowly dissociating GnRH receptor agonist. Conversely, in Chapter 5 a positive correlation between potency values and association rate was found for a set of NK1 receptor agonists. Additionally, while slow dissociation rates are often thought to increase E_{max} values the opposite was observed with the NK1 receptor agonists. Arguably, slowly dissociating agonists could be more efficacious in inducing receptor internalization while fastly dissociating agonists are less efficacious in inducing this process, thereby maintaining full receptor activation and a higher maximal effect. Lastly, in Chapter 6 it was demonstrated that a slowly dissociating NK1 antagonist can significantly decrease the initial kinetics of receptor activation. Moreover, these effects were stronger for a slowly associating

agonist than for a fastly associating agonist. These results indicate that the signaling kinetics can be significantly altered with divergent binding kinetics.

Altogether, the short review and examples in this thesis could provide a foundation for further research towards not only target binding kinetics but also the kinetics involved after a ligand is bound to its receptor. Additionally, knowledge of the kinetics of signaling pathways could provide more detailed input for mathematical models used to predict the translational effects of binding kinetics.

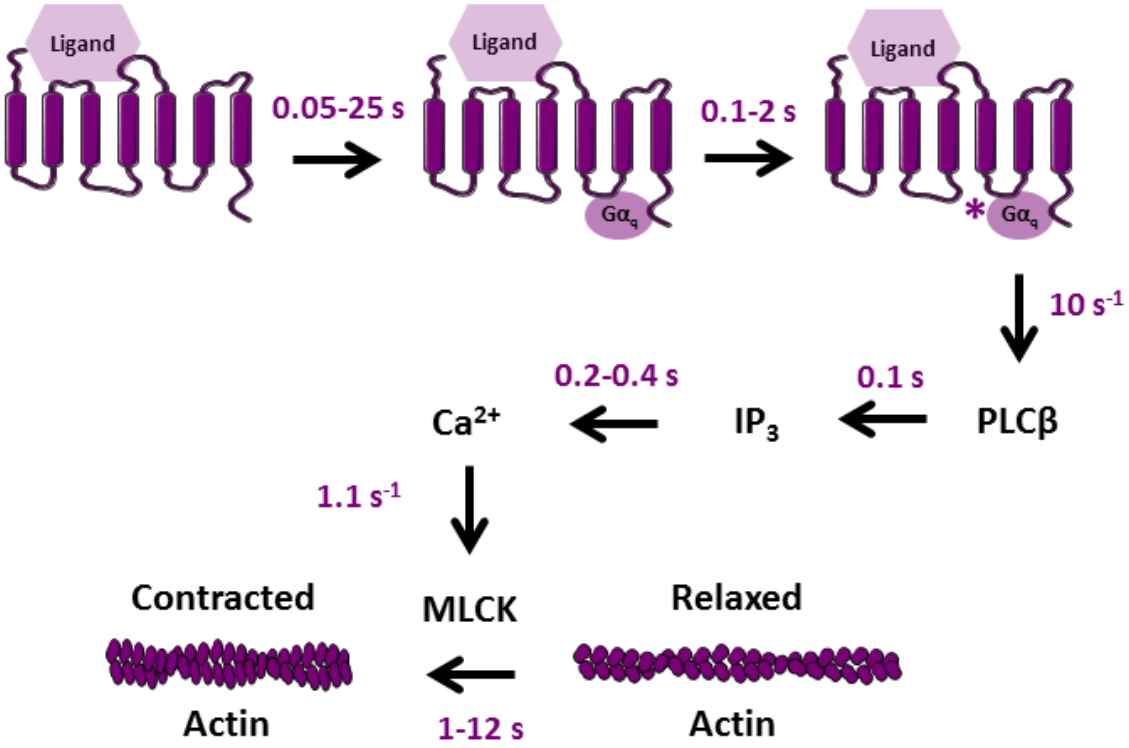

Figure 1: Upon agonist binding to a $G\alpha_q$ coupled receptor, the receptor undergoes a conformational change allowing the exchange of GDP to GTP and the time constant (tau) for this process ranges from 0.05 to 25 seconds [13-15], followed by activation of the G protein (*) within 0.1 to 2 seconds [13, 14, 16]. Following G protein activation, phospholipase C is activated with an activation rate of 10 s^{-1} [17]. Consequently, PLC induces hydrolysis of phosphoinositol 4,5-bisphosphate (PIP_2) into inositol 1,4,5-triphosphate (IP_3) with a maximum production after approximately 0.1 seconds [17, 18]. IP_3 can then bind to IP_3 receptors which results in the opening of Ca^{2+} channels, releasing Ca^{2+} into the cytosol within 0.2-0.4 seconds [19-21]. In turn, Ca^{2+} induces the activation of myosin light chain kinases (MLCKs) with a rate of 1.1 s^{-1} [22]. Activation of MLCKs will lead to actin contraction after 1-12 seconds [23, 24].

The potential role of binding kinetics in biased signaling

To date, the concept of biased signaling has gained increasing consideration in the GPCR field. Biased signaling or biased agonism can be described by the ability of an agonist to selectively activate a specific signaling pathway (Figure 2). For instance, ligand A may predominantly activate G proteins (Figure 2A) while ligand B may prefer β-arrestin activation (Figure 2B). Concurrently, ligands can also differentiate between different G proteins where ligand C could favor $G\alpha_i$ signaling while ligand D could favor $G\alpha_q$ signaling (Figure 2C). Biased agonism and its role in GPCR activation has already been extensively studied [25-27]. Interestingly, a recent publication proposed a new role of ligand-receptor binding kinetics in apparent biased agonism [28]. The authors examined the binding kinetics and functional effects of several dopamine D_2 receptor (D_2R) agonists. They were able to correlate differential binding kinetics to various biased signaling profiles of D_2R agonists. Moreover, it was shown that agonist bias could be reversed over time in different cell signaling processes. This research article provides a new perspective on binding kinetics and its role in functional processes and presents great potential for further research.

Illustratively, biased signaling at neuropeptide receptors such as the opioid receptor family is frequently observed [29-33]. The opioid receptor family consists of three members, i.e. δ opioid, κ opioid and μ opioid receptors, the latter being the most studied. For instance, Thompson *et al.* studied the potential for biased agonism of endogenous opioids [34]. They reported that several endogenous ligands showed distinct biased signaling profiles in comparison to the other endogenous ligands. The binding kinetics of these endogenous ligands have not been examined thus far and considering our findings in Chapter 5 it would be worthwhile to study the kinetic binding parameters of these ligands. Consequently, it should be investigated if the binding kinetics can be correlated with the various signaling profiles reported in the study of Thompson *et al* [34].

Another neuropeptide receptor that is known for biased signaling is the parathyroid hormone receptor type 1 (PTHR1) [35]. Recent studies have proposed that various PTH analogs can induce differential signaling pathways. More interestingly, it has been suggested that persistent signaling is induced by ligands that prefer G protein-independent pathways while ligands that prefer G protein-dependent pathways induce a more transient response [36]. Although the binding kinetics of the examined ligands were not reported, the authors did briefly discuss the possibility of long residence time being involved in inducing these persistent signaling profiles. Similarly, Hothersall *et al.* recently reviewed the role of residence time in sustained signaling profiles [37] which agreed with our findings in Chapter

4. To test if long residence time is involved in persistent signaling profiles, the binding kinetics of PTH analogs should be examined.

In conclusion, specific knowledge of how ligand binding kinetics can influence biased profiles of agonists for neuropeptide receptors, and GPCRs in general, could improve the discovery of novel drugs targeting this receptor family.

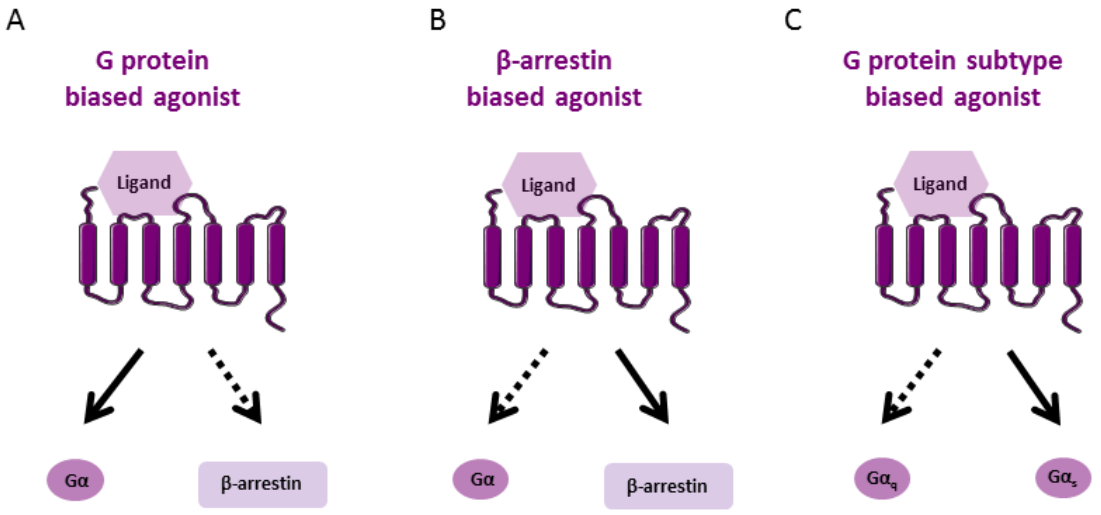

Figure 2: Schematic overview of various types of biased agonists. Upon agonist binding, biased agonism can be observed towards G protein activation (A), β-arrestin activation (B) or a specific G protein subtype, such as $G\alpha_s$ (C).

The future of binding kinetics at neuropeptide receptors

Neuropeptide receptors present an attractive drug target in the treatment of a wide range of therapeutic areas such as cancer, inflammation and reproduction [38]. In view of the latter, this receptor family is well-known for its role in the hypothalamic-pituitary-gon adal axis, playing a crucial role in reproductive functions. Over the past decade, kisspeptin and its receptor KISS1R (also known as GPR54) have gained interest in the treatment of sex hormone-dependent disorders such as infertility and precocious puberty [39]. More interestingly, increasing evidence indicates the benefits of long-acting kisspeptin analogues targeting KISS1R [39-43]. While current research is mainly focused on increasing the metabolic and plasma half-life of KISS1R ligands, another approach could be to design drugs with slow dissociation kinetics. It would be interesting to examine the binding kinetics of kisspeptin and its analogues and establish a structure-kinetics relationship (SKR) study with the aim of finding slowly dissociating ligands for KISS1R.

Kinetic ambition

This thesis evolves around the kinetic binding interactions between the endogenous ligand, the drug and the receptor followed by the cellular response. Three main conclusions are drawn;

1) Both kinetic binding assays such as radioligand binding and TR-FRET studies, and kinetic functional assays such as real-time cAMP and real-time morphology studies, are very suitable to qualitatively and quantitatively study the binding kinetics of numerous ligands.
2) The binding kinetics of endogenous neuropeptides are very divergent.
3) Differential binding kinetics will translate into differential functional effects *in vitro*.

In conclusion, the toolbox of kinetic assays is expanding which allows more accessible and high-throughput measurements of binding kinetics. Secondly, these kinetic assays enable the assessments of kinetic binding parameters of endogenous ligands and drug candidates. Lastly, including kinetic binding studies in the drug discovery paradigm will improve the understanding of drug-target interactions, translation to functional effects and predictions of *in vivo* responses.

Finally, I am hopeful that this thesis will contribute to an increased understanding of ligand-receptor interactions and that it provides a larger toolbox suitable for studying these kinetic interactions. My ambition is to transform binding kinetics into traditional, indispensable, drug discovery parameters and thereby improve the success rate of drug discovery in the future.

References

1. Treherne, J.M. and J.M. Young, *Temperature-dependence of the kinetics of the binding of [3H]-(+)-N-methyl-4-methyldiphenhydramine to the histamine H1-receptor: comparison with the kinetics of [3H]-mepyramine.* Br J Pharmacol, 1988. **94**(3): p. 811-22.
2. Sakai, S., *Effect of hormones on dissociation of prolactin from the rabbit mammary gland prolactin receptor.* Biochem J, 1991. **279 (Pt 2)**: p. 461-5.
3. Casado, V., et al., *Thermodynamic analysis of agonist and antagonist binding to membrane-bound and solubilized A1 adenosine receptors.* J Pharmacol Exp Ther, 1993. **266**(3): p. 1463-74.
4. Guo, D., et al., *Dual-point competition association assay: a fast and high-throughput kinetic screening method for assessing ligand-receptor binding kinetics.* J Biomol Screen, 2013. **18**(3): p. 309-20.
5. van Veldhoven, J.P., et al., *Affinity and kinetics study of anthranilic acids as HCA2 receptor agonists.* Bioorg Med Chem, 2015. **23**(14): p. 4013-25.
6. Pompeu, T.E., et al., *Partial agonism and fast dissociation of LASSBio-579 at dopamine D2 receptor.* Prog Neuropsychopharmacol Biol Psychiatry, 2015. **62**: p. 1-6.
7. Louvel, J., et al., *Agonists for the adenosine A1 receptor with tunable residence time. A Case for nonribose 4-amino-6-aryl-5-cyano-2-thiopyrimidines.* J Med Chem, 2014. **57**(8): p. 3213-22.
8. Glickman, J.F., A. Schmid, and S. Ferrand, *Scintillation proximity assays in high-throughput screening.* Assay Drug Dev Technol, 2008. **6**(3): p. 433-55.
9. Heise, C.E., S.K. Sullivan, and P.D. Crowe, *Scintillation proximity assay as a high-throughput method to identify slowly dissociating nonpeptide ligand binding to the GnRH receptor.* Journal of biomolecular screening, 2007. **12**(2): p. 235-9.
10. Xia, L., et al., *Scintillation proximity assay (SPA) as a new approach to determine a ligand's kinetic profile. A case in point for the adenosine A1 receptor.* Purinergic Signal, 2016. **12**(1): p. 115-26.
11. Vauquelin, G., I. Van Liefde, and D.C. Swinney, *On the different experimental manifestations of two-state 'induced-fit' binding of drugs to their cellular targets.* Br J Pharmacol, 2016. **173**(8): p. 1268-85.
12. Nuber, S., et al., *beta-Arrestin biosensors reveal a rapid, receptor-dependent activation/deactivation cycle.* Nature, 2016. **531**(7596): p. 661-4.
13. Vilardaga, J.P., *Theme and variations on kinetics of GPCR activation/deactivation.* J Recept Signal Transduct Res, 2010. **30**(5): p. 304-12.
14. Lohse, M.J., I. Maiellaro, and D. Calebiro, *Kinetics and mechanism of G protein-coupled receptor activation.* Curr Opin Cell Biol, 2014. **27**: p. 87-93.
15. Ayoub, M.A., et al., *Assessing Gonadotropin Receptor Function by Resonance Energy Transfer-Based Assays.* Front Endocrinol (Lausanne), 2015. **6**: p. 130.

16. Hoffmann, C., et al., *Comparison of the activation kinetics of the M3 acetylcholine receptor and a constitutively active mutant receptor in living cells.* Mol Pharmacol, 2012. **82**(2): p. 236-45.
17. Falkenburger, B.H., J.B. Jensen, and B. Hille, *Kinetics of PIP2 metabolism and KCNQ2/3 channel regulation studied with a voltage-sensitive phosphatase in living cells.* J Gen Physiol, 2010. **135**(2): p. 99-114.
18. Spielman, A.I., et al., *Rapid kinetics of second messenger production in bitter taste.* Am J Physiol, 1996. **270**(3 Pt 1): p. C926-31.
19. Somlyo, A.V., et al., *Kinetics of Ca2+ release and contraction induced by photolysis of caged D-myo-inositol 1,4,5-trisphosphate in smooth muscle. The effects of heparin, procaine, and adenine nucleotides.* J Biol Chem, 1992. **267**(31): p. 22316-22.
20. Sanchez, G., C. Hidalgo, and P. Donoso, *Kinetic studies of calcium-induced calcium release in cardiac sarcoplasmic reticulum vesicles.* Biophys J, 2003. **84**(4): p. 2319-30.
21. Meyer, T., T. Wensel, and L. Stryer, *Kinetics of calcium channel opening by inositol 1,4,5-trisphosphate.* Biochemistry, 1990. **29**(1): p. 32-7.
22. Hong, F., et al., *Kinetics of myosin light chain kinase activation of smooth muscle myosin in an in vitro model system.* Biochemistry, 2013. **52**(47): p. 8489-500.
23. Zimmermann, B., et al., *Kinetics of prephosphorylation reactions and myosin light chain phosphorylation in smooth muscle. Flash photolysis studies with caged calcium and caged ATP.* J Biol Chem, 1995. **270**(41): p. 23966-74.
24. Peiper, U. and J. Dee, *Smooth muscle contraction kinetics at different calcium concentrations.* Can J Physiol Pharmacol, 1994. **72**(11): p. 1338-44.
25. Violin, J.D., et al., *Biased ligands at G-protein-coupled receptors: promise and progress.* Trends Pharmacol Sci, 2014. **35**(7): p. 308-16.
26. Rankovic, Z., T.F. Brust, and L.M. Bohn, *Biased agonism: An emerging paradigm in GPCR drug discovery.* Bioorg Med Chem Lett, 2016. **26**(2): p. 241-50.
27. Liu, Y., et al., *Biased signalling: the instinctive skill of the cell in the selection of appropriate signalling pathways.* Biochem J, 2015. **470**(2): p. 155-67.
28. Klein Herenbrink, C., et al., *The role of kinetic context in apparent biased agonism at GPCRs.* Nat Commun, 2016. **7**: p. 10842.
29. Pradhan, A.A., et al., *Ligand-directed signalling within the opioid receptor family.* Br J Pharmacol, 2012. **167**(5): p. 960-9.
30. Al-Hasani, R. and M.R. Bruchas, *Molecular mechanisms of opioid receptor-dependent signaling and behavior.* Anesthesiology, 2011. **115**(6): p. 1363-81.
31. Busnelli, M., et al., *Functional selective oxytocin-derived agonists discriminate between individual G protein family subtypes.* J Biol Chem, 2012. **287**(6): p. 3617-29.
32. Sanger, G.J., *Ghrelin and motilin receptor agonists: time to introduce bias into drug design.* Neurogastroenterol Motil, 2014. **26**(2): p. 149-55.
33. Heasley, L.E., *Autocrine and paracrine signaling through neuropeptide receptors in human cancer.* Oncogene, 2001. **20**(13): p. 1563-9.

34. Thompson, G.L., et al., *Biased Agonism of Endogenous Opioid Peptides at the mu-Opioid Receptor.* Mol Pharmacol, 2015. **88**(2): p. 335-46.
35. Appleton, K.M., et al., *Biasing the parathyroid hormone receptor: relating in vitro ligand efficacy to in vivo biological activity.* Methods Enzymol, 2013. **522**: p. 229-62.
36. Hattersley, G., et al., *Binding Selectivity of Abaloparatide for PTH-Type-1-Receptor Conformations and Effects on Downstream Signaling.* Endocrinology, 2016. **157**(1): p. 141-9.
37. Hothersall, J.D., et al., *Can residence time offer a useful strategy to target agonist drugs for sustained GPCR responses?* Drug Discov Today, 2016. **21**(1): p. 90-6.
38. Brain, S.D. and H.M. Cox, *Neuropeptides and their receptors: innovative science providing novel therapeutic targets.* Br J Pharmacol, 2006. **147 Suppl 1**: p. S202-11.
39. Prague, J.K. and W.S. Dhillo, *Potential Clinical Use of Kisspeptin.* Neuroendocrinology, 2015. **102**(3): p. 238-45.
40. Skorupskaite, K., J.T. George, and R.A. Anderson, *The kisspeptin-GnRH pathway in human reproductive health and disease.* Hum Reprod Update, 2014. **20**(4): p. 485-500.
41. Oishi, S. and N. Fujii, *Neuropeptide derivatives to regulate the reproductive axis: Kisspeptin receptor (KISS1R) ligands and neurokinin-3 receptor (NK3R) ligands.* Biopolymers, 2016. **106**(4): p. 588-97.
42. Matsui, H. and T. Asami, *Effects and therapeutic potentials of kisspeptin analogs: regulation of the hypothalamic-pituitary-gonadal axis.* Neuroendocrinology, 2014. **99**(1): p. 49-60.
43. Curtis, A.E., et al., *A kisspeptin-10 analog with greater in vivo bioactivity than kisspeptin-10.* Am J Physiol Endocrinol Metab, 2010. **298**(2): p. E296-303.

Summary

In this thesis, the kinetic binding parameters of endogenous ligands and drug candidates and their effect on signal transduction are examined to provide a better understanding of drug-target interactions. While drug discovery programs are traditionally focused on equilibrium-based parameters such as affinity values, drug candidates often fail in clinical trials due to on and/or off target toxicity and/or lack of *in vivo* efficacy. In the past decade, drug-target binding kinetics, i.e. association and dissociation rate constants, are increasingly acknowledged as better predictive parameters of *in vivo* drug action and it is proposed to incorporate these parameters to decrease drug attrition rates and improve the drug discovery paradigm. To investigate the role of binding kinetics in ligand-receptor interactions, two G protein-coupled receptors (GPCRs) are used as model systems, namely the gonadotropin-releasing hormone (GnRH) receptor and the neurokinin 1 (NK1) receptor. Both receptors can be categorized in the neuropeptide receptor family and this receptor family plays a crucial role in the peripheral and central nervous system making them interesting targets in therapeutic areas such as epilepsy, pain and psychological disorders. An in-depth background on neuropeptide receptors, binding kinetics and kinetic assays is provided in **Chapter 1**.

Since drug candidates often compete with endogenous ligands in the body, more knowledge on the interactions between endogenous ligand and receptor could aid in understanding desired (kinetic) interactions of a drug candidate with that receptor. In **Chapter 2**, novel insights into the kinetic profile of endogenous neuropeptides and their receptors are considered. The binding kinetics, internalization kinetics and release kinetics of three exemplary neuropeptide-receptor pairs are reviewed and these kinetic parameters proved to be quite variable. Collectively, this review provides a perspective for future drug research to include the kinetic profile of the target receptor and its endogenous ligand(s). This will improve the understanding of desired drug-target binding kinetics and thus lead to more efficacious drugs.

One of the challenges in examining binding kinetics is the lack of robust kinetic assays suitable to study these kinetic binding parameters. To overcome this hurdle, a selection of well-known GnRH receptor drugs is used to design and validate kinetic radioligand binding and TR-FRET protocols in **Chapter 3**. A competition association assay is designed for both kinetic assays and this facilitated the determination of the kinetic binding parameters of 12 unlabeled GnRH analogs. Both affinity values and values of dissociation rate constant are highly correlated between both kinetic assays. Additionally, the association and dissociation rate constants of the tested GnRH drugs are very divergent, indicating a pivotal role of binding kinetics in drug-target interactions. This research provides new

perspectives by incorporating kinetic binding parameters in current research which could potentially improve future drug discovery targeting the GnRH receptor.

The functional effects of two kinetically diverse GnRH agonists, i.e. GnRH and buserelin, from **Chapter 3** are further studied in **Chapter 4**. A morphology-based real-time assay is found to be suitable for studying receptor-mediated responses. Persistent signal transduction profiles are observed for both agonists. However, wash-out experiments prove that the persistent signaling profile of fastly dissociating GnRH is most likely due to ligand rebinding while the persistent signaling profile of slowly dissociating buserelin is presumably due to a long-lasting receptor binding profile. This study stresses the impact of slow dissociation rates for long-lasting receptor activation and could support future research towards drugs with prolonged efficacy.

In **Chapter 5**, another well-known neuropeptide receptor is examined, namely the NK1 receptor. Considering the importance of knowledge of the binding kinetics of not only drug candidates but endogenous ligands discussed in **Chapter 2**, the association and dissociation rate constants of endogenous tachykinins and a few close analogs are examined. Interestingly, the binding kinetics of the tested tachykinins are very diverse, particularly the association rates. Furthermore, kinetic binding parameters are highly correlated to signal transduction values such as *in vitro* potency and maximal response values. Our findings demonstrate the great variability in binding kinetics of these tachykinins and underline the importance of measuring the kinetic binding parameters of not only drug candidates but also endogenous ligand(s).

Chapter 6 is focused on elucidating the missing link between binding kinetics and signal transduction to improve the understanding of drug action *in vivo*. The effects of two NK1 receptor antagonists with variable dissociation rates are examined using two endogenous tachykinins with variable association rates. We found that the divergent kinetic profiles of both antagonists and endogenous agonists resulted in different signal transduction profiles. Moreover, these findings are consistent throughout multiple assay formats, cellular backgrounds and mathematical simulations. This research emphasizes that knowledge of the relationship between drug-target binding kinetics and cellular responses is important for improved understanding of drug efficacy.

In summary, multiple kinetic binding assays (i.e. radioligand binding and TR-FRET studies) and kinetic functional assays (i.e. real-time cAMP and real-time morphology studies) are designed and validated to study binding kinetics and their role in signal transduction of numerous endogenous ligands and drug candidates. Significant differences in the kinetic profiles of endogenous neuropeptides and well-known drugs are observed and this kinetic

variability triggered differential functional effects *in vitro*. These overall conclusions are discussed in **Chapter 7**. Finally, the findings in this thesis could contribute to a larger toolbox suitable for studying kinetic ligand-receptor parameters. Moreover, knowledge of the kinetic binding parameters of drugs and endogenous ligands could play a pivotal role in understanding ligand-receptor interactions and result in an improved drug discovery paradigm.

Samenvatting

In dit proefschrift zijn de kinetische bindingparameters van endogene liganden en potentiële geneesmiddelen en hun effect op signaaltransductie onderzocht, om een beter inzicht te krijgen in geneesmiddel-receptor interacties. Geneesmiddelonderzoek programma's zijn voornamelijk gericht op evenwichtsparameters zoals affiniteit, maar potentiële geneesmiddelen stranden vaak in klinische onderzoeken door toxiciteit en/of een gebrek aan *in vivo* effectiviteit. In het afgelopen decennium wordt geneesmiddel-receptorkinetiek meer en meer gezien als een parameter die de *in vivo* geneesmiddelwerking beter kan voorspellen. Het verdient derhalve aanbeveling om deze kinetische bindingsparameters op te nemen in geneesmiddelonderzoeksprogramma's om het hoge percentage mislukkingen terug te dringen. Om de rol van bindingskinetiek in ligand-receptor interacties te onderzoeken zijn twee G-eiwit gekoppelde receptoren (GPCRs) gebruikt als modelsysteem, namelijk de gonadotropine-vrijgevend hormoon (GnRH) receptor en de neurokinine 1 (NK1) receptor. Beide receptoren vallen onder de neuropeptide receptorfamilie en deze receptorfamilie speelt een belangrijke rol in het perifere en centrale zenuwstelsel. Dit maakt deze receptorfamilie een aantrekkelijk aangrijpingspunt in therapeutische gebieden zoals epilepsie, pijn en psychologische aandoeningen. Een grondig overzicht van neuropeptide receptoren, bindingskinetiek en kinetische bepalingsmethoden wordt gegeven in **Hoofdstuk 1**.

Potentiële geneesmiddelen zijn vaak in competitie zijn met endogene liganden. Daarom is het van belang om meer kennis van de interacties tussen endogene liganden en de receptor te verkrijgen. Dit kan helpen bij het beter begrijpen van gewenste (kinetische) interacties tussen een potentieel geneesmiddel en de receptor. In **Hoofdstuk 2** worden nieuwe inzichten in het kinetische profiel van endogene neuropeptiden en hun receptoren behandeld. Uit een literatuurstudie van bindingskinetiek, receptor internaliseringskinetiek en ligand uitscheidingskinetiek voor drie voorbeelden van neuropeptide-receptor combinaties bleek dat de kinetische profielen van deze drie combinaties erg verschillend zijn. Samengevat geeft deze literatuurstudie aan dat het introduceren van het kinetische profiel van de receptor en z'n endogene ligand(en) tot een verbetering in het begrip van de gewenste bindingskinetiek van het potentiële geneesmiddel kan leiden. Dit kan dus resulteren in effectievere geneesmiddelen.

Eén van de uitdagingen in het onderzoeken van bindingskinetiek is het gebrek aan robuuste proeven die geschikt zijn voor het bestuderen van kinetische parameters. Om meer kinetische proeven beschikbaar te maken is een selectie van bekende GnRH receptor geneesmiddelen gebruikt om kinetische radioligand binding en TR-FRET (fluorescentie) studies op te zetten en te valideren in **Hoofdstuk 3**. Een competitieve associatie proef werd ontworpen voor beide kinetische proeven en hiermee konden de kinetische parameters van

twaalf GnRH geneesmiddelen bepaald worden. Zowel de affiniteit als de dissociatie snelheidswaardes kwamen goed overeen in de twee verschillende kinetische bepalingsmethoden. De associatie- en dissociatiesnelheden van de 12 GnRH geneesmiddelen waren erg verschillend, wat een belangrijke rol kan spelen in geneesmiddel-receptor interacties. Dit onderzoek heeft derhalve nieuwe kinetische perspectieven gegeven op bekende GnRH geneesmiddelen. Het meenemen van kinetische bindingsparameters kan toekomstige geneesmiddel onderzoek voor de GnRH receptor verbeteren.

De functionele effecten van twee kinetisch diverse GnRH agonisten, GnRH en busereline, uit **Hoofdstuk 3** zijn verder bestudeerd in **Hoofdstuk 4**. Een op morfologie-gebaseerde proef bleek erg geschikt voor het meten van receptor-gemedieerde responsen. Aanhoudende signaleringsprofielen werden waargenomen voor beide agonisten. Was-experimenten proeven toonden aan dat de aanhoudende signalering van snel dissociërend GnRH toe te schrijven was aan het opnieuw binden van de agonist aan de receptor. De aanhoudende signalering van langzaam dissociërend busereline werd hoogstwaarschijnlijk veroorzaakt door langdurige receptorbinding. Deze bevindingen leggen nadruk op de impact van een langzame dissociatiesnelheid op langdurige receptoractivatie. Dit kan toekomstig onderzoek naar geneesmiddelen met een lange werkingsduur bevorderen.

In **Hoofdstuk 5** wordt een andere welbekende neuropeptide receptor beschreven, namelijk de NK1 receptor. Het belang van kennis van de bindingskinetiek van niet alleen toekomstige geneesmiddelen, maar ook endogene liganden is al besproken in **Hoofdstuk 2**. Daarom zijn de associatie- en dissociatiesnelheidsconstanten van endogene tachykinines en een aantal vergelijkbare analogen onderzocht. Het was opmerkelijk dat de bindingskinetiek van de onderzochte tachykinines erg verschillend was, met name de associatie snelheden. Bovendien correleerden de kinetische bindingsparameters zeer goed met het maximale effect en ‘potency’ waarden *in vitro*. Deze resultaten tonen grote verschillen aan in de bindingskinetiek van endogene tachykines en benadrukken het belang van het meten van bindingskinetiek voor niet alleen potentiële geneesmiddelen, maar ook de endogene liganden waarmee zij in competitie zijn.

Hoofdstuk 6 is gericht op het ophelderen van de ontbrekende schakel tussen bindingskinetiek en signaaltransductie, om het begrip van geneesmiddel werking *in vivo* te verbeteren. De effecten van twee NK1 receptor antagonisten met variabele dissociatie snelheden werden onderzocht in combinatie met twee endogene tachykinines met variabele associatie snelheden. We toonden aan dat diverse kinetische bindingsprofielen van zowel antagonisten als endogene agonisten, tot verschillende signaaltransductieprofielen kunnen leiden. Deze resultaten waren consistent onder verschillende proef condities, cellulaire

achtergronden en in wiskundige modellen. Dit onderzoek toont aan dat kennis van de wisselwerking tussen bindingskinetiek en cellulaire responsen belangrijk is voor een verbeterd begrip van geneesmiddel effectiviteit.

Samenvattend, meerdere kinetische bindingsproeven (zoals radioligand binding en TR-FRET studies) en kinetische functionele proeven (zoals cAMP en morfologie studies) werde ontworpen en gevalideerd. Hiermee is de bindingskinetiek en de rol daarvan in signaaltransductie van verschillende endogene liganden en potentiële geneesmiddelen onderzocht. Significante verschillen in de kinetische profielen van endogene neuropeptiden en bekende geneesmiddelen werden waargenomen en deze verschillen zorgden ook voor variabele functionele effecten *in vitro*. Deze conclusies zijn besproken in **Hoofdstuk 7**. De bevindingen besproken in dit proefschrift kunnen bijdragen aan een uitgebreid instrumentarium, geschikt voor het onderzoeken van kinetische ligand-receptor interacties. Kennis van de kinetische bindingsparameters van potentiële geneesmiddelen en endogene liganden kan een belangrijke rol spelen in het ophelderen van ligand-receptor interacties en kan resulteren in betere geneesmiddel onderzoeksprogramma's.

List of publications

From receptor binding kinetics to signal transduction; a missing link in predicting in vivo drug-action. I. Nederpelt, M. Kuzikov, P. Schnider, B. Tuijt, A.P. IJzerman, E.C.M. de Lange, L.H. Heitman. *Manuscript in preparation*

Kinetic Profile of Neuropeptide-Receptor Interactions. I. Nederpelt, J. Bunnik, A.P. IJzerman, L.H. Heitman. *Trends in Neurosciences* **2016** 39 (12): 830–839

Kinetic binding and activation profiles of endogenous tachykinins targeting the NK1 receptor. I. Nederpelt, D. Bleeker, B. Tuijt, A.P. IJzerman, L.H. Heitman. *Biochemical Pharmacology* **2016** 118: 88-95

Persistent GnRH receptor activation in pituitary αT3-1 cells analyzed with a label-free technology. I. Nederpelt, R.D. Vergroesen, A P. IJzerman and L.H. Heitman. *Biosensors and Bioelectronics* **2016** 79: 721-727

Characterization of 12 GnRH peptide agonists – a kinetic perspective. I. Nederpelt, V. Georgi, F. Schiele, K. Nowak-Reppel, A.E. Fernández-Montalván, A.P. IJzerman and L.H. Heitman. *British Journal of Pharmacology* **2016** 173 (1): 128-41

Kinetics for Drug Discovery – An industry driven effort to target drug residence time. D.A. Schuetz, W.E.A. de Witte, Y.C. Wong, B. Knasmueller, L. Richter, R. Bosma, D. Kokh, S. Kashif, I. Nederpelt, E. Segala, M. Amaral, D. Guo, D. Andres, L.A. Stoddart, S. Hill, R.M. Cooke, R. Leurs, M. Frech, R. Wade, E.C.M de Lange, A.P. IJzerman, A. Müller-Fahrnow, G.F. Ecker. *Drug Discovery Today* in press

Mechanistic models enable the rational use of in vitro drug-target binding kinetics for better drug effects in patients. W.E. de Witte, Y.C. Wong, I. Nederpelt, L.H. Heitman, M. Danhof, P.H. van der Graaf, R.A. Gilissen, E.C. de Lange. *Expert Opinion in Drug Discovery* **2016** 11 (1): 45-63

Multiple binding sites for small-molecule antagonists at the CC chemokine receptor 2. A.J. Zweemer, I. Nederpelt, H. Vrieling, S. Hafith, M.L. Doornbos, H. de Vries, J. Abt, R. Gross, D. Stamos, J. Saunders, M.J. Smit, A.P. IJzerman, L.H. Heitman. *Molecular Pharmacology* **2013** 84 (4): 551-61

Curriculum Vitae

Indira Nederpelt was born in Rotterdam, The Netherlands on October 4th, 1988. After graduating high school at the IJsselcollege in Capelle aan den IJssel, she studied Biopharmaceutical Sciences at Leiden University starting in 2006. During her studies she performed two research internships under supervision of Dr. Annelien Zweemer, Dr. Laura Heitman and Prof. Dr. Ad IJzerman. These internships were both focused on designing and validating kinetic binding assays for the GnRH receptor and CCR2 receptor. Her contribution to the CCR2 project resulted in a co-publication in Molecular Pharmacology. Subsequently she moved to San Diego, CA, USA to perform a third internship at Vertex Pharmaceuticals under supervision of Akiko Nakatani and Dr. Julie Selkirk. She studied ligand selectivity at the extracellular and intracellular binding site of a tyrosine receptor kinase in an industrial setting. Upon her return to The Netherlands she finished her MSc. degree *cum laude* in 2012.

In 2013, Indira started her PhD study at Leiden University at the Department of Medicinal Chemistry, under supervision of Dr. Laura Heitman and Prof. Dr. Ad IJzerman. Her PhD research was part of an Innovative Medicine Initiative (IMI) project named Kinetics for Drug Discovery (K4DD) (grant number 115366) in collaboration with 20 partners throughout Europe in academia, small and medium-sized enterprises (SMEs) and pharmaceutical companies. This project was founded to improve measurement techniques and the understanding of ligand-receptor binding kinetics. Indira's research was focused on two G protein-coupled receptors, the GnRH receptor (a continuation of the project from her research internship) and the NK1 receptor. Throughout her PhD studies she presented the work described in this thesis at numerous national and international conference. In 2014 she was awarded the Young Investigator Award at the 11th international symposium on GnRH for best oral presentation. Later that year she was awarded for the best oral presentation at the Dutch Medicine Days in the section medicinal chemistry.

Acknowledgements

Throughout my PhD I have found support, advice and inspiration in my students, colleagues, friends and family. I'm truly appreciative of all your contributions and I have become a better scientist because of it.

I would like to thank K4DD for enabling this research and introducing me to a large group of junior and senior scientists working in academia and pharmaceutical companies. Amaury, Felix, Victoria, Patrick, Maria, Wilbert and Liesbeth, thank you for the wonderful collaborations, you've taught me a lot about team-work. All other K4DD fellows have been equally important for all the fruitful scientific (and non-scientific) discussions during our bi-annual meetings. I am grateful to all my students who've taught me how to be a supervisor. More importantly, I'm happy to have been part of the start of your scientific endeavors and without your hard work and dedication this thesis wouldn't exist. Laura, your ambition and work ethic inspired me to dream big. Ad, the combination of your dry humor and leadership skills made you the group leader I aspire to be. It has been a pleasure to start my scientific career working in your group. All my colleagues at medicinal chemistry, thank you for making me laugh during all our coffee breaks. My office mates, Joey, Miriam, Julia, Andrea, Maarten, Xuesong and Anna, all our interesting, weird and funny (non-)work related discussions never failed to give me new perspectives and put a smile on my face. Maarten, Henk and Miriam, thank you for always listening when I needed to vent and for helping me destress.

Mijn lieve vriendinnen, Bo, Michelle, Lisette, Tamar, bedankt voor jullie begrip en vriendschap in de afgelopen 4 jaar. Al onze spelletjesavonden, wandelingen, bootcamp en squash avonturen hebben mij ontzettend geholpen te ontspannen en geluk te vinden in jullie aanwezigheid. Rochelle, super bedankt voor onze eindeloze gesprekken, puzzelmiddagen en het ontwerpen van de cover. Akiko and Neelu, although we are separated by an ocean, your words of encouragement and unconditional friendship mean the world to me. Pap, je bent een man van weinig woorden maar je bent er altijd als ik je nodig heb. Mirjam, mijn onofficiële zusje, onze vriendschap begon 25 jaar geleden en vanaf dag 1 is onze band heel bijzonder. Jouw rust, steun en liefde is onschatbaar.

Tot slot, mam, jij bent de moeder en beste vriendin die iedereen verdient. Dankzij jouw humor, advies, steun, begrip en onvoorwaardelijke liefde schijnt de zon altijd in mijn leven. Met jou in mijn leven durf ik de grootste uitdagingen aan te gaan omdat ik weet dat jij er altijd bent om me te vangen als ik val.